Adaptive Parameter Estimation of Power System Dynamic Models Using Modal Information

SONG GUO

Abstract

Knowledge of the parameter values of the dynamic generator models is of paramount importance for creating accurate models for power system dynamics studies. Traditionally, power systems consists of a relatively limited numbers of large power stations and the values of generator parameters were provided by manufacturers and validated by utilities. Recently however, with the increasing penetration of distributed generation, the accuracy of these models and parameters cannot be guaranteed.

This thesis addresses the above concerns by developing a methodology to estimate the parameter values of a power system dynamic model online, employing dynamic system modes, i.e. modal frequencies and damping. The dynamic modes are extracted from real-time measurements.

The aim of the proposed methodology is to minimise the differences between the observed and modelled modes of oscillation. It should be emphasised that the proposed methodology does not aim to develop the dynamic model itself but rather modify its parameter using WAMS measurements. The developed methodology is general and can be used to identify any generator parameters., However, thesis concentrates on the estimation of generator inertia constants.

The results suggest that the proposed methodology can estimate inertias and replicate the dynamic behaviour of the power system accurately, through the inclusion of pseudo-measurements in the optimisation process. The pseudo-measurements not only improves the accuracy of the parameter estimation but also the robustness of it. Observability, a problem when there are fewer numbers of measurements than the numbers of parameters to be estimated, has also been successfully tackled. It has been shown that the damping measurements do not influence the accuracy and robustness of generator inertia estimation significantly.

Adaptive Parameter Estimation of Power System Dynamic Models Using Modal Information

by
Song Guo

A dissertation submitted for the degree of

Doctor of Philosophy in Power System Engineering

School of Engineering and Computing Sciences
Durham University
2014

Contents

Statement of Copyright

Acknowledgement

The joy of completion is to look over the entire journey, and remember the friends and family who have helped and supported me along this long but fulfilling road. Some sweat, tears and blood, but it is all worthy.

The author would like to express his heartfelt gratitude to **Professor Janusz Bialek**; an inspirational, supportive and patient advisor who brought me to power system industry, and guided me through my research journey. I will never forget his advice and suggestions from which benefited me significantly. Not only did he educate me with the technical knowledge but assisted with my development of my thoughts. Without his support this work cannot achieve completion. The encouragement from him was my main weapon when I confronted the challenges and difficulties.

I am grateful to obtain advice, knowledge and insightful discussions with **Professor Phillip Taylor**, **Dr. Chris Dent** and **Dr. Patrick McNabb** which form the steps for achieving my research target.

I also would like to thank my colleagues and friends, **Sean Norris**, **Peter Wyllie**, **Lei Wang**, **Jing Chen**, **Donatella Zappala**, **Terry Ho**, **Dr. Wenjuan Wang**, **Dr. Marco Autieri**, **Pengfei Wang**, **Dr. Yanchao Li, Dr. Padraig Lyons** and **Dr. Lorna Bang** who brought lots of fun to my life in Durham. I can still recall the days we playing squash, going to gym, and fishing on a boat in the sea near Whitby. A pub lunch together could always recharge my battery for the afternoon. It is the best three years in my life when I stayed in E215.

I appreciate **Dr. Douglas Wilson** and **Psymetrix**, **Alstom**, who provided me internship opportunities. This has significantly broadened my knowledge, and encouraged me to take an alternative route; walking out of the academic world into the industry.

I also would like to express my gratitude to my current company, **London Power Associates**, my regional director **Steve Elliot,** and my manager **Martin Luckett**, who has allowed me time to

complete my thesis. I am grateful to my colleague and friend, **Dr. Jhan Chan** who gave me a great amount of support for my career and life.

I also would like to thank **Energy CDT Network** and **Dr. Katie Daniels** who arranged the interesting trips to the power stations and wind farms.

I would like to express my gratitude to all the staff in the school of Engineering and Computing Sciences, especially **Trevor McCarron** who was always willing to fix my computer after I broke it.

I am grateful to my aunt, **Caihong Lan** who helped me to take care of my parents and my grandpa when I am eight thousand miles away.

Appreciation to my friends over in China and overseas, **Lei Yan** and **Lu Zhang** who spent most of time with me in my first year abroad. A football game, a cold shower and some beer were the best treatment after school; **An Chun**, **Yaping Li** and **Yafei Chen** who treat me like a brother and always cook me a delicious meal to cheer me up during my examination period; **Naveed Yasir** who always tackled the difficult questions in the past exam papers with me until midnight.

I would like to thank **Dr. Xuecheng Zhang** who gave me many useful advices when I just stepped into my career, and **Erica Li** who took care of my chinchillas when I was away from the country.

To my family

List of Publications

S. Guo, D. Wilson, S. Norris, J. Bialek, Increasing the Available Transmission Capacity by using a Dynamic Transient Stability Limit, IEEE-PES Innovative Smart Grid Technology Conference, Manchester, UK, 2011.

S. Norris, **S. Guo**, J. Bialek, Tracing of Power Flows applied to Islanding, IEEE general meeting, San Diego, USA, 2012.

S. Guo, J. Bialek, Synchronous Machine Inertia Constants Updating using Wide Area Measurements, IEEE-PES Innovative Smart Grid Technology Conference, Berlin, Germany, 2012.

S. Guo, J. Bialek, Adaptive Parameter Estimation of Power System Dynamic Model Using Modal Information, IEEE Transaction on power systems. (submitted)

S. Norris, **S. Guo**, J. Bialek and S. Ziemianek, Application of Power Tracing and Modal Voltage Analysis to Preventive Islanding, IEEE Transaction on power systems. (submitted)

Chapter 1 Introduction

1.1 Motivation

The management of power system stability has been extremely challenging due to significant changes in power system dynamic behaviours, especially power system oscillations. Power system oscillations were detected as soon as synchronous generators were interconnected to provide more power capacity. In conventional power systems, the synchronous generators were located closely to each other and amortiseur windings were applied to generator rotor to prevent the increase of oscillation amplitudes. The amortisuer windings provide a torque which is proportional to the rotor speed. In normal condition the rotor speed should match the synchronous speed. However if these two speed deviates the amortisuer winding can absorb the associated energy, thus reduce the oscillation amplitudes.

Recently, a number of issues have been identified that can change the power system dynamics properties, thus cause severe stability problems which may result in large area blackout. The changes can be due to the change in political policy, commercial strategies, current technology and existing infrastructure capabilities.

- The liberation of electricity energy market: The market determines the operation status of generators. It can push the system to a great many operational status. Due to the deregulation of the electricity market, the amount of power delivered becomes unpredictable. The bulk power transfer over long distances has been increased.
- Large power system interconnection: The expansion of synchronous areas can change the dynamic properties. For example, a growing number of oscillation modes have been observed in the UK power system after the connection with Scandinavian and continental European power systems.

- Integration of renewable generation: Different generation devices have different dynamic response. Policies have been issued to restrict the global carbon emission to promote the uptake of renewable generation, , to replace conventional carbon intensive generation.
- Existing electricity delivery infrastructure: Increasing electricity demand pushes the existing power system to operate closer to its limits. The tie line connecting two distant areas are normally heavily loaded, which increases potential risks.
- Plant-Grid separation: Due to commercial reasons, limited information is shared between parties. Dynamic testing and control tuning are restricted.
- Improper control tuning and system islanding: Improper control tuning can deteriorate existing oscillations. System islanding method is considered as an innovative approach in preventing further spread of wide area blackouts. However, the existing algorithms are based on historic system model that is an inaccurate representation of the current system.
- Increase penetration of distributed generation: the model accuracy and parameters cannot be guaranteed. This raises the need for a methodology that can estimate the parameters of generators utilising on-line measurements.

Measurement-based techniques have been implemented to diagnose problems related to oscillatory stability. These techniques aim to detect the location of the sources through poorly damped oscillatory modes. Through the usage of statistics, plants or network bottlenecks that degrade the oscillatory stability. This approach can be restricted due to the limited number of measuring devices in the network. If there are sources outside the observed network that degrades the stability, it can be very difficult to diagnose. Model-based methods are powerful. They help us understand the underlying conditions and assist the design of damping controllers. However, they are not always reliable. This thesis inspects possible model update schemes that can reconstruct near-real-time dynamic network models whilst retaining the network topology. The concept under investigation is to combine both model and measurement based methods to

create a linear dynamic model from noisy phasor measurements. The concept could be applied to update internal, external network models and generator parameters used by system operators. The ability to derive a near-real-time dynamic model that adapts to observed system conditions is thought to be a valuable addition to the management of system dynamics with large interconnection. This would provide a wider view of the system stability for the operators, and enable them to conduct Dynamic Security Assessment (DSA). The estimated parameters can also be useful for modelling or design purposes.

1.2 Research Objectives

The research objectives of this thesis focus on the follows:

- Introduce the 'model update' concept into power system engineering. The concept aim to estimate generator parameters in near-real-time base, and thus to update generator models.
- Develop the theory of model update technique. The update of generator inertia constants are used as an example to demonstrate the proposed methodology. However, the methodology is general and can be used to identify other generator parameters.
- Implement known sensitivity analysis technique for mode selection
- Investigate and evaluate different methods that could be used in model update scheme.
- Demonstrate the application of model update scheme using simulation studies.
- Execute comparative studies on different methods in model update scheme and outline their advantages and disadvantages.
- Draw conclusions and suggest future research.

1.3 Contributions

The contributions of this thesis are summarised as follows:

- The introduction of a novel concept, 'model update' to improve the management of power system stability. The concept is based on the application WAM which is captured by Phasor Measurement Units (PMUs) placed in different locations of the grid.
- The sensitivity analysis technique assist the selection of oscillatory modes.
- Several novel algorithms have been developed to update the parameters of power system dynamic models in near-real-time, using minimum system information, such as modal frequency and modal damping. These algorithms also present possible state estimation approaches to circumvent the problems of lack of measurements.
- The methodology presents a new way for the condition monitoring of a wider network. Model update schemes developed based on sensitivity analysis and model update algorithms can help to achieve more accurate power system models.
- External dynamic equivalents derived by model update scheme provides TSOs a whole picture of the system condition during normal operation and/or fault.
- The proposed method can be applied to model validation for network operators.

1.4 Outline

This thesis is organised as follows. Chapter 2 will introduce the background knowledge of power system dynamics and stability. The phenomena of power system oscillations will also be addressed. The modelling of synchronous generators and multi-machine system will also be included in this chapter. Chapter 3 introduces the techniques used for power system extraction. The two most commonly used methods are ringdown methods and ambient-signal methods. Dynamic equivalent methods are extensively discussed in Chapter 4. Conventional model reduction methods and measurement-based methods will be discussed within this chapter. Chapter 5 will describe the concept of 'model update'. Two simulation models are used to demonstrate the methodology. In chapter 6, the methods that depend on modal measurements will be discussed, and simulation tests are executed for different scenarios. Methods in Chapter 7 include pseudo-measurements along

with modal measurement. Conclusions and future work are presented in Chapter 8 and Chapter 9 respectively.

Chapter 2 Background

2.1 Power System Dynamics

Power system dynamics can be classified into four time dependent groups. These are shown in Figure 2.1 [1],

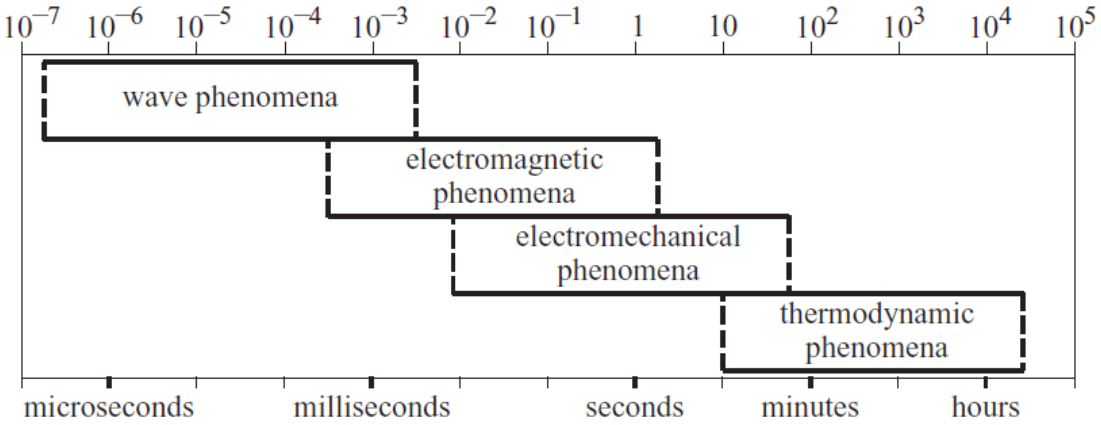

Figure 2. 1 classification of power system dynamics based on time frame [1]

The electromechanical phenomena has high relevance to power system oscillations is the prime concern in this thesis.

2.2 Power System Stability

Power system can be defined as a set of first-order nonlinear ordinary differential equations,

$$\dot{x} = f(x(t), u(t)) \quad (2.1)$$

$$y = g(x(t), u(t)) \quad (2.2)$$

where x indicates system states and u is input variables.

A general nonlinear system is stable in certain state space regions and unstable in others. Stability issues can be addressed as equilibrium points using Lyapunov theory reproduced in Figure 2.2. The origin of the state space is always at an equilibrium point, however multiple equilibrium points can exist.

- **Stable**: The origin is considered as a stable equilibrium point if for any given value $\varepsilon > 0$ there exists a scalar $\delta(\varepsilon, t_0) > 0$ such that if $\|x(t_0)\| < \delta$, then the resultant motion satisfies $\|x(t)\| < \varepsilon$ for any $t > t_0$.
- **Asymptotically Stable**: The origin is considered as an asymptotically stable equilibrium point if it is stable and there exists a scalar $\delta(t_0) > 0$ such that $\|x(t_0)\| < \delta$ the resultant motion satisfies $\|x(t)\| \to 0$ as $t \to \infty$.

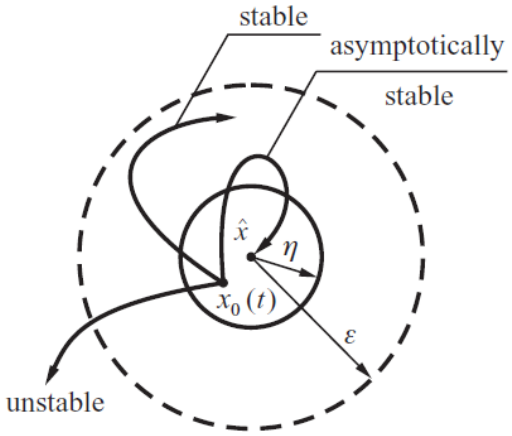

Figure 2. 2 definition for stability of nonlinear system in sense of Lyapunov [1]

Power system stability is the ability to regain an equilibrium point after subjected to a disturbance. For different stability study purposes, power system can be described differently by modelling corresponding variables. Classification of power system stability was produced in CIGRE Report No. 325 as shown in Figure 2.3.

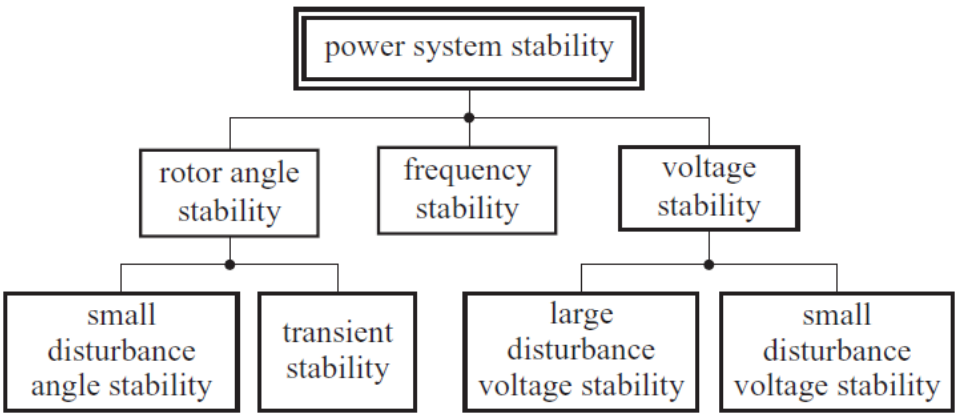

Figure 2. 3 classification of power system stability [2]

Due to nonlinear characteristics of power system, rotor angle stability and voltage stability can be further divided into two groups dependent on the size of disturbance. Rotor angle stability with small disturbance is the main concern of this research.

2.3 Stability Analysis Methods

Regarding to the size of a signal, the input signals to power systems are mainly recognised as small signal and ring-down signal.

- Constant perturbations are identified in power operation. These perturbations are mainly caused by random load variation and named small signal. During small signal perturbations, the system state stays around its original equilibrium points. The advantage of using small signal stability analysis is that the system studies can be executed online near real time.
- Ring-down signal is introduced to the system when a fault occurs. It pushes the system state from its origin to another equilibrium point.

2.4 System Linearisation and Modal Analysis

2.4.1 System Linearisation

Nonlinear system can be linearised at an equilibrium point under small disturbance, which can dramatically reduce numerical computation burden and reveal the system nature in a linear form. The linear model can be represented in state space form,

$$\Delta\dot{x} = A\Delta x + B\Delta u \tag{2. 3}$$

$$\Delta y = C\Delta x + D\Delta u \tag{2. 4}$$

In Equation (2.3) and (2.4), A, B, C and D are the matrices of derivatives of functions f, g with respect to x and u. A is the state matrix; B is the input matrix; C is the output matrix; D is the feedforward matrix.

2.4.2 Modal Analysis

Matrix A which indicates state matrix plays an important role in system modal analysis. The eigenvalues of the state matrix A determines the stability characteristics of a system and any eigenvalue λ must satisfy,

$$Aw = w\lambda \tag{2. 5}$$

where the non-zero column w is referred to as the right eigenvector regarding to λ.

(2. 5) can be rewritten as,

$$\det(A - \lambda I) = 0 \tag{2. 6}$$

A full expression is derived as,

$$AW = W\Lambda \tag{2. 7}$$

$W = [w_1, w_2, \dots, w_n]$ is a square matrix whose columns are the right eigenvectors of state matrix A. It indicates the relative activity of the state variables when a particular mode is excited, and thus is called mode shapes [3]. Right eigenvectors are not unique and may be scaled by a factor. The eigenvectors correspond to eigenvalues as complex conjugate pairs should be the same after scaled one by the selected factor.

Λ is a diagonal matrix contains eigenvalues of state matrix A.

$$\Lambda = \begin{bmatrix} \lambda_1 & 0 & \cdots & 0 \\ 0 & \lambda_2 & \cdots & 0 \\ \vdots & \vdots & \ddots & \vdots \\ 0 & 0 & \cdots & \lambda_n \end{bmatrix} \tag{2. 8}$$

Pre-multiplying (2.7) by W^{-1} gives,

$$\Lambda = UAW \tag{2. 9}$$

where $U = W^{-1} = \begin{bmatrix} u_1 \\ u_2 \\ \vdots \\ u_n \end{bmatrix}$ is also a square matrix whose rows are the left eigenvectors of A.

An eigenvalue can be described in a general complex form,

$$\lambda = \sigma \pm j\omega \tag{2. 10}$$

The modal frequency is defined as below,

$$f = \frac{\omega}{2\pi} \tag{2. 11}$$

The modal damping is determined by the real part of the eigenvalue. A damping ratio definition is presented in (2.12),

$$\zeta = -\frac{\sigma}{\sqrt{\sigma^2+\omega^2}} \tag{2. 12}$$

The damping conditions of a mode can be classified in terms of the damping ratio ζ,

- **Undamped:** When $\zeta = 0$, the mode response displays as $e^{j\omega}$.
- **Underdamped:** When $\zeta < 1$, the mode response decays exponentially with oscillation, as $e^{j\omega\sqrt{1-\zeta^2}}$.
- **Overdamped:** When $\zeta > 1$, the response decays exponentially without oscillsation.
- **Critical damped:** When $\zeta = 1$, this is the border between overdamped and underdamped.

The stability of the linear system is determined by the real part of the eigenvalue. It is interpreted by Lyapunov as:

- **Stable:** $\sigma \leq 0$, for all modes
- **Asymptotically stable:** $\sigma < 0$, for all modes

For a linear system, asymptotic stability is independent of initial conditions, and if a linear system is asymptotically stable, it is globally asymptotically stable.

2.5 Synchronous Generator Models

Synchronous generator models have been comprehensively illustrated in [1] and [4]. Generally, synchronous generator models are categorised as low-order and high-order synchronous generator models. Classical model and sixth-order model are briefly introduced in this section.

2.5.1 Classical Model

Classical synchronous generator model is derived from the swing equation,

$$M\Delta\dot{\omega} = P_m - P_e - D\Delta\omega \tag{2. 13}$$

$$\dot{\delta} = \Delta\omega \tag{2. 14}$$

where $\Delta\omega$ is the rotor speed deviation,

δ is the rotor angle,

$M = 2H$ which is the generator inertia constant,

P_m is the mechanical power input to the generator inertia,

P_e is the electrical power output from the generator,

D is the damping coefficient.

Single-machine infinite bus system shown in Figure 2.4, can be rewritten in the form of state space,

$$\begin{bmatrix} \dot{\delta} \\ \Delta\dot{\omega} \end{bmatrix} = \begin{bmatrix} 0 & \omega_0 \\ -\frac{K}{M} & -\frac{D}{M} \end{bmatrix} \begin{bmatrix} \delta \\ \Delta\omega \end{bmatrix} \tag{2. 15}$$

where $\omega_0 = 2\pi f_0$ is rated speed in electrical rad/s,

The eigenvalues of the state matrix in (2.15) were derived [1],

$$\lambda_{1,2} = -\frac{D}{2M} \pm j\sqrt{\frac{K}{M} - (\frac{D}{2M})^2} \tag{2. 16}$$

Thus the real part and imaginary part can be represented as,

$$\sigma = -\frac{D}{2M}, \omega = \sqrt{\frac{K}{M} - (\frac{D}{2M})^2} \quad (2.17)$$

K is the synchronising torque coefficient given by,

$$K = \frac{EE_B}{X_T} cos\delta_0 \quad (2.18)$$

E and E_B are generator end voltage and infinite bus voltage respectively; X_T is the line reactance; δ_0 is the voltage angle difference between generator bus and infinite bus.

The natural undamped frequency is

$$\omega_n = \sqrt{K\frac{\omega_0}{M}} \quad (2.19)$$

and the damping ratio is

$$\zeta = \frac{D}{2\sqrt{KM\omega_0}} \quad (2.20)$$

From (2.19) and (2.20), it can be seen that as K increases, the natural frequency increases whilst the damping ratio decreases. The damping ratio increases due to the increase of damping coefficient. An increase in inertia constant decreases both natural frequency and damping ratio.

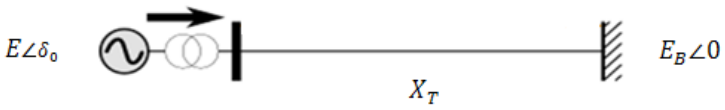

Figure 2. 4 Single-machine infinite bus system

2.5.2 Sixth-Order Model

The sixth-order model in state space form is given,

$$\dot{x} = Ax \quad (2.21)$$

where $x = \left[\delta, \Delta\omega, E'_q, E'_d, E''_q, E''_d\right]^T$, and state matrix,

$$A = \begin{bmatrix} 0 & \omega_0 & 0 & 0 & 0 & 0 \\ -\frac{K_s}{M} & -\frac{D}{M} & 0 & 0 & K_{1sq} & K_{1sd} \\ K_{1\delta} & 0 & -(T'_{do})^{-1} & 0 & K_{2sq} & K_{2sd} \\ K_{2\delta} & 0 & 0 & -\left(T'_{qo}\right)^{-1} & K_{3sq} & K_{3sd} \\ K_{3\delta} & 0 & -(T''_{do})^{-1} & 0 & K_{4sq} & K_{4sd} \\ K_{4\delta} & 0 & 0 & \left(T''_{qo}\right)^{-1} & K_{5sq} & K_{5sd} \end{bmatrix} \quad (2.\ 22)$$

The notations in the above matrix are defined as,

$$K_{1\delta} = (T'_{do})^{-1}\Delta X'_d \frac{\partial I_d}{\partial \delta} \quad (2.\ 23)$$

$$K_{2\delta} = (T'_{qo})^{-1}\Delta X'_q \frac{\partial I_q}{\partial \delta} \quad (2.\ 24)$$

$$K_{3\delta} = (T''_{do})^{-1}\Delta X''_d \frac{\partial I_d}{\partial \delta} \quad (2.\ 25)$$

$$K_{4\delta} = (T''_{qo})^{-1}\Delta X''_q \frac{\partial I_q}{\partial \delta} \quad (2.\ 26)$$

$$K_{1sq} = -M^{-1}\frac{\partial P}{\partial E''_q} \quad (2.\ 27)$$

$$K_{2sq} = (T'_{do})^{-1}\Delta X'_d \frac{\partial I_d}{\partial E''_q} \quad (2.\ 28)$$

$$K_{3sq} = (T'_{qo})^{-1}\Delta X'_q \frac{\partial I_q}{\partial E''_q} \quad (2.\ 29)$$

$$K_{4sq} = (T''_{do})^{-1}(\Delta X''_d \frac{\partial I_d}{\partial E''_q} - 1) \quad (2.\ 30)$$

$$K_{5sq} = -(T''_{qo})^{-1}\Delta X''_q \frac{\partial I_q}{\partial E''_q} \quad (2.\ 31)$$

$$K_{1sd} = -M^{-1}\frac{\partial P}{\partial E''_d} \quad (2.\ 32)$$

$$K_{2sd} = (T'_{do})^{-1}\Delta X'_d \frac{\partial I_d}{\partial E''_d} \quad (2.\ 33)$$

$$K_{3sd} = (T'_{qo})^{-1}\Delta X'_q \frac{\partial I_q}{\partial E''_d} \quad (2.\ 34)$$

$$K_{4sd} = (T''_{do})^{-1}\Delta X''_d \frac{\partial I_d}{\partial E''_d} \quad (2.\ 35)$$

$$K_{5sd} = -\left(T''_{qo}\right)^{-1}(\Delta X''_q \frac{\partial I_q}{\partial E''_d} + 1) \quad (2.\ 36)$$

where E'_q and E'_d are transient emfs behind the transient reactances X'_q and X'_d;

E_q'' and E_d'' are subtransient emfs behind the transient reactances X_q'' and X_d'';

$I_q$and $I_d$are current in q-axis and d-axis armature circuit;

T_{qo}' is the q-axis transient open-circuit time constant;

T_{do}' is the d-axis transient open-circuit time constant;

T_{qo}'' is the q-axis subtransient open-circuit time constant;

T_{do}'' is the d-axis subtransient open-circuit time constant.

2.6 Multi-Machine Power System Models

Based on (2.15), a multi-machine system is presented in (2.37) using classical synchronous generator model,

$$\begin{bmatrix} \dot{\delta}_1 \\ \Delta\dot{\omega}_1 \\ \vdots \\ \dot{\delta}_i \\ \Delta\dot{\omega}_i \\ \vdots \\ \dot{\delta}_n \\ \Delta\dot{\omega}_n \end{bmatrix} = \begin{bmatrix} 0 & \omega_0 & \cdots & 0 & 0 & \cdots & 0 & 0 \\ -\frac{K_{11}}{M_1} & -\frac{D_1}{M_1} & \cdots & -\frac{K_{1i}}{M_1} & 0 & \cdots & -\frac{K_{1n}}{M_1} & 0 \\ \vdots & \vdots & \vdots & \vdots & \vdots & \vdots & \vdots & \vdots \\ 0 & 0 & \cdots & 0 & \omega_0 & \cdots & 0 & 0 \\ -\frac{K_{i1}}{M_i} & 0 & \cdots & -\frac{K_{ii}}{M_i} & -\frac{D_i}{M_i} & \cdots & -\frac{K_{in}}{M_i} & 0 \\ \vdots & \vdots & \vdots & \vdots & \vdots & \vdots & \vdots & \vdots \\ 0 & 0 & \cdots & 0 & 0 & \cdots & 0 & \omega_0 \\ -\frac{K_{n1}}{M_n} & 0 & \cdots & -\frac{K_{ni}}{M_n} & 0 & \cdots & -\frac{K_{nn}}{M_n} & -\frac{D_n}{M_n} \end{bmatrix} \begin{bmatrix} \delta_1 \\ \Delta\omega_1 \\ \vdots \\ \delta_i \\ \Delta\omega_i \\ \vdots \\ \delta_n \\ \Delta\omega_n \end{bmatrix} \quad (2.37)$$

The multi-machine system can be also represented by sixth-order generator model, but this will not be presented within this thesis.

2.7 Power System Oscillations

The oscillatory modes can be classified by frequency ranges and oscillation source [3].

- Inter-area modes: 0.1-0.7 Hz. A group of generators located in different coherent area are involved.

- Local modes: 0.7-2.0 Hz. One or more generators located in the same coherent area are involved.
- Control modes: 0.1- 50Hz. This mode is caused by control devices, such as speed governor, AVR, HVDC converters, SVC and etc..

Inter-area modes are of particular concern, since they indicate that oscillations are not caused by high loading of a particular generator or generators, but a certain power flow pattern in tie-lines connecting two areas [3]. Factors that can influence inter-area oscillations are discussed extensively in [5] and categorised as:

- System structure
- Operation conditions
- Excitation systems
- System loads
- DC links

2.8 Power System Dynamics Analysis

Generally, power system analysis methods include model-based methods and measurement-based methods.

2.8.1 Measurement-Based Methods

The measurement-based methods are prevailing after WAMS are widely installed in power systems. The main advantage of these methods are no prior information is required on the power system and all analysis are based on the measurements gathered by the WAMS. Neglecting the system model, measurement-based methods focus on first-hand information captured by the measuring devices, and implements signal processing techniques and intelligent identification to detect the sources of problems. However, these methods give rise to a number of problems:

- System physics is not provided. Rather than detecting problems through investigating physical systems, these methods analyse system conditions directly through sensor data.
- Accurate data measurement are required. Large measurement errors restrict decision making. Cyber attacks may also reduce the reliability of using measurement-based methods.
- A large amount of data is needed for statistical analysis. However, in practice, the lack of system information is common.
- Full system condition cannot be described by incomplete system data.

2.8.2 Model-Based Methods

Model-based methods aim to reveal the system's natural characteristics though the construction of an equivalent model. As interconnection of large modern power systems increases, it becomes very time-consuming to model each individual electrical element. Computer programs have been developed to aid the research on large power systems. However, difficulties still exist in computational analysis due to the complexity of system.

Power system model equivalencing methods are widely used to approximate unknown network models. The necessity to construct equivalent large interconnected power systems has been extensively explained in [1]. As a mature technique, the methodology of dynamic equivalencing has been comprehensively discussed in [1] and [4]. To derive power system dynamic equivalents, generally, methods can be classified into two categories:

- Modal-based dynamic equivalents: This method derives external network equivalents using modal analysis.
- Coherency-based dynamic equivalents: Dynamic aggregation of generator components, control devices and buses is proposed in this method by using transient stability analysis.

The limitation of conventional model-based approaches are as follows:

- Model validation is required -Parameter tuning is compulsory based on off-line analysis, which means real-time and/or near-real-time analysis for online studies cannot be conducted.
- Rather than small signal analysis, equivalents are developed for transient analysis. These can be only developed when a large disturbance is applied to excite certain modes in the system.
- Detailed and accurate prior knowledge on modal data and rotor angle is essential for coherency-based equivalencing -This prior knowledge may be out of date and cannot represent current system configuration.
- Equal or nearly equal eigenvalues are not cannot be differentiated in conventional modal-based methods [6].
- Simplified model equivalents are produced -As a consequence of simplicity, problems associated with real complex power system may not be detected.

2.9 Conclusions and Discussions

This chapter introduced the fundamental definitions of power system dynamics, stability and modelling. Measurement-based and model-based techniques are well established for power system analysis and stability management. However, the existing techniques have significant limits in dealing with practical problems.

This thesis aims to investigate a novel method which can circumvent the proposed difficulties and is more practically applicable.

Chapter 3 Power Dynamics Extraction

3.1 Introduction

Power system oscillations are observed relatively easily through the measurement of power flow, voltage angles and system frequency within certain time frame, using existing measuring devices. However, oscillatory modes information such as modal frequencies, damping and mode shapes cannot be captured directly. These information are of paramount importance to indicate power system stress [7]. Modal data thus provides critical information to make control decisions and operate power systems.

Power Dynamics Extraction (PDX) techniques were developed to extract information on the power system oscillations through the use of real-time or field test measurements. Typical measurement data can be divided into three types [8], ringdown algorithms, ambient-signal algorithms and probing-signal algorithms. It should be noted that the former two are the most commonly used methods. Probing-signal is difficult to generate. Experiments have designed to achieve useful measurements to estimate using the probing-signal method. [9] and [10] described the two methods which utilises probing signal for the mode estimation. Both ringdown approaches and ambient-signal approaches will be discussed later in this chapter due to the lack of feasibility of practical application.

3.2 Ringdown Techniques

Ringdown techniques utilises ringdown signals generated from large system disturbance. These techniques are normally performed to estimate modal data after a system event when ringdown signal is available. However, it does not provide the feasibility to conduct continuous modal estimation.

3.2.1 Prony Method

Prony method [11-15] is a technique widely used to extract modal information directly from a given signal. It was developed centuries ago, but the practical use occurred with the birth of digital computer. It has been employed to estimate the modal information of power system oscillations from ringdown signals. It aims to fit a linear combination of exponential terms to a measured signal which consists of equally spaced samples. For a signal with N evenly spaced samples, Prony method fits a function shown in (3.1) to the observed signal $y(t)$ in a least squares sense [16]. This method allows the identification of low order linear system [17, 18].

$$y(t) = \sum_{i=1}^{n} A_i e^{\lambda_i t} \tag{3. 1}$$

where A_i is the signal residue associated with the mode λ_i, and n is the number of desired modes.

(3.1) can be written in the discrete form if the signal y is sampled at a constant time period,

$$y(k) = \sum_{i=1}^{n} A_i z_i^k \tag{3. 2}$$

where is $z_i = e^{\lambda_i t}$ represents the z-transform operator.

(3.2) is then expanded as (3.3) for N data samples,

$$\begin{bmatrix} y(0) \\ y(1) \\ \vdots \\ y(N-1) \end{bmatrix} = \begin{bmatrix} 1 & 1 & \cdots & 1 \\ z_1 & z_2 & \cdots & z_n \\ \cdots & \cdots & \cdots & \cdots \\ z_1^{N-1} & z_2^{N-1} & \cdots & z_n^{N-1} \end{bmatrix} \begin{bmatrix} A_1 \\ A_2 \\ \vdots \\ A_n \end{bmatrix} \tag{3. 3}$$

As a necessary condition, z satisfies (3.4),

$$z^n - (a_1 z^{n-1} + a_2 z^{n-2} + \cdots + a_n z^0) = 0 \tag{3. 4}$$

where $a = [a_1, a_2, \cdots a_n]$ is a set of unknown coefficients,

(3.5) can be achieved if a left vector, $[0, -a_n, -a_{n-1}, \cdots, -a_1, 1, 0, \ldots 0]$, is left multiplied to (3.3),

$$\begin{bmatrix} y(n) \\ y(n+1) \\ \vdots \\ y(N-1) \end{bmatrix} = \begin{bmatrix} y(n-1) & y(n-2) & \cdots & y(0) \\ y(n) & y(n-1) & \cdots & y(1) \\ \cdots & \cdots & \cdots & \cdots \\ y(N-2) & y(N-3) & \cdots & y(N-n-1) \end{bmatrix} \begin{bmatrix} a_1 \\ a_2 \\ \vdots \\ a_n \end{bmatrix} \quad (3.5)$$

Then, the set of unknown coefficients can be obtained by solving (3.5). z_i and $A_i$can also be determined by solving (3.4) and (3.3) respectively.

Conventional Prony method is a signal identification approach that is not suitable for transfer functions estimation. Transfer functions are necessary for control design and mode shape estimation. Prony method is further extended to transfer function analysis [19-23]. The general idea is to extend Prony analysis by analysing multiple signals simultaneously to improve the accuracy of modal estimates.

Other identification techniques similar to Prony method were also used in the estimation of modal content. Matrix Minimal Realisation (MMR) was employed to identify modal data in transient simulation [24, 25]. MMR method is very similar to Prony method. The Hankle matrix in MMR [24] is almost identical to the linear prediction matrix in Prony method [19]. [16] addressed the similarity between Eigenvalue Realisation Algorithm (ERA) [26].

3.2.2 Matrix Pencil Method

Matrix Pencil (MP) method introduced in [27, 28] extracts modal data z_i from a given signal $y(t)$ is. The method defines two matrices,

$$Y_1 = \begin{bmatrix} x(0) & x(1) & \cdots & x(L-1) \\ x(1) & x(2) & \cdots & x(L) \\ \vdots & \vdots & & \vdots \\ x(N-L-1) & x(N-L) & \cdots & x(N-2) \end{bmatrix} \quad (3.6)$$

$$Y_2 = \begin{bmatrix} x(1) & x(2) & \cdots & x(L) \\ x(2) & x(3) & \cdots & x(L+1) \\ \vdots & \vdots & & \vdots \\ x(N-L) & x(N-L+1) & \cdots & x(N-1) \end{bmatrix} \quad (3.7)$$

where L is the pencil parameter [29].

Y_1 and Y_2 then can be rewritten as,

$$Y_1 = Z_1 A Z_2 \tag{3. 8}$$

$$Y_2 = Z_1 A Z_0 Z_2 \tag{3. 9}$$

where,

$$Z_1 = \begin{bmatrix} 1 & 1 & \cdots & 1 \\ z_1 & z_2 & \cdots & z_n \\ \vdots & \vdots & & \vdots \\ z_1^{(N-L-1)} & z_2^{(N-L-1)} & \cdots & z_n^{(N-L-1)} \end{bmatrix} \tag{3. 10}$$

$$Z_2 = \begin{bmatrix} 1 & z_1 & \cdots & z_1^{(L-1)} \\ 1 & z_2 & \cdots & z_2^{(L-1)} \\ \vdots & \vdots & & \vdots \\ 1 & z_n & \cdots & z_n^{(L-1)} \end{bmatrix} \tag{3. 11}$$

$$Z_0 = diag[z_1, z_2, \dots, z_n] \tag{3. 12}$$

$$A = diag[A_1, A_2, \dots, A_n] \tag{3. 13}$$

The matrix pencil is defined as,

$$Y_2 - \lambda Y_2 = Z_1 A (Z_0 - \lambda I) Z_2 \tag{3. 14}$$

where I is identity matrix.

Matrix Y contains the actual measured data with noise is defined in (3.15). The eigenvalues can be extracted from the roots of this matrix. Significant modes can be determined by applying Singular Value Decomposition (SVD) to Y. The roots of (3.15) can then be found as the generalised eigenvalues of the matrix pair $[Y_2 : Y_1]$.

$$Y = \begin{bmatrix} y(0) & y(1) & \cdots & y(L) \\ y(1) & y(2) & \cdots & y(L+1) \\ \vdots & \vdots & & \vdots \\ y(N-L-1) & y(N-L) & \cdots & y(N-1) \end{bmatrix} \tag{3. 15}$$

3.2.3 Hankel Total Least Square Method

Hankel Total Least Square (HTLS) method is applied to extract modal data [30]. The Hankel matrix is factorised by a noise-free signal as shown(3.2),

$$H = SRT^T \tag{3. 16}$$

where S and T are Vandermone matrices defined in [30].

The following relationship can be found by applying SVD to the Hankel matrix,

$$H = U\Sigma V^H \tag{3. 17}$$

where the superscript H denotes the operator, complex conjugate transpose.

Total least square method is then utilised to solve for the eigenvalues. The same method is used to determine the residues A_i as that in Prony method.

[30] also executed a comparison study between Prony method, MP method and HTLS method to estimate modal data. The simulation results indicated that all three methods had similar accuracy when estimating modal frequency, while MP and HTLS performed better at the identification of modal damping.

3.3 Ambient-Signal Techniques

Ambient-signal-based mode estimation can be carried out in both time domain and frequency domain. Time domain estimation methods operate directly on the data samples, while power spectral density has to be calculated for frequency domain estimation [7].

Estimation methods are divided into two categories in [7]:

- Block processing methods:

  Block processing method estimates modes from data framed by a time window. The estimates are updated for each new window of data.

- Recursive methods:

The recursive estimation methods are updated for every new sample of data. The new estimates are based on previous mode estimates and new data sample. A forgetting factor is introduced to enable current data to have a greater weight than previous.

3.3.1 Yule-Walker Method

Yule-Walker (YW) method was first implemented in block processing [31] to estimate system modes using an Autoregressive (AR) model. An AR model is defined as,

$$x_{i+1} = \phi_1 x_i + \phi_2 x_{i-1} + \cdots + \phi_p x_{i-p+1} + e_{i+1} \tag{3. 18}$$

Consider a lag of 'k' by multiplying x_{i-k+1} to the two sides of (3.18),

$$x_{i-k+1} x_{i+1} = \sum_{j=1}^{p} (\phi_j x_{i-k+1} x_{i-j+1}) + x_{i-k+1} e_{i+1} \tag{3. 19}$$

The following can be achieved by taking the expectance of (3.19),

$$\langle x_{i-k+1} x_{i+1} \rangle = \sum_{j=1}^{p} (\phi_j \langle x_{i-k+1} x_{i-j+1} \rangle) \tag{3. 20}$$

Given in [31], the estimated autocorrelation matrix is,

$$R = \begin{bmatrix} r(0) & r(1) & \dots & r(p-1) \\ r(1) & r(2) & \dots & r(p-2) \\ \vdots & \vdots & & \vdots \\ r(p-1) & r(p-2) & \dots & r(0) \end{bmatrix} \tag{3. 21}$$

The estimated correlation vector is,

$$r = [r(1), r(2), \dots, r(p)]^T \tag{3. 22}$$

Thus, the relationship shown in (3.23) can be formed,

$$R\Phi = r \tag{3. 23}$$

where $\Phi = \left[\phi_1, \phi_2, \dots, \phi_p\right]^T$

Defining,

$$\Phi(z) = 1 + \phi_1 z^{-1} + \phi_2 z^{-2} + \cdots + \phi_p z^{-p} \tag{3. 24}$$

After the roots of (3.24) has being determined, the modes can then be found.

The Modified Yule-Walker (MYW) method was used to estimate an Autoregressive Moving Average (ARMA) model in [32]. In [33], YW was extended to multiple signals.

3.3.2 Subspace Method

Subspace identification methods have also been implemented in online estimation of eletromechanical modes using ambient signals, such as Canonical Variate Algorithm (CVA) [34] and Subspace State Space System Identification (N4SID) [9].

Subspace method is applied to a discrete stochastic state-space model as shown in (3.25) and (3.26),

$$\Delta x_{k+1} = A\Delta x_k + w_k \tag{3. 25}$$

$$\Delta y_k = C\Delta x_k + v_k \tag{3. 26}$$

where Δx_{k+1} is the discrete time state vector; $\Delta y_k$is the output vector; w_k and v_k are white noise.

The method suggested the inclusion of the outputs in a Hankel matrix as two subspaces, 'past' and 'future'. The method aims to determine the state matrix A in (3.25) and thus the eigenvalues (modes).

Based on subspace method, [35] the combined Two-Sided Arnoldi (TSA) method and Sensitive Pole Algorithm (SPA) can be used to evaluate sensitive eigenvalues in large power systems. The proposed TSA-SPA method aims to compute sensitive modes to control parameters. Rather than focusing on the whole complex plane, it reduces the computational burden considerably by only concentrating on a particular region of interest, providing more flexibility in stability analysis.

A revised subspace method was proposed in [36]. The proposed method reduces the computation complexity through the introduction of reference channels into the conventional subspace method. Mode shapes can also be assessed along with modal frequencies and damping.

3.3.3 Recursive Methods

As stated, recursive methods implements both new data sample and previous estimation to calculate new estimates. The recursion method has been addressed in many publications for parameter estimation, and is commonly applied to modal data estimation. The advantages of

recursive methods is that it can include the prior knowledge of the unknown modes into the estimation, and the impacts of missing or inaccurate raw data can be reduced.

[37] introduces a recursive Least-Mean Square (LMS) method to estimate electromechanical modes using real-time measured ambient signals. A whitening filter was developed based LMS method and the dominant modes of the whitening filter correspond to the dominant modes of the power system. The following relationship was established in [37] ,

$$y(n) = w^H(n)u(n-1) \tag{3. 27}$$

$$e(n) = u(n) - y(n) \tag{3. 28}$$

$$w(n+1) = w(n) + \mu u(n-1)e(n) \tag{3. 29}$$

where $y(n)$ is the filter output and $u(n)$ is the power system data; $w(n)$ is a vector contains time-varying filter weights; $e(n)$ is the output of the white noise filter; μ is the step-size parameter.

Then, $w(n)$ was obtained from the LMS process, it can then be used to determine the modes of the input data $u(n)$.

A Robust Recursive Least Square (RRLS) is proposed in [38]. It was advocated that RRLS method can identify modes from both ambient signals and ringdown signals with outliers and missing data without noticeable degradation in performance. This method was then extended to Regularised Robust Recursive Least Squares (R3LS) [8] which was used to identify the Autoregressive Moving Average Exogenous (ARMAX) model.

[39] developed a novel method for electromechanical mode identification. The concept uses an ARMAX model to represent a linearised power system model which is normally written in the form of state-space. The state-space was first converted to transfer function, and then to a multichannel

ARMAX. The ARMAX model characterises modes and mode shapes of the system. The Two-stage Least Squares method is used to demonstrate this concept in [39].

A significant improvement was made in [40] through the estimation of both modal data and their variance. The proposed Recursive Maximum Likelihood (RML) method was used due to the fact that it provides both the recursive estimates of the electromechanical modes and the covariance matrix of the polynomial coefficients of an AR model. The variance of the estimates is important as it provides a wider picture of the estimation results, thus estimates can be used in a better sense.

Combined with recursion, a Recursive Adaptive Stochastic Subspace Identification (RASSI) method was developed in [41] to identify electromechanical modes using ambient data. This method originated from civil engineering, and have proved to be a powerful estimation method. In [41], it was shown that the proposed method provides an accurate estimates of electromechanical modes. The recursive version also enables real-time implementation.

[42] presents a Recursive Least Squares algorithm based on the Inverse QR Decomposition (IQRD-RLS) with an exact initialisation procedure. The method estimates electromechanical modes using ambient signals. It was also compared with LSM algorithm. Unlike LSM, IQRD-RLS method is independent of the selection of an initial weights vector through the addition of an exact initialisation procedure.

3.3.4 Hilbert Transform Method

[43-45] introduces modal identification techniques based on Hilbert Transform (HT) [46] and Empirical Mode Decomposition (EMD) [47]. The HT $H(u(t))$ of a signal $u(t)$ is defined as,

$$H\big(u(t)\big) = \frac{1}{\pi t} * u(t) = \frac{1}{\pi}\int_{-\infty}^{\infty} \frac{u(\tau)}{t-\tau} d\tau = \frac{1}{\pi}\int_{-\infty}^{\infty} \frac{u(t-\tau)}{\tau} d\tau \qquad (3.30)$$

The HT of $u(t)$ is the convolution of $u(t)$ with the signal $1/\pi t$. It can be seen that HT is the response to $u(t)$ of a linear time-invariant filter having impulse response $1/\pi t$. Further, the HT was properly defined as the Cauchy principle value of the integral in (3.31),

$$H\big(u(t)\big) = \frac{1}{\pi}\lim_{\epsilon\to 0+}\left(\int_{t-\frac{1}{\epsilon}}^{t-\epsilon}\frac{u(\tau)}{t-\tau}d\tau + \int_{t+\epsilon}^{t+1/\epsilon}\frac{u(\tau)}{t-\tau}d\tau\right) \quad (3.31)$$

HT is normally combined with EMD (known as Hilbert-Huang transform) to identify modal content. For a given oscillatory signal $z(t)$, EMD technique decomposes the time series into Intrinsic Mode Function components using temporal and structural characteristics of the data [44]. The decomposition is shown in (3.32),

$$z(t) = \sum_{j=1}^{n} c_j(t) + r_n(t) \quad (3.32)$$

where n is the number of IMF components, and $r_n(t)$ is the residue of the signal.

[48] presents a method based on EMD and Orthogonal Decomposition (OD) to extract dynamic information from Wide-Area Measurements (WAM). The technique valuably contributes to the determination of phase relationships between dominant modes and the identification of dynamic trends.

Signals captured by Wide Area Measurement Systems (WAMS) is processed by Hilbert domain analysis. Comparison with Prony method was made in [49]. It was found that the two methods generates a similar accuracy. Since Prony method assumes a stationary signal, whereas the Hilbert Transform and EMD are able to identify non-stationary and nonlinear signal. It was suggested that the two methods could be used in a complementary fashion [49].

3.4 Other Methods

[50] introduces an offline method, Associate Hermite Expansion (AHE) method. It allows the estimation of oscillatory system performance by fitting an orthogonal polynomial expansion to

ringdown data. The spectrum of the data was extrapolated for the identification of the electromechanical modes. A sliding window technique combined with a linear prediction algorithm was developed to assess the damping of each mode. The method was then compared against the least square Prony method and the YW method. From the simulation results, it can be seen that the performance of the three methods under single-mode test condition are similar. However, AHE method and Prony method displayed high precision in mode estimation under multiple-mode test condition. AHE method also has superior performance in the presence of white noise. [51] also examined the performance of five mode estimators, including Prony method, YW method, Fast Fourier Transform (FFT) method, HT method and AHE method under identical test conditions. The results showed that Prony method has great advantages in resolving modal frequency, which is hard to be accomplished by using the other methods. With the presence of white noise, the AHE method performs much better than the other estimation methods in low signal-to-noise relationship (SNR). It should be noted that HT, FFT and YW have relatively stable performance when SNR varies, whilst the performance of the Prony method becomes less robust due to moving SNR.

3.5 Conclusions

In this chapter, two types of techniques were introduced, ringdown signal techniques and ambient-signal techniques. The former identify electromechanical modes based on measured ringdown signals during a system event, while the latter can extract modal information continuously from real-time online measurements. Prony analysis is most representative and commonly used method among ringdown techniques. Many new techniques uses ringdown signals based on Prony analysis. Various approaches have been developed using ambient-signals in both time-domain and frequency domain. In some comparison studies, recursive methods shows its advantages on fast converging and estimation accuracy.

Chapter 4 Dynamic Equivalent

4.1 Introduction

Normally, with accurate internal network information, greater interests lie upon understanding the external network. The internal network is defined as the network modelled in detail, whilst the external network is represented by a simplified model. This is due to the fact that the information of external network is very limited. Thus, modelling external network in great details is not feasible.

There is a wide diversity in external network representation [52]. Two main types of methods to derive external network equivalents are introduced in [1], model reduction methods and measurement-based methods. Recently, Artificial Intelligence (AI) techniques, such as Generic Algorithm (GA) and Neural Networks (NN) were also introduced to solve identification problems.

Model reduction methods require prior knowledge of the system. These methods are usually applied in offline studies. One of the drawbacks of the equivalent model which is derived from these methods is that the real-time system dynamic characteristics under various operational conditions cannot be revealed. Thus, the equivalent is a static model.

Today, online Dynamic Security Assessment (DSA) becomes more prevalent in utility control centres [52]. DSA on modern power systems is required to be real time or near-real-time, thus dynamic equivalents are highly desirable to meet such requirement.

4.2 Model Reduction Methods

Conventionally, mathematical modelling of dynamic equivalents of large electrical power system was widely adopted in power system analysis, especially for stability purposes. Modal-based methods and aggregation methods are the two means to produce valid static equivalents. The target of modal-based methods is to derive an equivalent that can reflect the modes of interest. Aggregation methods, also known as coherency-based methods, aim to eliminate or aggregate model nodes to reduce the size of the model. The foundation of model reduction methods are discussed

comprehensively in [1, 53]. The methods were highly dependent on existing constituent system parameters which may be out of date.

Three types of power system simulation equivalents were mentioned in [54] for different study purposes. High-frequency equivalents (HFE) were derived to simulate high-frequency transients, such as lightning, switching overvoltage and the effects of power electronics devices on power system behaviour. In HFE models, the generators in the external network are modelled as power frequency voltage sources which eliminate low-frequency behaviour from the model. Low-frequency equivalents (LFE) are developed for low-frequency electromechanical oscillation studies. In LFE, the generators can be modelled without stator winding transients and the transmission lines can be modelled as constant impedances. Wideband Equivalents (WE) are designed for investigating subsynchronous oscillations. In WE, turbine-generator dynamics and network transients must be modelled properly.

4.2.1 Modal-based Method

[55] and [6] specified the technical details to model dynamic equivalents using modal-based dynamic equivalents approach. The dynamic equivalents are achieved by neglecting the fast decaying and high frequency eigenvalues from the diagonalised linear external network model. In this approach, a large interconnected power system is divided into three parts, shown in Figure 4.1. The surroundings of the internal network are named as external network which is the key part for an equivalent model. Beyond the external network, the remainder is represented by a few equivalent generators with highly simplified model.

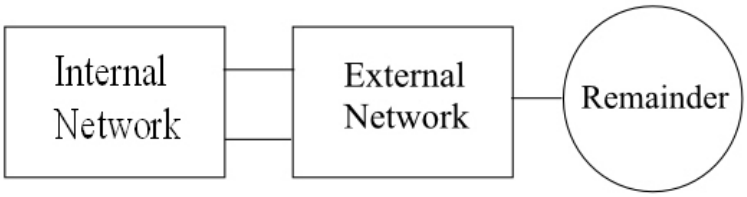

Figure 4. 1 Network separation for eigenvalue-based method

This approach focused on constructing an electro-mechanical equivalent through eigenvalue analysis method. The steps are:

1) Describe the external system by high-order nonlinear differential equations.
2) Conduct linearization to nonlinear external network model.
3) Diagonalise the linearised system model
4) Neglect the fast decaying and high frequency modes.

The method was tested on the Northeast Power Coordinating Council (NPCC) system [56]. It was also addressed in [56] that the reference machine in the external network for the linearization process must be chosen properly.

Selective Modal Analysis (SMA) offers a systematic framework to understand, simplify and analyse complex linear time-invariant models of a dynamic system [57, 58]. The SMA demonstrates a linear system reduction approach based on selected modes. The reduced order model can adequately reflect the selected modes. The steps for SMA are summarised as,

1) Separate the states associated with the selected modes from the least relevant states. The state space form of a linear system in (2.21) can be rewritten as,

$$\begin{bmatrix} \dot{r} \\ \dot{a} \end{bmatrix} = \begin{bmatrix} A_{11} & A_{12} \\ A_{21} & A_{22} \end{bmatrix} \begin{bmatrix} r \\ a \end{bmatrix} \quad (4.1)$$

   where r are the relevant states and a are the irrelevant states.

2) A transformation matrix needs to be determined at this step to reflect the changes of neglecting irrelevant states.

It was advocated that the reduced model could always retain the physical properties of the selected modes. SMA was also proved to be an effective approach to the control design of moderate size system [59].

4.2.2 Coherency-Based Method

Coherency-based methods are well established methods widely used in power system studies to model external equivalents [60, 61]. This method is based on coherency of swinging generators [1, 62-65]. The identification of coherency has been extensively illustrated in the literature. The procedures are:

1) Identify coherent groups
2) Aggregate generator terminal buses and eliminate load buses.
3) Aggregate coherent generator models and controls.

The dynamic aggregation includes the following,

- Equivalent bus: The generators in the same coherent group are connected to an equivalent bus through transformers that can match their terminal voltages and angles with those of the equivalent bus. The transformer ratio is complex and can be defined as,

$$a_j = \frac{V_j}{V_t} \tag{4. 2}$$

  Where V_j and V_t are the voltage phasors of the generator and the equivalent bus respectively. The equivalent bus voltage is chosen from the voltage of any individual bus or the average values of the coherent group in [4].

- Generating units: The aggregation of rotor dynamics is based on the identical speed of generators in the same coherent group. It can be represented as,

$$\sum_j M\,\dot{\omega} = \sum_j P_{mj} - \sum_j P_{ej} - \sum_j D_j\omega \tag{4. 3}$$

  It should be noted that the MVA and kV bases should be the same for each machine.

  The aggregation of the equivalent's transient reactance and time constant are clearly defined in [66].

- Turbine governor: The equations of turbine governors in a coherent group is represented as,

$$P_{mj}(s) = G_j(s)\Delta\omega(s) \tag{4. 4}$$

Then, the aggregated equation can be written as,

$$\sum_j P_{mj}(s) = \sum_j G_j(s)\,\Delta\omega(s) \tag{4. 5}$$

Least-square-error curve-fitting technique is used to identify unknown parameters in [4].

- Excitation systems: Similar technique is applied to aggregate excitation systems. The excitation system of individual machine can be represented as,

$$e_j(s) = G_{Ej}(s)\Delta v_t(s) \tag{4. 6}$$

Thus, the equivalent transfer function is thus written as,

$$G_E(s) = \frac{e(s)}{\Delta v_t(s)} = \sum_j W_j(s) G_{Ej}(s) \tag{4. 7}$$

where $G_{Ej}(s)$ represents the transfer function of the excitation system of each machine, $G_E(s)$ is the transfer function of the excitation system of the equivalent,

$e_j(s)$ is the field voltage of each machine,

$e(s)$ is the equivalent field voltage,

$\Delta v_t(s)$ is the equivalent terminal voltage,

Weighting factor $W_j(s)$ is introduced in [63].

It is noted that the high wind energy penetration has significantly impacted on the dynamic properties of the power system. Coherency-based methods are also widely implemented in the aggregation of large scale wind farms. The study of the effects are normally performed by the aggregation of individual wind generator in a large wind farm. Aggregation of a wind farm into one or more wind generators is a prevailing technique. [67] compares the representation of a single and multiple wind generator through transient stability analysis. [68-71] specifies the methods of wind farms aggregation with fixed-speed wind turbines. It is discussed in [72] the accuracy of the reduced order of the Doubly-Fed Induction Generator (DFIG) models under different operating conditions.

A modal-coherency technique based on Modal Tree Algorithm (MTA) was presented in [73]. The system modes were mapped onto a tree diagram according to the number of machines involved as shown in Figure 4.2. The number of machines in the modal tree confirm with the rule $N > M > K$.

It was advised that the modes which involved the machines within the study area should be retained. The MTA provides a direct guidance on dividing coherent groups and model reduction. However, it is difficult to find out the machines related to a particular mode in a large power system. Moreover, full system eigenvalues and eigenvectors were required to derive the modal tree, is a major obstacle for practical application.

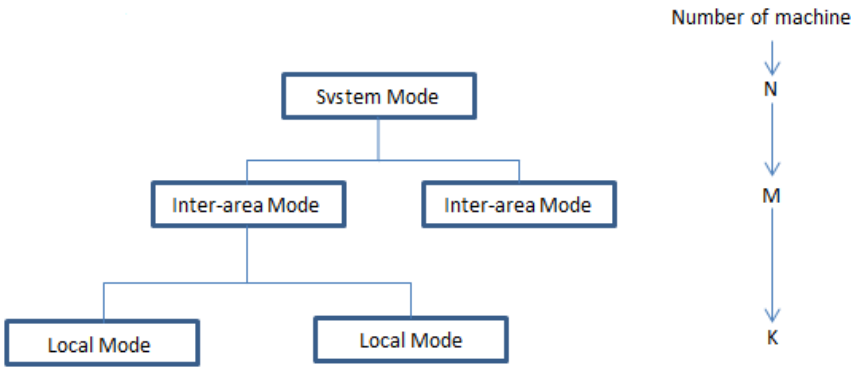

Figure 4. 2 Modal Tree Algorithm

4.3 Measurement-Based Equivalent

[74] illustrated a dynamic equivalent method based on direct measurements from Phasor Measurement Unit (PMU), such as voltage phasors and current phasors. The principles are shown in Figure 4.3. Rather than to execute model reduction to coherent groups, this method simplifies groups of generators connected by transfer paths. The generators in the same group are represented by a single classical generator model without damping coefficient. Line reactance and generator inertia constants can be estimated through physical relationship between measurements and these parameters. It was addressed in the literature that a minimum of three PMUs must be installed, two at the terminal buses and the other one is located at the transfer path between the terminals.

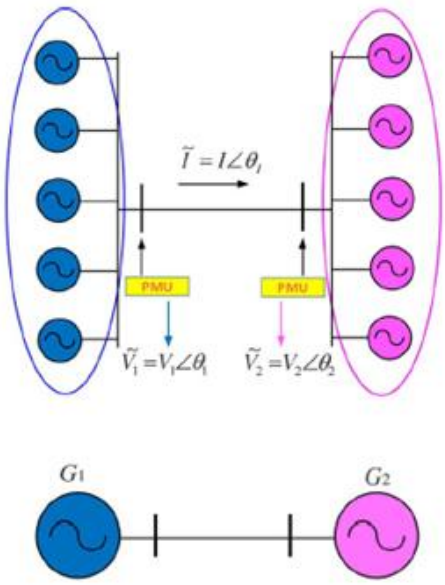

Figure 4. 3 Dynamic equivalent based on direct measurement method [74]

The solution to measurement noise was also discussed separately in [74]. Cramer-Rao bounds (CRB) suggested that this was to be incorporated within the problem description. It was found that the estimation error depends on the location of the PMU on the transfer path. Therefore, the problem is to find the optimal location such that the estimation error is minimised.

This approach aggregates system model without referring to parameters of individual generator. However, it has high requirements for PMU locations. Corresponding inter-area modes have to be excited and captured in order to provide necessary information. The equivalent model is represented by a significantly simplified network topology and generator model. The dynamic characteristics cannot be reflected adequately.

[75] and [76] introduced a voltage and frequency measurements based method to identify the equivalent for a distribution network. Due to increasing penetration of renewable generation although their size are much smaller in comparison to conventional generation, the impact on power grids becomes significant. However, the details of these Distributed Generators (DGs) are normally unknown ,thus, the dynamic modelling of the DGs is of great importance and becomes challenging. In [75] and [76], identification of ARX and state-space models of distribution network was conducted

in MATLAB identification toolbox. Nevertheless, the method has high requirements on disturbance locations, which makes it impractical for the industry to implement. Moreover, the methods that rely on measurements generated by large system disturbances cannot be used for online identification.

[77] proposed an automatic online calibration method using the measured response captured by the PMU. The method is based on the Extended Kalman Filter (EKF). This method seeks a solution through the minimisation of the discrepancy between model response and the measurements captured by PMU. This method is mainly utilised in the validation of generator models. Real and reactive power at Point of Connection (POC) were considered as the inputs.

A grey-box approach in [78] was developed to validate the dynamic equivalent of distribution network cell. Similar to [77], the approach derives a dynamic equivalent through the minimisation of the discrepancy between the measured and the simulated power flow at a certain location.

4.4 Artificial Intelligence Methods

4.4.1 Artificial Neural Networks

Artificial Neural Network (ANN) is a new computational technique which mimics the function of the brain. The understanding of the neuron functions and its pattern of interconnections prompts the use of ANN in mathematical modelling [79-83]. A simple diagram is shown in Figure 4.4 an illustration of the basic structure of a MultiLayer Perceptron (MLP) or a multilayer feedforward network. The circle represents neurons and the arrow represents the interconnections. Modelling an effective ANN model requires two stages, training and validation. The perceptron can be trained by adjusting the weights of the inputs with a larger proportion of data, and the trained model is validated with the remaining data.

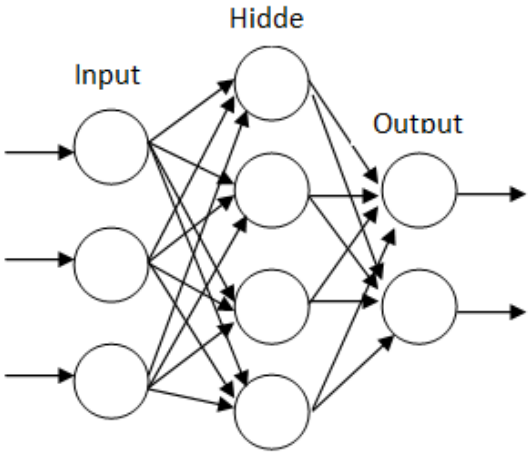

Figure 4. 4 Basic Structure of ANN

The complexity of modern power systems is increasing due to their large size, component nonlinearity and operational uncertainty. In order to cope this, ANN is widely used in power system as a very effective computational technique [84-88] to derive the external network equivalents. MLP is the most commonly used approach.

[85, 86] presents an approach to model a dynamic equivalent of a system that is to be reduced. Measurements captured from the location between the retained system and the system which is to be reduced is fed into a first-stage ANN to extract estimates of states of the reduced order equivalent. A second-stage ANN embedded in an Ordinary Differential Equation (ODE) solver was trained to approximate a continuous-time system with the same states which was extracted at the first stage.

Back-propagation and Radial-Basis Function (RBF) neural networks were employed to identify the dynamic equivalent of an external power system in [87]. The identification is restricted from online use as transient stability indices, such as peak overshoot, decay constant and the frequency of oscillation were utilised as the input in training the ANN.

[89] demonstrates a hybrid method to combine both coherency-based method and ANN method in deriving a dynamic equivalent. The proposed method is illustrated in Figure 4.5,

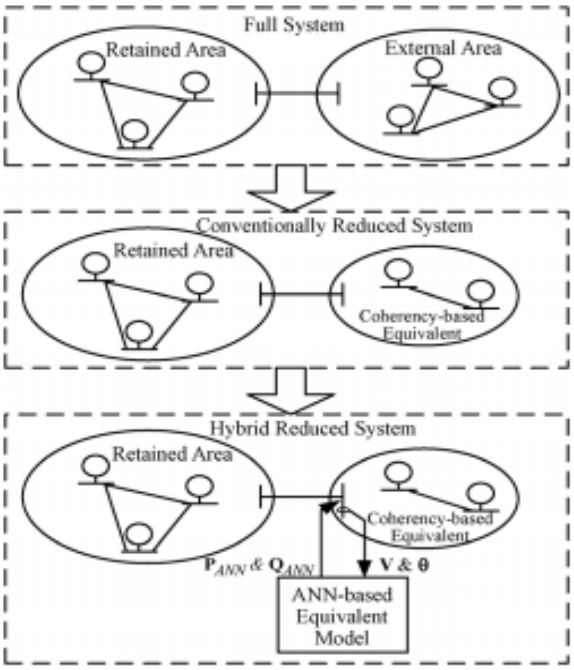

Figure 4. 5 Dynamic Equivalent Based On Hybrid Method [89]

The network was first reduced using the conventional coherency-based approach. Then an ANN-based equivalent as developed to adjust power injection at the boundary bus, in order to minimise the discrepancy of voltage response between the real system and the reduced model. Voltage at the boundary bus was taken as the input of the ANN-based equivalent.

4.4.2 K-means Clustering

The k-means algorithm is a clustering method that aims to partition n observations into k clusters [90]. For a set of observations $\{x_1,\ x_2 \dots x_n\}$, the k-means method aims to allocate each observation to a cluster in order to minimise the sum of the squares, as shown:

$$\arg min_K \sum_{i=1}^{k} \sum_{x_j \in K} \left\| x_j - \mu_i \right\| \tag{4. 8}$$

Where K is the cluster centres and μ_i is the mean point in the ith cluster centre.

In [91], K-means method was employed to develop a dynamic equivalent for the distribution network. A grey-box equivalent model was presented in the form of a nonlinear state space.

$$\dot{x} = Ax + Bu + f(x)$$

$$y = Cx + Du + f(x) \quad (4.9)$$

where A, B, C and D are the coefficient matrices, x is the state vector, u is the input vector, y is the output vector and $f(x)$ a function that represents the nonlinear parts of the model.

The input vector includes the bus voltage and frequency. A nonlinear least square method was utilised to estimate the unknown parameters in the coefficient matrices of the grey-box model. The clustering method was tested under a series of disturbance scenarios. Simulation results showed that it was indiscernible from the standard grey box parameter estimation value, which could closely approximate to the dynamic response of the network.

4.4.3 Genetic Algorithms

Genetic Algorithms (GAs) are new artificial intelligent computation methods which mimics the evolution [92]. They are especially developed to solve problems that require searching through a large amount of possibilities. GAs are broadly used in power system for optimisation. [93] demonstrates the application of GAs in the generator scheduling. It is specified in [94] the implementation of GAs in optimal power flow studies.

[95] presented the techniques to deriving a dynamic equivalent of a permanent synchronous motor using GAs. [96, 97] introduced the application of GAs to model the dynamic equivalent for a multi-machine system.

4.5 Conclusions

It was found that the equivalent models derived by model-based methods cannot timely reflect the dynamic characteristics of the system. Often, there are a large discrepancy between the model-based equivalent and the real system. Moreover, these methods require comprehensive knowledge on the external network. In some countries private utilities compete with each other and not intend

to disclose any information about their business, which makes it impractical to get access to detailed information.

In contrast, measurement-based methods and AI techniques can effectively circumvent the problem that occurs in the model-based methods. These methods normally rely on both system measurements and prior knowledge. The models achieved by these two methods can retain certain topology, whilst enable the parameters to be updated in a timely manner according to the measurements.

In comparison, it is evident that the measurement-based methods and AI methods have advantages over the conventional modelling techniques. For the purpose of retaining the physical information of the network, trade-off has to be made between model-based methods and measurement-based methods. In the following chapters, a new measurement-based approach which could retain network information will be proposed and tested.

Chapter 5 Modal Analysis of Multi-Machine System

5.1 Introduction

Oscillatory modes are constantly monitored in power systems. Generator dynamics provide great contribution to this phenomenon. By modelling the generator dynamics property in a linear form for small signal analysis, the oscillations are reflected as complex eigenvalues. As mentioned in Chapter 2, the oscillatory information, such as oscillatory frequency, damping and mode shapes can be extracted from direct Wide Area Measurements (WAM) with considerable accuracy [98] .

This chapter presents a deep insight between oscillatory information and multi-machine system dynamics. A Modal Assurance Criterion (MAC) technique will be used to differentiate between the various modes. Those with similar oscillatory information will also be introduced. This knowledge constructs a concrete theoretical foundation to develop the model update scheme.

5.2 Simulation Models

5.2.1 Two-Area Model

Two-area models are adequate representation of the network topology for a general study in many countries [99]. The Great Britain power flow pattern in 2009/2010 provided by National Grid in GB Seven Year Statement 2009 is shown in Figure 5.1. The pattern indicates that the GB network can be divided into Scotland and England by the boarder B6.

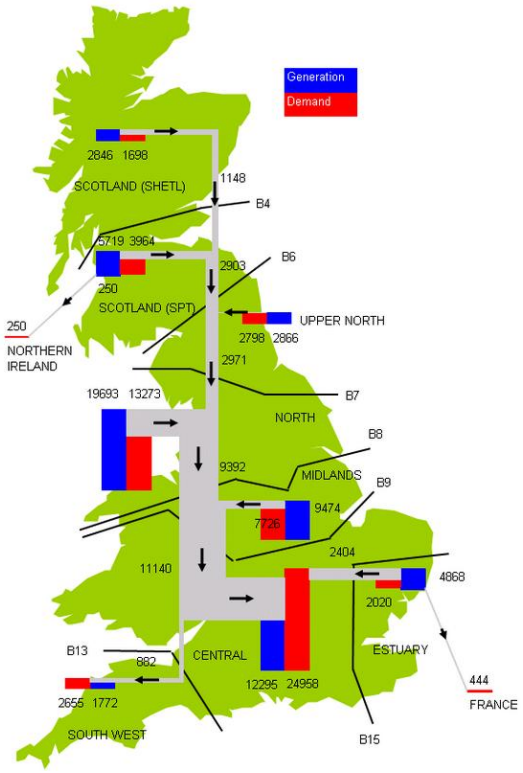

Figure 5. 1 Power Flow Pattern in GB Network [100]

The two-area model is shown in Figure 5.2 marked with the length of each part of the transmission lines. The system consists of two areas, each with two generators and two loads located at bus 7 and bus 9. The system details are specified in [101]. This artificial model was created by the Canadian Electrical Association [5] to demonstrate the types of oscillations in an interconnected power system.

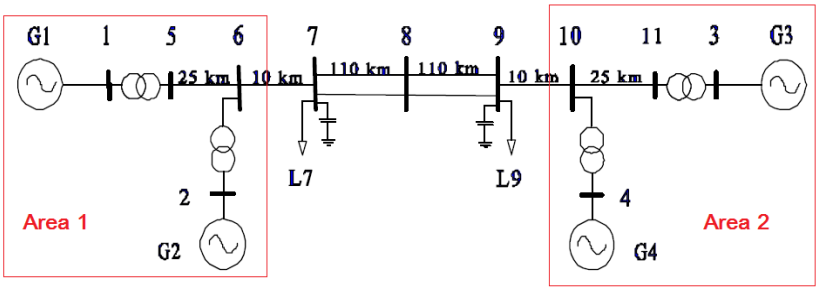

Figure 5. 2 Two-area System Diagram

5.2.2 New York-New England (NY-NE) Model

The NY-NE model which consists of sixteen generators and five coherent groups is described in Figure 5.3.

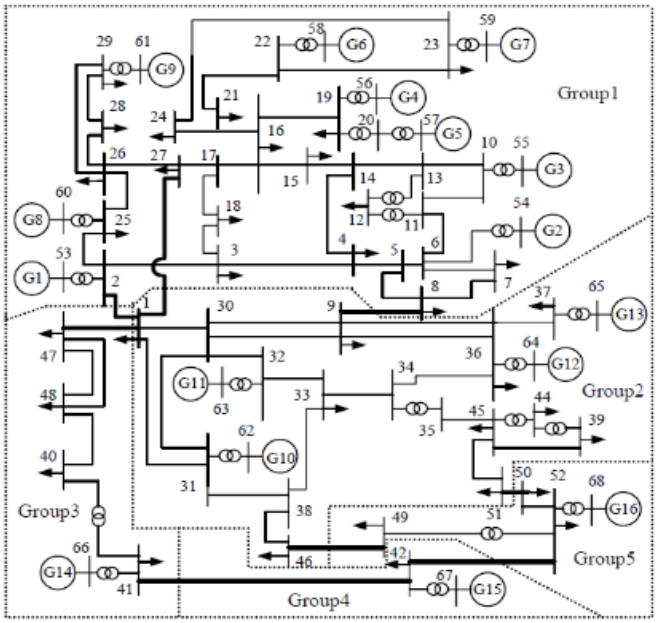

Figure 5. 3 NY-NE Power System Model

The division of coherency is given in Table 5.1,

Table 5. 1 Coherent Groups of NY-NE Model

Group	Generator	Number of Generators
Group 1	G1,G2,G3,G4,G5,G6,G7,G8,G9	9
Group 2	G10,G11,G12,G13	4
Group 3	G14	1
Group 4	G15	1
Group 5	G16	1

5.3 Modal Sensitivity Analysis

The sensitivity of an eigenvalue to a particular system parameter indicates how much the variation of this parameter can be reflected in this eigenvalue. If the eigenvalue is insensitive to a certain parameter, the estimation of this parameter using this eigenvalue may result in large deviation from the real value or algorithm divergence. Three system parameters are concerned and shown in Equation (2.16), inertia constant M, damping coefficient D and synchronising torque coefficient K.

For a particular mode λ_j, it is given in Equation (2.5) that,

$$Aw_j = w_j\lambda_j \tag{5. 1}$$

where $j = 1,2,\dots,n$. n is the number of modes in the system and w_j is the right eigenvector (mode shape) for jth mode and λ_j is the j-th eigenvalue.

5.3.1 Modal Sensitivity to Inertia Constants

To investigate the modal sensitivity to inertia constants, Equation (5.2) was employed by simply differentiation (5.1) with respect to any inertia constant M_i,

$$\frac{\partial A}{\partial M_i}w_j + A\frac{\partial w_j}{\partial M_i} = \frac{\partial \lambda_j}{\partial M_i}w_j + \lambda_j\frac{\partial w_j}{\partial M_i} \tag{5. 2}$$

Premultiplying by j-th left eigenvector u_j, and noting that $u_j(A - \lambda_j I) = 0$, the sensitivity function can be written as,

$$\frac{\partial \lambda_j}{\partial M_i} = u_j\frac{\partial A}{\partial M_i}w_j \tag{5. 3}$$

Hence, for a classical generator model given by Equation (2.16), the full sensitivity function of the j-th mode to the i-th inertia constant can be expanded as,

$$\frac{\partial \lambda_j}{\partial M_i} = \begin{bmatrix}u_1,\dots,u_j,\dots,u_n\end{bmatrix}_j \begin{bmatrix} 0 & \dots & 0 & \dots & 0 & \dots & \dots & 0 \\ \vdots & \vdots & \vdots & \vdots & \vdots & \vdots & \vdots & \vdots \\ \frac{K_{i1}}{M_i^2} & 0 & \cdots & \frac{K_{ii}}{M_i^2} & \frac{D_i}{M_i^2} & \cdots & \frac{K_{in}}{M_i^2} & 0 \\ \vdots & \vdots & \vdots & \vdots & \vdots & \vdots & \vdots & \vdots \\ 0 & \cdots & 0 & \cdots & 0 & \cdots & \cdots & 0 \end{bmatrix} \begin{bmatrix} w_1 \\ \vdots \\ w_j \\ \vdots \\ w_n \end{bmatrix}_j \tag{5. 4}$$

The polynomial form is derived from (5.4),

$$\frac{\partial \lambda_j}{\partial M_i} = u_{j,2i}\sum_{k=1}^{n}\frac{K_{ik}}{M_i^2}w_{2k-1,j} + u_{j,2i}\sum_{k=i}\frac{D_i}{M_i^2}w_{2k,j} \tag{5. 5}$$

Based on (2.17), the sensitivity of the real parts and the imaginary parts to the inertia constant are,

$$\frac{\partial \sigma}{\partial M} = \frac{D}{2M^2} \tag{5. 6}$$

$$\frac{\partial \omega}{\partial M} = \frac{D^2 - 2MK_S}{2M^2\sqrt{4MK_S - D^2}} \tag{5. 7}$$

Similarly, the sensitivity for sixth-order generator model in (2.20) is derived as,

$$\frac{\partial A}{\partial M_i} = \begin{bmatrix} \cdots & \cdots & 0 & 0 & \cdots & 0 & 0 & \cdots \\ \vdots & \vdots & \vdots & \vdots & \vdots & \vdots & \vdots & \vdots \\ \cdots & \frac{K_{ii}}{M_i^2} & \frac{D_i}{M_i^2} & 0 & 0 & \frac{1}{M_i^2}\frac{\partial P_i}{\partial E_{qi}''} & \frac{1}{M_i^2}\frac{\partial P_i}{\partial E_{di}''} & \cdots \\ \vdots & \vdots & \vdots & \vdots & \vdots & \vdots & \vdots & \vdots \\ \cdots & \cdots & 0 & 0 & \cdots & 0 & 0 & \cdots \end{bmatrix} \tag{5. 8}$$

The corresponding sensitivity function in the form of polynomial can then be represented as,

$$\frac{\partial \lambda_j}{\partial M_i} = \frac{u_{j,6i-4}}{M_i^2}\sum_{k=1}^{n}(K_{ik}w_{6k-5,j} + \frac{\partial P_i}{\partial E_{qi}''}w_{6k-1,j} + \frac{\partial P_i}{\partial E_{di}''}w_{6k,j}) + u_{j,6i-4}\sum_{k=i}\frac{D_i}{M_i^2}w_{6k-4,j} \tag{5. 9}$$

The full sensitivity matrix consists of all sensitivity function as its elements,

$$S_M = \begin{bmatrix} \frac{\partial \lambda_1}{\partial M_1} & \cdots & \frac{\partial \lambda_1}{\partial M_i} & \cdots & \frac{\partial \lambda_1}{\partial M_m} \\ \vdots & \ddots & \vdots & \ddots & \vdots \\ \frac{\partial \lambda_j}{\partial M_1} & \cdots & \frac{\partial \lambda_j}{\partial M_i} & \cdots & \frac{\partial \lambda_j}{\partial M_m} \\ \vdots & \ddots & \vdots & \ddots & \vdots \\ \frac{\partial \lambda_n}{\partial M_1} & \cdots & \frac{\partial \lambda_n}{\partial M_i} & \cdots & \frac{\partial \lambda_n}{\partial M_m} \end{bmatrix} \tag{5. 10}$$

where m denotes the number of generators,

n is the number of oscillatory modes.

5.3.2 Modal Sensitivity to Damping Coefficients

The modal sensitivity to damping coefficient can be achieved by differentiating (5.1) with respect to any damping coefficient D_i, and premultiplying the outcome by jth left eigenvector u_j.

$$\frac{\partial \lambda_j}{\partial D_i} = u_j \frac{\partial A}{\partial D_i} w_j \tag{5. 11}$$

For a classical generator model, the sensitivity can be written as,

$$\frac{\partial \lambda_j}{\partial D_i} = -\frac{u_{j,2i} w_{2i,j}}{M_i} \tag{5. 12}$$

Based on (2.17), the sensitivity of the real parts and the imaginary parts to the damping coefficient can be derived as,

$$\frac{\partial \alpha}{\partial D} = -\frac{1}{2M} \tag{5. 13}$$

$$\frac{\partial \omega}{\partial D} = \frac{D}{2M\sqrt{4MK_s - D^2}} \tag{5. 14}$$

The eigenvalue sensitivity to damping coefficient for sixth-order generator model as,

$$\frac{\partial \lambda_j}{\partial D_i} = -\frac{u_{j,6i-4} w_{6i-4,j}}{M_i} \tag{5. 15}$$

The full sensitivity matrix with respect to damping coefficients is then formed,

$$S = \begin{bmatrix} \frac{\partial \lambda_1}{\partial D_1} & \cdots & \frac{\partial \lambda_1}{\partial D_i} & \cdots & \frac{\partial \lambda_1}{\partial D_m} \\ \vdots & \ddots & \vdots & \ddots & \vdots \\ \frac{\partial \lambda_j}{\partial D_1} & \cdots & \frac{\partial \lambda_j}{\partial D_i} & \cdots & \frac{\partial \lambda_j}{\partial D_m} \\ \vdots & \ddots & \vdots & \ddots & \vdots \\ \frac{\partial \lambda_n}{\partial D_1} & \cdots & \frac{\partial \lambda_n}{\partial D_i} & \cdots & \frac{\partial \lambda_n}{\partial D_m} \end{bmatrix} \tag{5. 16}$$

5.3.3 Modal Sensitivity to Synchronising Torque Coefficients

The same technique was applied to develop the relationship between modes and synchronising torque coefficients. The sensitivity of a particular eigenvalue to the synchronising torque coefficient can be written as,

$$\frac{\partial \lambda_j}{\partial K_{ik}} = \begin{bmatrix} u_1, \dots, u_j, \dots, u_n \end{bmatrix}_j \begin{bmatrix} 0 & \cdots & 0 & \dots & 0 \\ \vdots & \vdots & \vdots & \vdots & \vdots \\ 0 & \cdots & -\frac{1}{M_i} & \cdots & 0 \\ \vdots & \vdots & \vdots & \vdots & \vdots \\ 0 & \cdots & 0 & \cdots & 0 \end{bmatrix} \begin{bmatrix} w_1 \\ \vdots \\ w_j \\ \vdots \\ w_n \end{bmatrix}_j \tag{5. 17}$$

For classical model, the polynomial form is,

$$\frac{\partial \lambda_j}{\partial K_{ik}} = -u_{j,2i} \frac{1}{M_i} w_{2k-1,j} \tag{5. 18}$$

For sixth-order model, it can be expressed as,

$$\frac{\partial \lambda_j}{\partial K_{ik}} = -u_{j,6i-4} \frac{1}{M_i} w_{6k-5,j} \tag{5. 19}$$

5.4 Model Update

5.4.1 Linear Approximation

For a mode $\lambda(\theta)$, its full Taylor series expansion at a given value θ_a can be written as,

$$\lambda(\theta) = \lambda(\theta_a) + \frac{\lambda'(\theta_a)}{1!}(\theta - \theta_a) + \frac{\lambda''(\theta_a)}{2!}(\theta - \theta_a)^2 + \frac{\lambda^{(3)}(\theta_a)}{3!}(\theta - \theta_a)^3 + \cdots \tag{5. 20}$$

By neglecting high order terms in (5.20), a linear approximation can be derived,

$$\Delta\lambda = S\Delta\theta \tag{5. 21}$$

where $\Delta\theta = \theta - \theta_a$, is the perturbation of the parameter. θ indicates the parameter; $\Delta\lambda = \lambda - \lambda_a$, is the change of eigenvalues; λ indicates eigenvalues and λ_a is the eigenvalues at θ_a; S is the modal sensitivity matrix.

5.4.2 Model Update Foundation

To make the parameters best reflect any measured oscillatory mode λ_m, a model update theory was proposed in [102]. The model update theory estimates the parameters based on an iterative algorithm,

$$\lambda_m - \lambda_k = S_k(\theta_{k+1} - \theta_k) \tag{5. 22}$$

where λ_k is the corresponding eigenvalue at k-th iteration; S_k is the sensitivity matrix at k-th iteration; θ_k and θ_{k+1} are the parameter estimates at k-th and $(k+1)$-th iteration respectively.

5.4.3 Objective Function

The optimal estimate can be achieved through the minimisation of the following objective function:

$$J(\Delta\theta) = \varepsilon^T \varepsilon \tag{5. 23}$$

where $\varepsilon = \Delta\lambda - S_k \Delta\theta$,

$$\Delta\theta = \theta_{k+1} - \theta_k \tag{5. 24}$$

$$\Delta\lambda = \lambda_m - \lambda_k \tag{5. 25}$$

When ${\partial J(\Delta\theta)}/{\partial \Delta\theta} = 0$, the minimum of $J(\Delta\theta)$ can be obtained at

$$\Delta\theta = \left[S_k^T S_k\right]^{-1} S_k^T \Delta\lambda \tag{5. 26}$$

Equation (5.26) can be further expanded as (5.27) which is the update algorithm,

$$\theta_{k+1} = \left[S_k^T S_k\right]^{-1} S_k^T [\lambda_m - \lambda_k] + \theta_k \tag{5. 27}$$

In practice, the measured modal data are not necessarily accurate. The accuracy of measurements can be incorporated into the update algorithm through the minimisation of the weighted objective function,

$$J(\Delta\theta) = \varepsilon^T W_m \varepsilon \tag{5. 28}$$

W_m in (5.28) is a positive definite weighting matrix. The weighting matrix is normally a diagonal matrix whose elements are given by the reciprocals of the variance of the corresponding measurements. If the variances of the measurements are uncorrelated then,

$$E[(b - E[b])(b - E[b])^T] = V \tag{5. 29}$$

where $V = diag(v_1^2, v_2^2, \dots, v_i^2, \dots v_m^2)$ and v_i^2 is the variance of the i-th measurement.

The weights are given by the inverse measurement variances,

$$W_m = V^{-1} \tag{5. 30}$$

If

$$W_m = diag(w_1, w_2, \dots, w_i, \dots w_m) \tag{5. 31}$$

Then,

$$w_i = \frac{1}{v_i^2} \tag{5. 32}$$

Through the minimisation of (5.28), gives,

$$\Delta\theta = \left[S_k^T W_m S_k\right]^{-1} S_k^T W_m \Delta\lambda \tag{5. 33}$$

Thus, the weighted update algorithm is

$$\theta_{k+1} = \theta_k + \left[S_k^T W_m S_k\right]^{-1} S_k^T W_m (\lambda_m - \lambda_k) \tag{5. 34}$$

5.5 Modal Assurance Criterion

It is insufficient to simply rearrange the modal frequencies in ascending order of magnitude, especially when two modes are close together in frequency, because the magnitudes of different modes vary in different operational conditions. This gives rise to a higher possibility of mis-pairing.

The modal frequencies and mode shapes of the measured and updated data must relate to the same mode, i.e. they must be paired correctly for the model update process. The Modal Assurance Criterion (MAC) was used to assess the degree of correlation between mode shapes. In model update, MAC is applied to pair mode shapes derived from initial model and updated the model at each stage of iteration, with those from the measured modes. The advantage of this method is that it does not require prior system matrices.

Normally, it can be difficult to collect a full set of modes due to the limited system observability. The MAC can help to pair the measured modes with the calculated ones computed from the initial model.

The MAC between a measured mode ϕ_{mj} and a given mode ϕ_{ak} is defined as,

$$MAC_{jk} = \frac{\left|\phi_{mj}^T \phi_{ak}\right|^2}{(\phi_{ak}^T \phi_{ak})(\phi_{mj}^T \phi_{mj})} \quad (5.35)$$

From (5.35), it can be seen that the value of the MAC is between 0 and 1. A value of 1 means that one of the mode shape vector is a multiple of the other, i.e. they are correlated, while a value of 0 means that the two modes are uncorrelated. The measured and computed mode shapes must contain the same number of elements, although their scaling does not have to be the same. Note that the complex mode shapes may be correlated using the MAC as long as the transpose is taken to be conjugate transpose. Usually, the calculated modes are correlated with all the measured modes. An example was used to demonstrate MAC below. For the two-area system, the calculated mode shapes are given as Φ_0,

$$\Phi_0 = \begin{bmatrix} -0.5000 & -0.3399 & -0.6653 & 0.0027 \\ -0.5000 & -0.2598 & 0.7420 & -0.0224 \\ -0.5000 & 0.6760 & -0.0800 & -0.6504 \\ -0.5000 & 0.6000 & -0.0205 & 0.7593 \end{bmatrix}$$

Due to unknown perturbations in the system, the snapshot measurements captured are shown,

$$\Phi_1 = \begin{bmatrix} -0.3790 & 0.0120 & -0.5000 & -0.6320 \\ -0.2904 & -0.0383 & -0.5000 & 0.7688 \\ 0.6592 & -0.6489 & -0.5000 & -0.0973 \\ 0.5809 & 0.7598 & -0.5000 & 0.0047 \end{bmatrix}$$

MAC is calculated based on (5. 31),

$$MAC = \begin{bmatrix} 0.0814 & 0.9969 & 0.0008 & 0.0003 \\ 0.0018 & 0.0005 & 0.0000 & 0.9997 \\ 1.0000 & 0.1143 & 0.0001 & 0.0020 \\ 0.0005 & 0.0023 & 0.9972 & 0.0023 \end{bmatrix}$$

The correlated mode shapes are:

Original mode 1 with measured mode 3;

Original mode 2 with measured mode 1;

Original mode 3 with measured mode 4;

Original mode 4 with measured mode 2;

The pairing results can be validated based on the nature of the modes. There are four types of electrical mechanical modes excited in this model, local mode 1 (G1 and G2 participating), local mode 2 (G3 and G4 participating), interarea mode, and a zero mode. These can be found by checking their participation factors as introduced in previous chapters. The validation are shown in the diagram below,

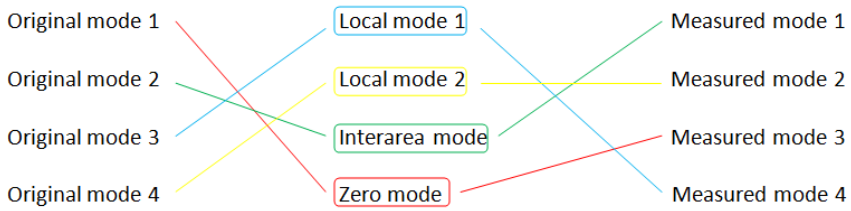

Figure 5. 4 Validation of MAC in two-area system model

5.6 Conclusions

The main contribution of this chapter is to establish the relationship between modal information and system parameters. By focusing on the system dynamic properties, parameters such as the generator inertia constants, the damping coefficients and the synchronising torque coefficients are of particular concern. Modal sensitivity matrices for these parameters were derived analytically for different generator models. It can be found that the inertia constant was involved in all three sensitivity matrices. Thus, the precision of inertia constant contributes most to the sensitivity computation.

The model update concept was initially introduced to power system in this chapter. This concept was originally used in structural engineering to monitor the health of a structure through vibration tests. WAMS, have been successfully introduced to power system engineering [103] for real-time power system dynamics analysis. In comparison to conventional online study methods, this technique only requires system modal information that can be easily measured from the grid.

The objective function is a key part in this method. Through the minimisation of the discrepancy between the measured modes and the estimated modes, an iterative algorithms was developed to estimate parameter values that best reflect the measured modes in a timely manner. The weighted model update method was also developed based on the initial method, to achieve more accurate estimation results. The Modal Assurance Criterion (MAC) was proposed to pair measured modes with calculated modes. Some difficulties were encountered when attempt to pair modes close in frequency for a large power system. The advantage of MAC is that it can work without any system matrices and associate corresponding modes with high accuracy.

Chapter 6 Iterative Parameter Estimation Without Pseudomeasurement

6.1 Introduction

Least Square Method (LSM) is a standard approach to approximate the solution of over-determined equations where the number of equations is more than that of the unknowns. The method seeks a solution by minimising the sum of the squares of the errors in the results of every equation.

LSM can be classified into two categories: Linear Least Squares (LLS) and Non-linear Least Squares (NLS). The classification depends on whether the residuals are linear or not in all unknowns. The LLS has a closed-form solution, i.e., any formula can be evaluated in a finite number of standard operations, while the NLS has no closed-form solution and is normally solved by iterative refinement. A linear system is used to approximate the nonlinear one at each iteration stage. The NLS requires the initial conditions of the parameters whilst the LLS does not have such requirement.

The objective of LSM is to adjust the model parameters to fit a set of data. The adjusted parameters should best fit the data set. Through minimisation of the sum of the squares of the errors in the results, the optimal solution can be achieved. A residual is defined as the difference between the actual values and the estimated values.

In this work, a truncated Taylor series expansion of the modal data is used to linearise the relationship between the modal data and the system parameters at each iteration stage. As an example to demonstrate the methodology, the system inertia constants are adjusted/ updated to fit the modal data (eigenvalues). The problem is formulated as an over-determined systems of nonlinear equations and solved using weighted least squares method.

The modal measurements used in this thesis are extracted using ambient signal methods which conducts modal data estimation continuously under small system disturbance. This method is more practical to provide real time modal information in industry.

The measurement errors of modal data are considered in this thesis. They are mainly produced due to measuring devices and mode estimation methods. The errors are in certain ranges. It was suggested by manufacturers that (-1%, 1%) error is applicable for modal frequencies, and (-10%, 10%) is applicable for modal damping. In the simulation tests of this thesis, measurement errors are generated from the standard uniform distribution on an open interval. For example, modal frequency error $\pm a\%$ means the errors are pseudorandom scalars drawn from the standard uniform distribution on the open interval $(-a\%, a\%)$. This will be applied throughout this thesis as the indication of measurement error ranges.

In the simulation using a particular set of measurements, measurements with their errors will be sampled only once. Then, the algorithms will work on updating current parameters. However, this could lead to divergence of the algorithms due to the nonlinearity of the process with random inputs.

6.2 Frequency Method

In this section, the proposed method is employed to estimate the inertia constants of the generators in multi-machine power systems based on the modal frequency measurements only, since modal frequencies are more closely related to inertia constants. The optimal estimation can be obtained through the minimisation of (6.1),

$$J(\Delta M) = \varepsilon_f^T W_f \varepsilon_f \tag{6. 1}$$

where ε_f is a vector contains the errors between measured modal frequency and estimated modal frequency,

W_f is a weighting matrix that allows relative uncertainty in the frequency measurements.

The optimal solution is given in (6.2) for (5.34),

$$M_{k+1} = M_k + \left[S_{fk}^T W_f S_{fk}\right]^{-1} S_{fk}^T W_f (\omega_m - \omega_k) \tag{6. 2}$$

where S_{fk} is the modal frequency sensitivity matrix at the k-th step,

ω_m is a vector consists of measured modal frequencies,

ω_k is a vector contains calculated modal frequencies computed based on the updated system at the k-th step,

M_k is a vector contains the updated inertia constants at the k-th step.

The modal frequency sensitivity matrix S_f is defined as,

$$S_f = \begin{bmatrix} \frac{\partial \omega_1}{\partial M_1} & \cdots & \frac{\partial \omega_1}{\partial M_i} & \cdots & \frac{\partial \omega_1}{\partial M_m} \\ \vdots & \ddots & \vdots & \ddots & \vdots \\ \frac{\partial \omega_j}{\partial M_1} & \cdots & \frac{\partial \omega_j}{\partial M_i} & \cdots & \frac{\partial \omega_j}{\partial M_m} \\ \vdots & \ddots & \vdots & \ddots & \vdots \\ \frac{\partial \omega_n}{\partial M_1} & \cdots & \frac{\partial \omega_n}{\partial M_i} & \cdots & \frac{\partial \omega_n}{\partial M_m} \end{bmatrix} \quad (6.3)$$

The algorithm is illustrated in Figure 6.1. The oval blocks represent the input data and the rectangular ones are the necessary modules for the model update method.

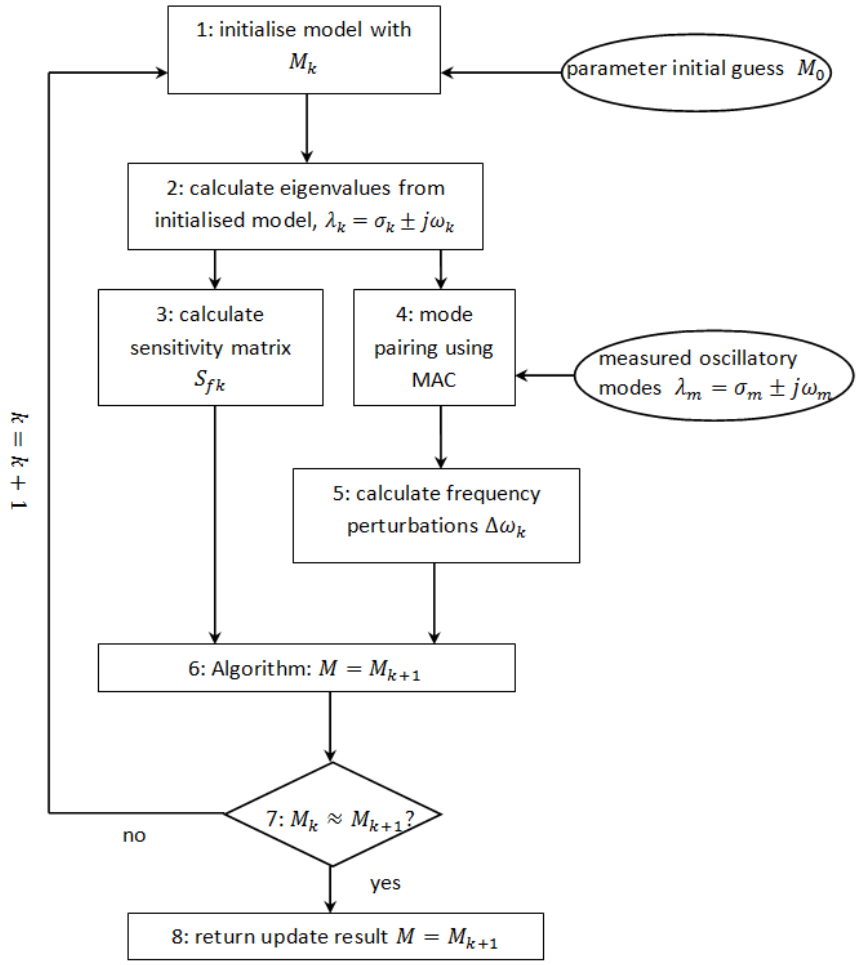

Figure 6.1 Frequency method

The flow chart is summarised,

1. Initialise system model with M_k (M_0, for the first time);
2. Calculate the eigenvalues of the initialised system model;
3. Calculate sensitivity matrix of modal frequency;
4. Pair eigenvalues calculated at step 2, with the measured eigenvalues;
5. Calculate perturbations between corresponding calculated frequencies and measured frequencies;
6. Update inertia constants using equation (6.2);
7. If the updated results are approximately equal to last update, then return results. Otherwise, go back to step 1.

The estimation errors in this thesis are defined as,

$$Err = \left|\frac{M_a - M_e}{M_a}\right| \times 100\% \quad (6.4)$$

where M_a is the actual value of inertia constant and M_e is the estimated value.

6.3 Test on Two-Area System

6.3.1 Sensitivity Analysis for Two-Area System

Tests are conducted under three sets of scenarios of the two-area system, for single machine, two machines and three machines. It is assumed that the full observability for this system is available in the tests. Frequency Measurement Error (FME) is introduced in each test within the range of $\pm$0.2%-$\pm$10%. Initial guess and true values of inertia constants are given in Table 6.1, and the discrepancies are also presented,

Table 6.1 Initial guess and true values for inertia constants in Two-area system

Generator Inertia	Initial	True	Discrepancy (%)
M1	13	12	8.33
M2	13	12	8.33
M3	9	10	10.00
M4	9	10	10.00

For different cases, only the inertia constant(s) to be estimated are changed to their true values, whilst the inertia constants of the generators at rest remain the same as initial guess. The purpose of doing so is to simulate a operational status which is different from the initial one. The sensitivity matrix of modal frequencies to inertia constants calculated based on the initial guess is given in Table 6.2. We can see that the frequency of mode 1 is sensitive to M3 and M4, whilst the changes in M1 and M2 can hardly affect it. The frequency of mode 2 is more sensitive to M1 and M2. The frequency of mode 3 is sensitive to all four inertia constants but more dependent on those of M3 and M4. Figure 6.2 visualises the sensitivity of modal frequencies in a bar diagram.

Table 6. 2 frequency sensitivity matrix

	M1	M2	M3	M4
ω_1	-0.0000j	-0.0000j	-0.1812j	-0.2416j
ω_2	-0.0861j	-0.1269j	-0.0020j	-0.0006j
ω_3	-0.0180j	-0.0037j	-0.0837j	-0.0641j

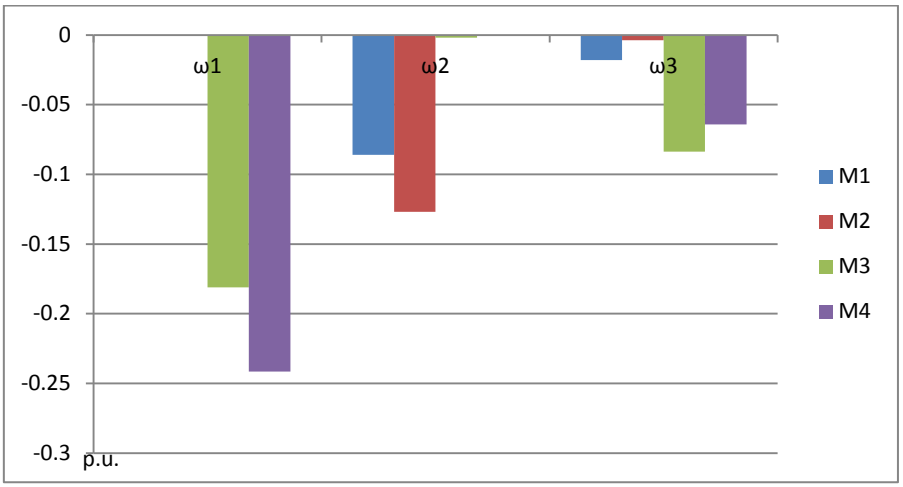

Figure 6.2 Sensitivity of modal frequencies to inertia constants for two-area system

6.3.2 Single-Machine Estimation

The estimates of M1 for different FME are shown in Table 6.3. From the table, it can be seen that the number of iterations to produce the optimal estimate increases with the increase of FME, while the estimation accuracy decreases. Clearly as shown in the table, $\pm$1% FME is the boarder of 'good' and 'bad' parameter estimates. When FME is less than $\pm$1%, the method produces precise estimates with less than 5.48% errors which are smaller than original discrepancy, (8.33%) shown in Table 6.1. However, the estimates are not acceptable when FME is over $\pm$1%.

Table 6.3 Estimation errors of M1

FME (%)	$\pm$0.2	$\pm$0.5	$\pm$0.8	$\pm$1	$\pm$2	$\pm$5	$\pm$10
M1 Estimation Error (%)	1.03	1.05	2.17	5.48	11.40	9.41	127.00
steps	3 steps	3 steps	4 steps	2 steps	3 steps	5 steps	9 steps

Table 6.4-6.6 show the estimation errors for M2, M3 and M4 individually. Similar conclusions can be drawn, as the measurement error increases, the estimation errors increase and a slightly longer

estimation time is required for the algorithm to converge. In general, the resultant estimates are poor when FME is over ±1%.

Table 6. 4 Estimation errors of M2

FME (%)	±0.2	±0.5	±0.8	±1	±2	±5	±10
M2 Estimation Error (%)	0.63	1.23	2.27	3.22	6.67	11.20	44.87
steps	3 steps	3 steps	2 steps	3 steps	2 steps	4 steps	5 steps

Table 6. 5 Estimation errors of M3

FME (%)	±0.2	±0.5	±0.8	±1	±2	±5	±10
M3 Estimation Error (%)	0.06	0.31	0.00	0.58	5.35	6.56	17.16
steps	3 steps	3 steps	3 steps	4 steps	4 steps	6 steps	9 steps

Table 6. 6 Estimation errors of M4

FME (%)	±0.2	±0.5	±0.8	±1	±2	±5	±10
M4 Estimation Error (%)	0.15	0.19	0.76	0.536	1.28	0.58	1.64
3 steps	4 steps	4 steps	4 steps	4 steps	6 steps	9 steps	3 steps

6.3.3 Two-Machine Estimation

There are six scenarios in the test for the two machines. When the change is applied to M1 and M2 the results for the estimation are provided in Table 6.7. For this scenario, the resultant estimates become unacceptable when FME exceeds ±0.5%, which significant limits the implementation of this methodology when measurement noise exists. The number of iterations required to reach convergence increases slightly when FME is growing. Similar results are found in the estimation of M1 and M3, and M1 and M4 shown in Table 6.8 and 6.9 respectively.

Table 6. 7 Estimation errors of M1 and M2

FME (%)	±0.2	±0.5	±0.8	±1	±2	±5	±10
M1 Estimation Error (%)	2.51	7.53	13.71	14.10	25.61	83.20	285.77
M2 Estimation Error (%)	1.03	5.74	15.82	4.96	6.84	29.69	13.58
steps	3 steps	3 steps	4 steps	3 steps	4 steps	6 steps	6 steps

Table 6. 8 Estimation errors of M1 and M3

FME (%)	±0.2	±0.5	±0.8	±1	±2	±5	±10
M1 Estimation Error (%)	1.07	1.22	2.27	5.65	12.04	11.72	196.10
M3 Estimation Error (%)	0.14	0.54	0.38	0.46	1.39	8.32	12.90
steps	3 steps	3 steps	3 steps	4 steps	4 steps	7 steps	24 steps

Table 6. 9 Estimation errors of M1 and M4

FME (%)	±0.2	±0.5	±0.8	±1	±2	±5	±10
M1 Estimation Error (%)	1.10	1.02	2.00	5.87	12.45	9.55	204.89
M4 Estimation Error (%)	0.28	0.07	0.53	1.26	2.81	1.00	17.76
steps	3 steps	3 steps	4 steps	4 steps	4 steps	6 steps	16 steps

The proposed method has robust performance up to ±2% FME when it is employed to estimate the scenarios of 'M2 and M3', and 'M2 and M4'. Relatively, the estimates of M2 have larger errors than those of M3 and M4 at the same FME level.

Table 6. 10 Estimation errors of M2 and M3

FME (%)	±0.2	±0.5	±0.8	±1	±2	±5	±10
M2 Estimation Error (%)	0.63	1.24	2.27	3.22	6.69	11.39	43.73
M3 Estimation Error (%)	0.02	0.37	0.01	0.41	0.50	6.04	13.69
steps	3 steps	3 steps	3 steps	4 steps	5 steps	5 steps	8 steps

Table 6. 11 Estimation errors of M2 and M4

FME (%)	±0.2	±0.5	±0.8	±1	±2	±5	±10
M2 Estimation Error (%)	0.64	1.21	2.24	3.25	6.75	11.14	45.23
M4 Estimation Error (%)	0.16	0.16	0.71	0.64	1.49	0.30	0.22
steps	3 steps	4 steps	3 steps	3 steps	4 steps	5 steps	8 steps

Accurate estimates can be achieved when the method is applied to estimate M3 and M4, when FME level is less than ±0.5 %. However, the results in Table 6.12 shows that the algorithm has poor robustness in this test. Convergence cannot be achieved when FME is ±0.8% and ±10%. Large estimation errors also occurred when FME is higher than ±1%.

Table 6. 12 Estimation errors of M3 and M4

FME (%)	±0.2	±0.5	±0.8	±1	±2	±5	±10
M3 Estimation Error (%)	2.59	5.77	N/A	10.84	17.48	36.54	N/A
M4 Estimation Error (%)	2.41	5.06	N/A	9.13	14.08	23.79	N/A
steps	3 steps	3 steps	N/A	4 steps	4 steps	5 steps	N/A

6.3.4 Three-Machine Estimation

In this section four scenarios are presented for the estimation of three inertia constants. The estimation results are given in Table 6.13 to Table 6.16. It is found that the algorithm could encounter divergence problems. In the estimation of 'M1, M2 and M3', and 'M1, M2 and M4', valid estimates cannot be produced at FME level, ±0.8%, ±5% and ±10%, due to divergence. Moreover, the estimates have large errors in the resultant estimates of M1 and M2 in these two scenarios when FME is larger than ±0.2%.

Table 6. 13 Estimation of M1, M2 and M3

FME (%)	±0.2	±0.5	±0.8	±1	±2	±5	±10
M1 Estimation Error (%)	5.72	14.57	N/A	30.17	60.29	N/A	N/A
M2 Estimation Error (%)	2.97	9.00	N/A	10.87	15.25	N/A	N/A
M3 Estimation Error (%)	0.86	1.93	N/A	4.20	7.99	N/A	N/A
steps	3 steps	4 steps	N/A	4 steps	5 steps	N/A	N/A

Table 6. 14 Estimation of M1, M2 and M4

FME (%)	±0.2	±0.5	±0.8	±1	±2	±5	±10
M1 Estimation Error (%)	4.40	11.70	N/A	23.46	45.16	N/A	N/A
M2 Estimation Error (%)	2.20	7.74	N/A	8.72	12.35	N/A	N/A
M4 Estimation Error (%)	0.64	1.44	N/A	3.13	6.02	N/A	N/A
steps	3 steps	4 steps	N/A	4 steps	4 steps	N/A	N/A

In the estimation of 'M1, M3 and M4', and 'M2, M3 and M4', large errors occur in M3 and M4 when FME level is larger than ±1%. Still, the proposed algorithm cannot converge at ±0.8% and ±10% FME.

Table 6. 15 Estimation of M1, M3 and M4

FME (%)	±0.2	±0.5	±0.8	±1	±2	±5	±10
M1 Estimation Error (%)	0.85	1.90	N/A	4.35	9.23	16.01	N/A
M3 Estimation Error (%)	2.00	6.92	N/A	8.69	13.53	43.67	N/A
M4 Estimation Error (%)	2.01	5.72	N/A	8.07	12.56	25.07	N/A
steps	3 steps	4 steps	N/A	4 steps	4 steps	6 steps	N/A

Table 6. 16 Estimation of M2, M3 and M4

FME (%)	±0.2	±0.5	±0.8	±1	±2	±5	±10
M2 Estimation Error (%)	0.59	1.36	N/A	2.97	6.22	12.23	N/A
M3 Estimation Error (%)	2.46	6.06	N/A	10.42	16.70	38.35	N/A
M4 Estimation Error (%)	2.32	5.23	N/A	8.90	13.77	24.06	N/A
steps	3 steps	3 steps	N/A	4 steps	4 steps	5 steps	N/A

6.4 Test on NY-NE System

The proposed method is tested on a larger system which consists of sixteen generators. To avoid a large amount of testing scenarios, the inertia constants of G1, G10, G14, G15 and G16 from different coherent groups were selected. The initial guess and actual values of the inertia constants of these generators are shown in Table 6.17.

Table 6. 17 Initial guess and true values for inertia constants of selected group in NY-NE system

Generator Inertia	Initial	True	SD(%)
M1	6.8000	7.8000	12.82
M10	5.8210	4.8210	20.74
M14	6.0000	6.8000	14.71
M15	6.0000	6.8000	14.71
M16	8.9000	9.9000	10.10

For a large power system, it is not practical to assume that the full observability is known. Thus, it is necessary for the algorithm to deal with the condition when the number of measurements is less than the number of parameters to be estimated. Two conditions are hence defined to test the proposed method, in terms of the number of measurements,

- Condition 1: more measurements than parameters
- Condition 2: more parameters than measurements

Three scenarios are designed based on the two conditions, because full observability is considered as a special scenario under the condition when there are more measurements than parameters. As it is shown, s_1 and s_2 are designed based on 'Condition 1', while s_3 is designed in terms of 'Condition 2'. Full observability is desirable for state estimation and system condition monitoring, but it is difficult to be obtained in practice. s_2 and s_3 are quite practical, while s_1 is ideal for testing purposes.

$$s_1: \{full\ observability\}$$

$$s_2: \{2, 6, 11, 12, 14, 15\}$$

$$s_3: \{2, 6, 12\}$$

It should be noted that s_3 which includes three modes is highly associated with all parameters to be estimated, because misusing non-sensitive modes would not contribute towards the estimation. Even worse, it may lead the algorithm to divergence or return irrational results. This can be explained mathematically. If we assume that there are more measurements than parameters to be estimated, the simultaneous equations (6.2) becomes over-determined. Therefore, according to the nature of least square method, relatively reasonable results can be obtained. However, if the number of measured modes is less than the number of parameters, (6.2) becomes under-determined, i.e. infinite number of solutions satisfies the equation. This suggests the results are invalid and do not have a physical meaning.

The sensitivity of the frequencies of all oscillatory modes to selected generator inertia constants is presented in Table 6.18. It is also illustrated in the bar charts from Figure 6.3 to Figure 6.7,

Table 6. 18 Frequency sensitivity to selected generator inertia constants

	M1	M10	M14	M15	M16
ω_1	-0.0426j	-0.0290j	-0.0001j	-0.0000j	-0.0002j
ω_2	-0.6690j	-0.0066j	-0.0000j	-0.0000j	-0.0000j
ω_3	-0.0002j	-0.0001j	-0.0000j	0.0000j	-0.0000j
ω_4	0.0000j	0.0000j	0.0000j	0.0000j	0.0000j
ω_5	-0.0108j	0.0514j	0.0001j	0.0000j	0.0001j
ω_6	-0.0023j	-0.6277j	-0.0006j	-0.0000j	-0.0004j
ω_7	-0.0001j	-0.0013j	-0.0000j	-0.0000j	-0.0000j
ω_8	-0.0000j	-0.0105j	-0.0001j	-0.0000j	-0.0002j
ω_9	-0.0000j	-0.0000j	0.0000j	0.0000j	0.0000j
ω_{10}	-0.0002j	-0.0029j	-0.0001j	-0.0000j	-0.0000j
ω_{11}	-0.0005j	-0.0004j	-0.0000j	-0.0000j	-0.0000j
ω_{12}	-0.0000j	-0.0001j	-0.1063j	-0.2423j	-0.0212j
ω_{13}	-0.0017j	0.0000j	-0.0008j	-0.0000j	-0.0017j
ω_{14}	-0.0001j	-0.0001j	-0.0997j	-0.0049j	-0.0949j
ω_{15}	-0.0007j	-0.0015j	-0.0321j	-0.0364j	-0.0140j

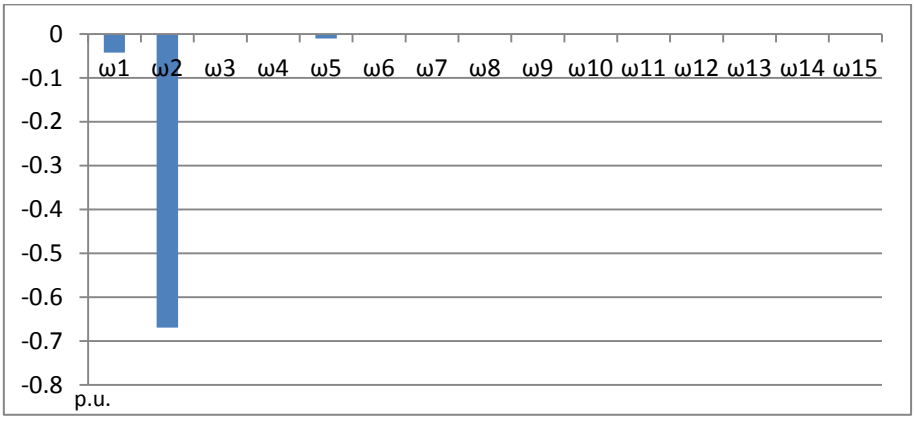

Figure 6.3 Sensitivity of modal frequencies to M1

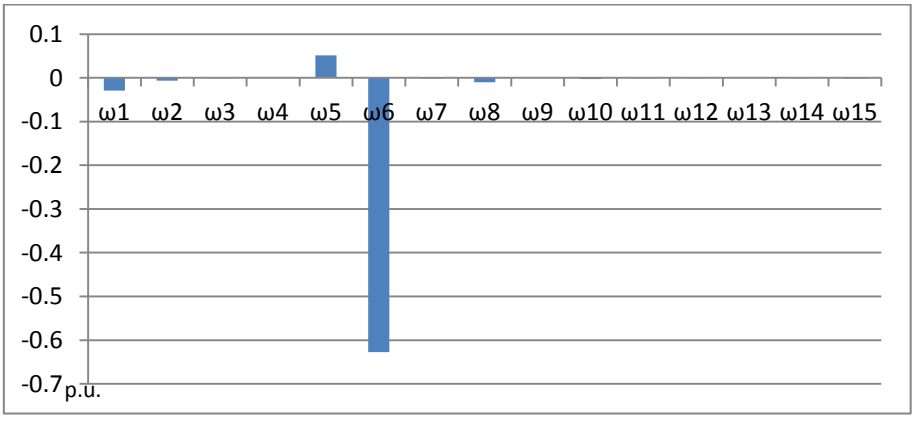

Figure 6.4 Sensitivity of modal frequencies to M10

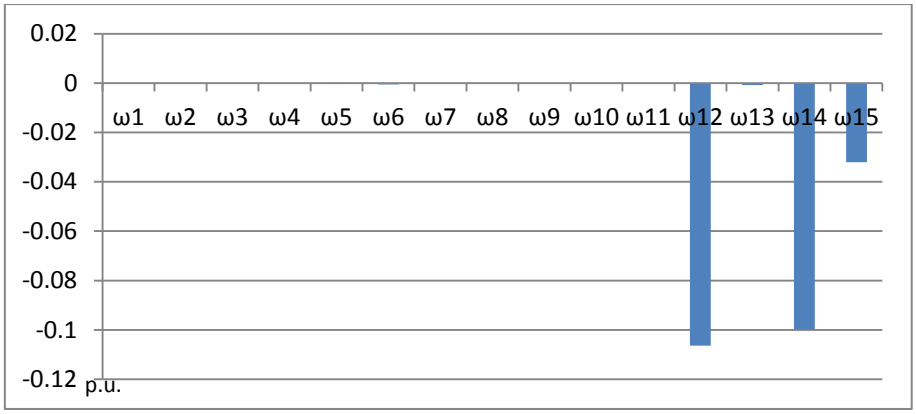

Figure 6.5 Sensitivity of modal frequencies to M14

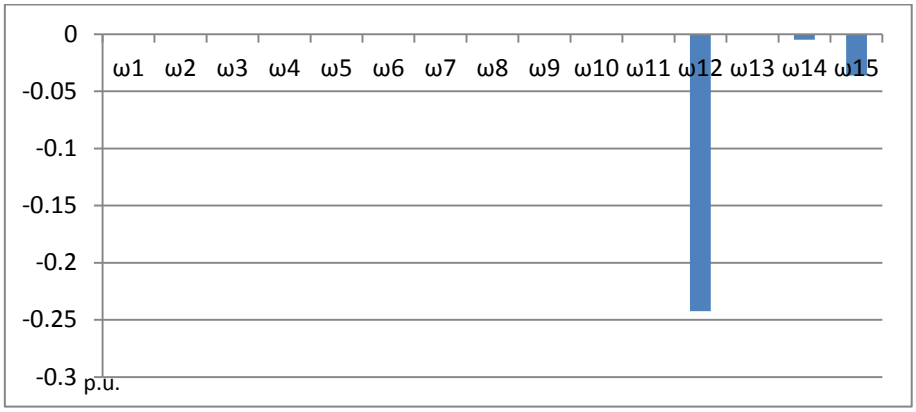

Figure 6.6 Sensitivity of modal frequencies to M15

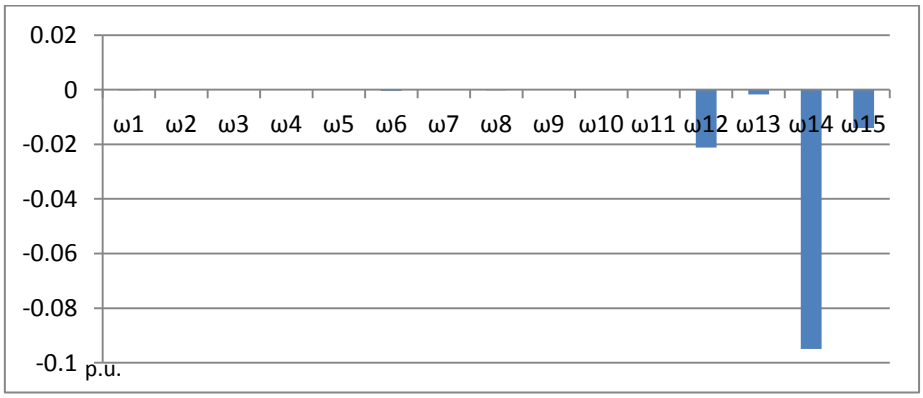

Figure 6.7 Sensitivity of modal frequencies to M16

6.4.1 Estimation with redundant measurements

The estimation results based on full observability are described in Table 6.19. The algorithm displays its limitation to use in large power systems. It cannot provide valid results when FME level is $\pm$0.5%, $\pm$2%, $\pm$5% and $\pm$10%. Accurate estimates can be achieved when FME is less $\pm$2%. Relatively accurate results are obtained when estimating M1, M10 and M15 at $\pm$0.8% and $\pm$1% FME level. However, the identified values of M14 and M16 were deviated significantly from their true values.

Similar results were obtained when the estimation is based on s_2. The accuracy did not vary much by using fewer measurements, as shown in Table 6.20. In addition, the results for the two cases are very similar.

Table 6. 19 Estimation based on s_1

FME (%)	$\pm$0.2	$\pm$0.5	$\pm$0.8	$\pm$1	$\pm$2	$\pm$5	$\pm$10
M1 Estimation Error (%)	0.42	N/A	1.28	2.10	N/A	N/A	N/A
M10 Estimation Error (%)	0.30	N/A	1.12	1.47	N/A	N/A	N/A
M14 Estimation Error (%)	3.97	N/A	13.91	12.41	N/A	N/A	N/A
M15 Estimation Error (%)	1.03	N/A	4.94	2.21	N/A	N/A	N/A
M16 Estimation Error (%)	3.00	N/A	9.04	9.32	N/A	N/A	N/A
steps	4 steps	N/A	5 steps	4 steps	N/A	N/A	N/A

Table 6. 20 Estimation based on s_2

FME (%)	$\pm$0.2	$\pm$0.5	$\pm$0.8	$\pm$1	$\pm$2	$\pm$5	$\pm$10
M1 Estimation Error (%)	0.40	N/A	1.35	2.03	N/A	N/A	N/A
M10 Estimation Error (%)	0.29	N/A	1.21	1.43	N/A	N/A	N/A
M14 Estimation Error (%)	3.90	N/A	13.94	12.33	N/A	N/A	N/A
M15 Estimation Error (%)	1.00	N/A	4.94	2.11	N/A	N/A	N/A
M16 Estimation Error (%)	2.95	N/A	9.06	9.27	N/A	N/A	N/A
steps	3 steps	N/A	4 steps	4 steps	N/A	N/A	N/A

6.4.2 Estimation with inadequate measurements

The proposed method does not converge to any results when the number of measurements is less than the number of parameters. This constrains the practical implementation of this method.

Table 6. 21 Estimation based on s_3

FME (%)	$\pm$0.2	$\pm$0.5	$\pm$0.8	$\pm$1	$\pm$2	$\pm$5	$\pm$10
M1 Estimation Error (%)	N/A	N/A	N/A	N/A	N/A	N/A	N/A
M10 Estimation Error (%)	N/A	N/A	N/A	N/A	N/A	N/A	N/A
M14 Estimation Error (%)	N/A	N/A	N/A	N/A	N/A	N/A	N/A
M15 Estimation Error (%)	N/A	N/A	N/A	N/A	N/A	N/A	N/A
M16 Estimation Error (%)	N/A	N/A	N/A	N/A	N/A	N/A	N/A
steps	N/A	N/A	N/A	N/A	N/A	N/A	N/A

6.5 Summary of Frequency Method

The frequency method minimises the difference of imaginary parts for the selected eigenvalues by moving the estimated frequencies as close as possible to the measured frequencies. The results showed that the method is not robust or accurate enough. This is due to high nonlinearity of the model, and thus the estimation was very sensitive to measurement noise. More importantly, the least square method can be under-determined when the number of measurements is less than the number of parameters. Thus, modal damping will be taken into account in the next step development of the method.

6.6 Frequency-Damping Method

Frequency method shows its limitation when estimating the inertia constants of the generators in a multi-machine system. The performance of this method is not robust, even in the case of the redundant measurements that are available. Thus, a new technique which minimises the difference of the entire eigenvalues is proposed in this section. By adding modal damping as an extra measurements to the objective function, the new objective function can be expressed as,

$$J(\Delta M) = \varepsilon_f^T W_f \varepsilon_f + \varepsilon_d^T W_d \varepsilon_d \quad (6.5)$$

where ε_d is a vector contains the errors between measured modal damping and estimated modal damping,

W_d is the weighting matrix that allows damping measurement uncertainty.

The optimal solution is written as,

$$\Delta M = \left(S_f^T W_f S_f + S_d^T W_d S_d\right)^{-1} (S_d^T W_d \Delta\sigma + S_f^T W_f \Delta\omega) \tag{6. 6}$$

Equation (6.5) is rewritten in iterative form as,

$$M_{k+1} = M_k + \left(S_{fk}^T W_f S_{fk} + S_{dk}^T W_d S_{dk}\right)^{-1} (S_{dk}^T W_d \Delta\sigma + S_{fk}^T W_f \Delta\omega) \tag{6. 7}$$

where S_{dk} is the modal damping sensitivity matrix at the k-th step.

The modal damping sensitivity matrix S_d can be defined as,

$$S_d = \begin{bmatrix} \frac{\partial\sigma_1}{\partial M_1} & \cdots & \frac{\partial\sigma_1}{\partial M_i} & \cdots & \frac{\partial\sigma_1}{\partial M_m} \\ \vdots & \ddots & \vdots & \ddots & \vdots \\ \frac{\partial\sigma_j}{\partial M_1} & \cdots & \frac{\partial\sigma_j}{\partial M_i} & \cdots & \frac{\partial\sigma_j}{\partial M_m} \\ \vdots & \ddots & \vdots & \ddots & \vdots \\ \frac{\partial\sigma_n}{\partial M_1} & \cdots & \frac{\partial\sigma_n}{\partial M_i} & \cdots & \frac{\partial\sigma_n}{\partial M_m} \end{bmatrix} \tag{6. 8}$$

The algorithm is illustrated in Figure 6.8,

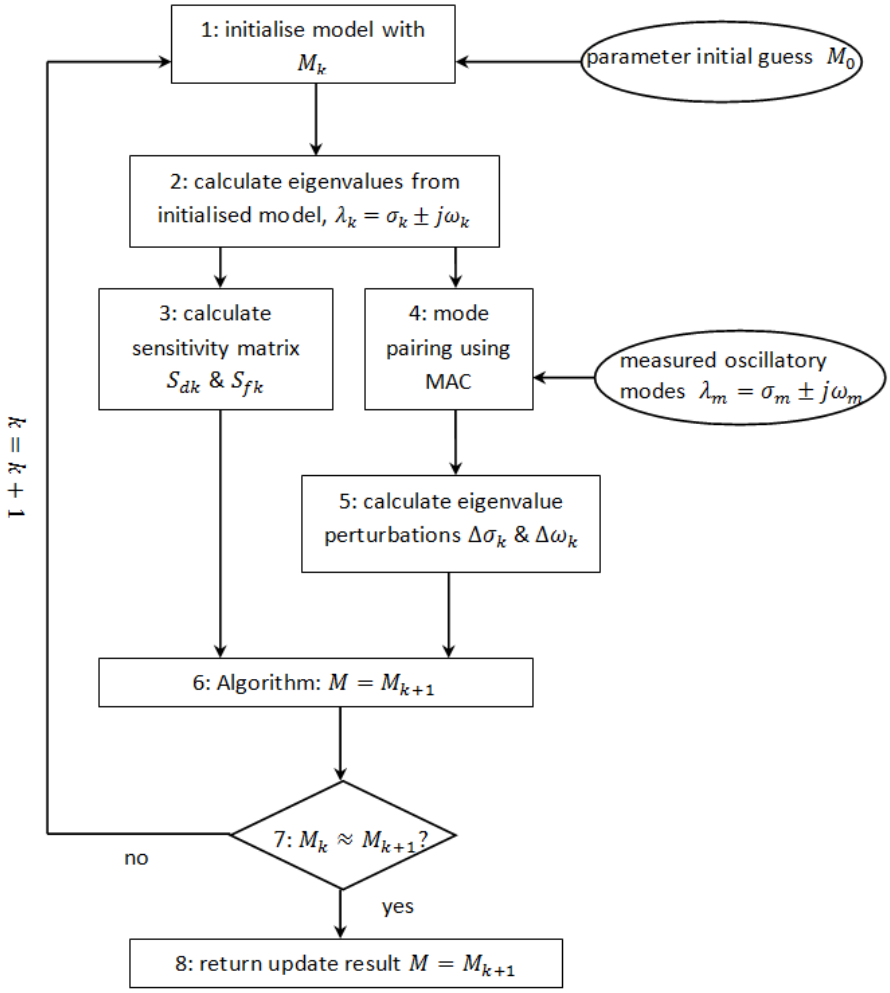

Figure 6. 8 Frequency-Damping method

By the inclusion of the damping measurements into the objective function, the measurement errors of damping also need to be introduced. The Damping Measurement Error (DME) range in the test was set to $\pm$5%, $\pm$10% and $\pm$20%., which will be used to form damping weighting matrix W_d. The flow chart is summarised,

1. Initialise system model with M_k (M_0, for the first time);
2. Calculate the eigenvalues of the initialised system model;
3. Calculate sensitivity matrix of modal frequency;
4. Pair eigenvalues calculated at step 2, with the measured eigenvalues;
5. Calculate perturbations between corresponding calculated frequencies and measured frequencies;

6. Update inertia constants using equation (6.7);
7. If the updated results are approximately equal to last update, then return results. Otherwise, go back to step 1.

6.7 Test on Two-Area System

Still, three categories of tests can be executed based on the number of inertia constants to be estimated. In all the tests, only the inertia constants to be identified change from their initial guess to the actual values, while the rest remain unchanged as initial values. The full observability is also assumed in this test.

The complex sensitivity matrix is shown in Table 6.22 where the real values are damping sensitivity and imaginary parts are frequency sensitivity. The sensitivity of modal frequencies to inertia constants are the same as that is shown in Table 6.2 and Figure 6.2, and the sensitivity of modal damping is presented in Figure 6.9. By comparing Figure 6.2, clearly the changes of inertia constants can be better reflected by the modal frequencies. However, the variances of modal damping is much smaller. By comparing this with to the summary of frequency method, the introduction of modal damping measurements can improve the estimation accuracy for selected cases.

Table 6. 22 mode sensitivity matrix

	M1	M2	M3	M4
ω_1	-0.0000-0.0000j	0.0001-0.0000j	0.0244-0.1812j	0.0213-0.2416j
ω_2	0.0111-0.0861j	0.0056-0.1269j	-0.0002-0.0020j	-0.0000-0.0006j
ω_3	0.0071-0.0180j	0.0051-0.0037j	-0.0028-0.0837j	-0.0018-0.0641j

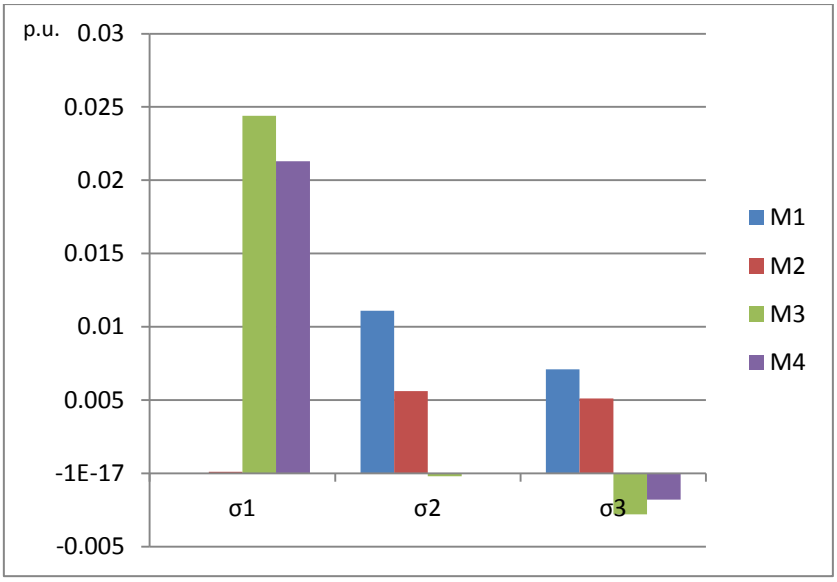

Figure 6. 9 Sensitivity of modal damping to inertia constants for two-area system

6.7.1 Single-Machine Estimation

The proposed method produces good estimates when identifying single machine inertia constant. Especially, the estimated results at ±10% DME level have been significantly improved in comparison to those in the frequency method. However, in some cases estimates that are significantly deviated from the true values still exist, especially when measurement errors are high. The estimation time increases with the growth of FME and DME.

In the estimation of M1, the algorithm shows the capability to produce estimates within 5.69% deviation when FME is within ±1%. When FME is more than ±1%, large errors occur in three cases, ±20% DME with ±2% FME, ±10% DME with ±5% FME, and ±20% DME with ±10% FME.

From Table 6.24 and 6.25, it can be seen that the algorithm can generate highly accurate estimates within ±2% FME in the identification of M2 and M3. However, large estimation errors still occur when FME becomes higher than ±2%.

The accuracy of the estimation results of M4 is shown in Table 6.26. Results with less than ±8% errors can be achieved when FME is within ±5% as.

Table 6. 23 Estimation of M1

FME(%) / DME(%)	±0.2	±0.5	±0.8	±1	±2	±5	±10
±5	1.03	0.92	2.16	4.95	7.31	0.07	5.46
	3 steps	3 steps	3 steps	2 steps	3 steps	5 steps	4 steps
±10	0.98	1.31	1.42	4.11	5.39	16.16	7.84
	3 steps	3 steps	3 steps	3 steps	2 steps	5 steps	3 steps
±20	1.04	0.97	2.33	5.69	11.78	0.95	38.73
	3 steps	3 steps	3 steps	2 steps	3 steps	4 steps	5 steps

Table 6. 24 Estimation of M2

FME(%) / DME(%)	±0.2	±0.5	±0.8	±1	±2	±5	±10
±5	0.64	1.16	2.36	3.33	6.72	3.54	14.61
	3 steps	3 steps	3 steps	3 steps	3 steps	6 steps	6 steps
±10	0.62	1.31	2.02	2.81	4.93	15.49	0.94
	3 steps	3 steps	2 steps	3 steps	2 steps	3 steps	4 steps
±20	0.63	1.21	2.31	3.27	6.78	8.37	29.46
	3 steps	3 steps	2 steps	2 steps	2 steps	4 steps	10 steps

Table 6. 25 Estimation of M3

FME(%) / DME(%)	±0.2	±0.5	±0.8	±1	±2	±5	±10
±5	0.03	0.15	0.39	0.08	1.59	6.10	10.78
	3 steps	3 steps	3 steps	4 steps	4 steps	4 steps	2 steps
±10	0.07	0.42	0.26	1.00	2.50	13.95	36.71
	3 steps	3 steps	3 steps	4 steps	4 steps	6 steps	7 steps
±20	0.06	0.30	0.03	0.53	0.63	3.74	9.35
	3 steps	3 steps	3 steps	4 steps	4 steps	6 steps	11 steps

Table 6. 26 Estimation of M4

FME(%) / DME(%)	±0.2	±0.5	±0.8	±1	±2	±5	±10
±5	0.16	0.31	0.45	1.00	3.00	7.96	13.24
	3 steps	3 steps	3 steps	3 steps	4 steps	3 steps	3 steps
±10	0.13	0.11	0.95	0.22	0.02	7.68	30.85
	3 steps	3 steps	3 steps	4 steps	4 steps	6 steps	10 steps
±20	0.15	0.20	0.74	0.58	1.46	1.82	4.69
	3 steps	3 steps	3 steps	4 steps	4 steps	7 steps	11 steps

6.7.2 Two-Machine Estimation

The estimates of the two inertia constants have been significantly improved when compared with those produced by frequency method, especially when FME is high. However, more number of iterations is required for the production of such results. It should be noted that convergence when estimating M3 and M4 at ±0.8% and ±10% FME still cannot be reached.

Moreover, the accuracy of the estimation do not change with FME and DME regularly. For example, the errors of the estimates at ±1% FME and ±5% DME result in 10.70% errors in the estimates of M1 and 3.64% in the estimates of M2. For the same FME, the increase of DME to ±10% caused a dramatic reduction in the error of M1 estimate from 10.70% to 0.48%, and a slight increase in the estimation of M2 from 3.64% to 5.00%. It should be noted that the resultant estimates changed significantly again for M1 from 0.48% to 13.37% when DME is increased to ±20%. It should be noted that high FME and DME can lead to divergence during the estimation of M1 and M2.

The two machine estimation tests showed that the method was not robust enough to deal with some cases, e.g. in the case of the estimation of M1 and M2. Also, divergence may occur when FME and DME at certain levels.

Table 6. 27 Estimation of M1 and M2

FME(%) / DME(%)		±0.2	±0.5	±0.8	±1	±2	±5	±10
±5	M1	2.56	7.56	17.61	10.70	14.88	27.01	13.50
	M2	1.06	5.74	22.53	3.64	26.95	25.63	33.82
		3 steps	4 steps	13 steps	9 steps	15 steps	4 steps	6 steps
±10	M1	2.17	5.48	15.72	0.48	7.35	6.40	16.17
	M2	0.83	4.72	18.24	5.00	11.94	11.22	16.63
		3 steps	3 steps	11 steps	3 steps	4 steps	9 steps	25 steps
±20	M1	2.58	7.56	7.13	13.37	19.34	21.17	N/A
	M2	1.07	5.74	8.30	4.56	4.20	17.29	N/A
		3 steps	4 steps	18 steps	6 steps	12 steps	57 steps	N/A

Table 6. 28 Estimation of M1 and M3

FME(%) / DME(%)		±0.2	±0.5	±0.8	±1	±2	±5	±10
±5	M1	1.09	1.00	2.36	5.22	7.66	0.54	3.66
	M3	0.17	0.32	0.76	0.91	2.36	6.23	9.92
		3 steps	3 steps	3 steps	4 steps	4 steps	6 steps	5 steps
±10	M1	1.02	1.52	1.39	4.00	4.86	16.85	5.94
	M3	0.11	0.70	0.03	0.26	1.64	15.84	35.28
		3 steps	3 steps	3 steps	4 steps	6 steps	5 steps	7 steps
±20	M1	1.08	1.13	2.45	5.89	12.48	1.91	38.18
	M3	0.14	0.51	0.45	0.56	1.66	4.13	2.11
		3 steps	3 steps	3 steps	3 steps	4 steps	6 steps	10 steps

Table 6. 29 Estimation of M1 and M4

FME(%) / DME(%)		±0.2	±0.5	±0.8	±1	±2	±5	±10
±5	M1	1.11	0.85	2.11	5.33	7.71	0.53	3.72
	M4	0.30	0.22	0.23	1.58	3.49	8.20	12.76
		3 steps	3 steps	3 steps	4 steps	4 steps	5 steps	5 steps
±10	M1	1.05	1.31	1.19	4.30	5.47	19.72	6.37
	M4	0.26	0.05	0.82	7.43	0.64	9.11	28.45
		3 steps	3 steps	3 steps	4 steps	5 steps	6 steps	8 steps
±20	M1	1.11	0.94	2.17	6.08	12.78	0.69	41.78
	M4	0.28	0.09	0.49	1.33	3.01	1.65	12.17
		3 steps	3 steps	3 steps	3 steps	4 steps	6 steps	11 steps

Table 6. 30 Estimation of M2 and M3

FME(%) / DME(%)		±0.2	±0.5	±0.8	±1	±2	±5	±10
±5	M2	0.64	1.16	2.38	3.37	6.77	4.52	11.56
	M3	0.00	0.19	0.48	0.21	1.61	6.89	8.59
		3 steps	3 steps	3 steps	4 steps	4 steps	6 steps	7 steps
±10	M2	0.61	1.33	2.00	2.79	4.86	15.44	4.21
	M3	0.04	0.48	0.18	0.86	2.29	13.96	37.89
		3 steps	3 steps	3 steps	4 steps	5 steps	6 steps	7 steps
±20	M2	0.64	1.22	2.30	3.27	6.80	8.55	29.48
	M3	0.02	0.36	0.13	0.36	0.27	4.21	8.52
		3 steps	3 steps	3 steps	4 steps	4 steps	6 steps	11 steps

Table 6. 31 Estimation of M2 and M4

FME(%) / DME(%)		±0.2	±0.5	±0.8	±1	±2	±5	±10
±5	M2	0.65	1.20	2.35	3.38	6.72	4.52	11.55
	M4	0.18	0.17	0.40	1.10	2.94	8.60	11.78
		3 steps	3 steps	3 steps	3 steps	3 steps	6 steps	6 steps
±10	M2	0.62	1.30	1.98	2.83	4.92	15.43	2.91
	M4	0.15	0.08	0.91	0.30	0.10	7.58	31.97
		3 steps	3 steps	3 steps	5 steps	4 steps	6 steps	10 steps
±20	M2	0.64	1.20	2.27	3.30	6.86	8.32	29.46
	M4	0.16	0.17	0.68	0.68	1.66	1.65	5.60
		3 steps	3 steps	3 steps	4 steps	4 steps	6 steps	10 steps

Table 6. 32 Estimation of M3 and M4

FME(%) / DME(%)		±0.2	±0.5	±0.8	±1	±2	±5	±10
±5	M3	0.18	5.43	N/A	9.80	14.18	21.21	21.06
	M4	0.65	4.92	N/A	8.89	13.74	22.45	26.34
		3 steps	3 steps	N/A	4 steps	5 steps	6 steps	7 steps
±10	M3	0.62	5.95	N/A	11.32	18.84	41.68	N/A
	M4	0.15	5.12	N/A	9.16	13.79	20.57	N/A
		3 steps	3 steps	N/A	4 steps	5 steps	7 steps	N/A
±20	M3	0.64	5.77	N/A	10.88	17.70	38.15	N/A
	M4	0.17	5.07	N/A	9.20	14.39	25.39	N/A
		3 steps	3 steps	N/A	5 steps	5 steps	7 steps	N/A

6.7.3 Three-Machine Estimation

Divergence still exists when FME is at ±0.8%, ±5% and ±10% in three-machine estimation. However, the ability for the algorithm to converge is improved by using this method.

During the estimation of M1, M2 and M3, at ±0.5% FME, the proposed method can converge when DME is less than ±5%. At ±5% and ±10% FME, convergence can be achieved when DME is up to ±10%. In comparison to frequency method, the accuracy of the estimation for this case has been significantly improved, especially when FME is greater than ±0.8%. Similar results can be obtained for the estimation of M1, M2 and M4 as shown in Table 6.14. However, divergence still exists in some cases.

Table 6. 33 Estimation of M1, M2 and M3

FME(%) / DME(%)		±0.2	±0.5	±0.8	±1	±2	±5	±10
±5	M1	5.94	14.38	18.74	16.47	9.86	26.27	13.39
	M2	3.09	9.00	24.35	6.53	1.25	25.58	31.70
	M3	0.91	2.00	1.36	2.50	2.65	5.29	6.52
		5 steps	5 steps	8 steps	8 steps	35 steps	5 steps	6 steps
±10	M1	4.74	8.58	N/A	4.45	12.94	18.37	17.62
	M2	2.41	6.36	N/A	0.15	18.43	1.88	24.44
	M3	0.69	0.87	N/A	0.41	3.86	16.17	39.81
		4 steps	4 steps	N/A	6 steps	10 steps	11 steps	17 steps
±20	M1	5.81	14.09	N/A	25.02	31.52	N/A	N/A
	M2	3.01	8.77	N/A	9.17	8.50	N/A	N/A
	M3	0.87	1.87	N/A	3.51	4.57	N/A	N/A
		4 steps	5 steps	N/A	5 steps	10 steps	N/A	N/A

Table 6. 34 Estimation of M1, M2 and M4

FME(%) / DME(%)		±0.2	±0.5	±0.8	±1	±2	±5	±10
±5	M1	4.54	12.04	18.76	15.36	10.59	25.78	13.28
	M2	2.28	7.97	24.35	6.02	1.82	25.35	31.00
	M4	0.67	1.56	1.73	2.56	3.73	7.57	10.18
		4 steps	5 steps	8 steps	6 steps	23 steps	4 steps	5 steps
±10	M1	3.83	8.19	N/A	8.00	8.93	12.78	17.80
	M2	1.87	6.15	N/A	2.24	13.66	4.73	23.68
	M4	0.56	0.97	N/A	1.17	0.74	8.65	34.32
		3 steps	4 steps	N/A	4 steps	5 steps	23 steps	12 steps
±20	M1	4.47	11.48	N/A	20.80	28.87	24.86	N/A
	M2	2.23	7.63	N/A	7.68	7.68	18.25	N/A
	M4	0.64	1.42	N/A	2.90	4.72	5.03	N/A
		4 steps	4 steps	N/A	4 steps	8 steps	45 steps	N/A

Convergence still cannot be reached for the two cases, during the estimation of 'M1, M3 and M4', and 'M2, M3 and M4' at ±0.8% FME. However, it can be achieved when FME is ±10% and DME is within ±5%. The estimation errors in these two cases are also reduced in comparison with that are estimated by frequency method.

Table 6. 35 Estimation of M1, M3 and M4

FME(%) / DME(%)		±0.2	±0.5	±0.8	±1	±2	±5	±10
±5	M1	0.88	1.61	N/A	4.30	6.77	0.70	8.06
	M3	1.92	6.41	N/A	7.91	12.66	22.13	32.96
	M4	1.96	5.51	N/A	7.92	13.11	22.89	29.97
		3 steps	4 steps	N/A	5 steps	5 steps	6 steps	7 steps
±10	M1	0.79	2.21	N/A	2.75	2.95	17.41	N/A
	M3	2.09	7.25	N/A	10.32	17.74	45.10	N/A
	M4	2.07	5.86	N/A	8.54	13.38	21.23	N/A
		3 steps	4 steps	N/A	4 steps	4 steps	8 steps	N/A
±20	M1	0.86	1.81	N/A	4.60	9.82	5.77	N/A
	M3	1.99	6.87	N/A	8.60	13.56	40.54	N/A
	M4	2.00	5.70	N/A	8.04	12.80	25.82	N/A
		3 steps	3 steps	N/A	4 steps	5 steps	7 steps	N/A

Table 6. 36 Estimation of M2, M3 and M4

FME(%) / DME(%)		±0.2	±0.5	±0.8	±1	±2	±5	±10
±5	M2	0.60	1.27	N/A	3.20	6.76	2.30	26.83
	M3	2.39	5.69	N/A	9.45	14.27	20.15	50.12
	M4	2.28	5.08	N/A	8.70	13.77	22.13	33.63
		3 steps	3 steps	N/A	5 steps	4 steps	5 steps	9 steps
±10	M2	0.57	1.45	N/A	2.55	4.48	15.47	N/A
	M3	2.51	6.25	N/A	10.99	18.43	41.72	N/A
	M4	2.34	5.30	N/A	8.98	13.61	20.41	N/A
		3 steps	3 steps	N/A	4 steps	4 steps	6 steps	N/A
±20	M2	0.59	1.34	N/A	3.02	6.34	9.31	N/A
	M3	2.46	6.06	N/A	10.45	16.93	39.41	N/A
	M4	2.32	5.24	N/A	8.97	14.08	25.54	N/A
		3 steps	3 steps	N/A	3 steps	4 steps	6 steps	N/A

6.8 Test on NY-NE System

The same tests are performed in this section as those in section 6.4 by using frequency-damping method instead of frequency method. The tests are also based on the two conditions, redundant measurements and inadequate measurements, and three scenarios are designed.

The sensitivity of both modal frequency and modal damping calculated based on initial guess is given in Table 6.37. Figure 6.3-6.7 already illustrated sensitivity of modal frequencies to each inertia

constants to be estimated. The modal damping sensitivity to inertia constants are presented in Figure 6.10 to Figure 6.14. Clearly, the sensitivity of the modal damping is much lower than the sensitivity of frequency.

Table 6. 37 Modal sensitivity to inertia constants

	M1	M10	M14	M15	M16
ω_1	-0.0083-0.0426j	0.0002-0.0290j	0.0000-0.0001j	-0.0000-0.0000j	0.0000-0.0002j
ω_2	0.0832-0.6690j	-0.0022-0.0066j	-0.0000-0.0000j	-0.0000-0.0000j	-0.0000-0.0000j
ω_3	-0.0000-0.0002j	-0.0001-0.0001j	-0.0000-0.0000j	-0.0000+0.0000j	0.0000-0.0000j
ω_4	0.0000+0.0000j	0.0000+0.0000j	-0.0000+0.0000j	-0.0000+0.0000j	-0.0000+0.0000j
ω_5	0.0171-0.0108j	-0.1135+0.0514j	0.0001+0.0001j	0.0000+0.0000j	-0.0000+0.0001j
ω_6	-0.0057-0.0023j	0.1366-0.6277j	-0.0001-0.0006j	0.0000-0.0000j	-0.0000-0.0004j
ω_7	-0.0001-0.0001j	-0.0006-0.0013j	-0.0000-0.0000j	-0.0000-0.0000j	-0.0000-0.0000j
ω_8	0.0000-0.0000j	0.0042-0.0105j	0.0000-0.0001j	0.0000-0.0000j	-0.0000-0.0002j
ω_9	-0.0000-0.0000j	-0.0000-0.0000j	0.0000+0.0000j	0.0000+0.0000j	-0.0000+0.0000j
ω_{10}	0.0001-0.0002j	0.0009-0.0029j	-0.0000-0.0001j	-0.0000-0.0000j	-0.0000-0.0000j
ω_{11}	0.0001-0.0005j	-0.0001-0.0004j	-0.0000-0.0000j	-0.0000-0.0000j	-0.0000-0.0000j
ω_{12}	-0.0000-0.0000j	0.0000-0.0001j	0.0046-0.1063j	0.0099-0.2423j	0.0004-0.0212j
ω_{13}	0.0002-0.0017j	-0.0000+0.0000j	0.0001-0.0008j	-0.0001-0.0000j	0.0003-0.0017j
ω_{14}	0.0000-0.0001j	0.0000-0.0001j	0.0064-0.0997j	0.0009-0.0049j	0.0033-0.0949j
ω_{15}	0.0001-0.0007j	0.0002-0.0015j	0.0022-0.0321j	0.0028-0.0364j	0.0016-0.0140j

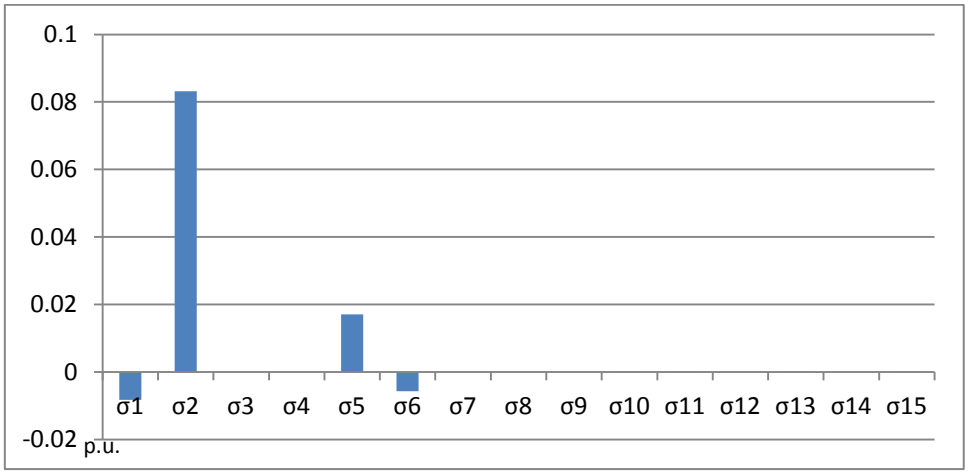

Figure 6.10 Sensitivity of modal damping to M1

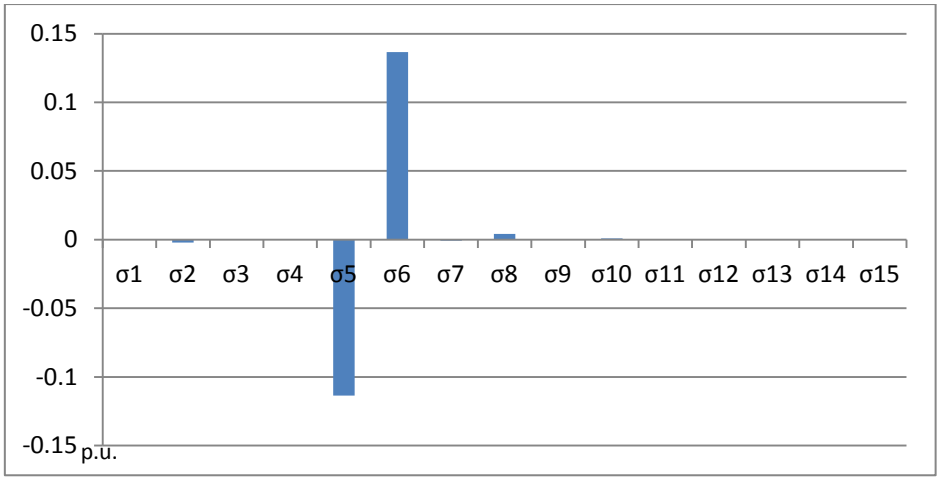

Figure 6.11 Sensitivity of modal damping to M10

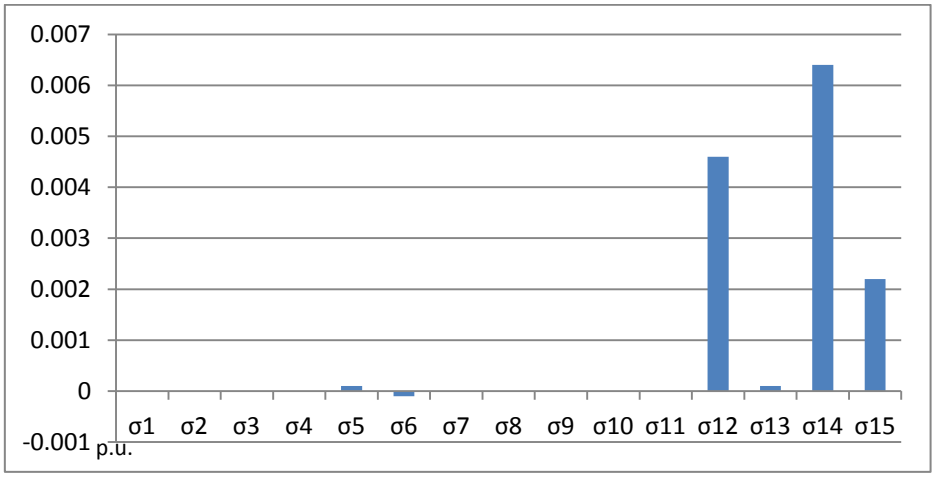

Figure 6.12 Sensitivity of modal damping to M14

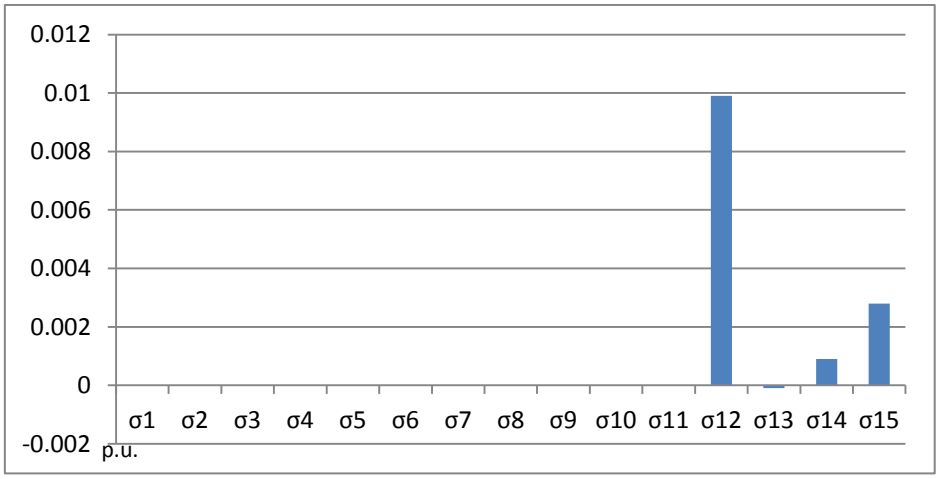

Figure 6.13 Sensitivity of modal damping to M15

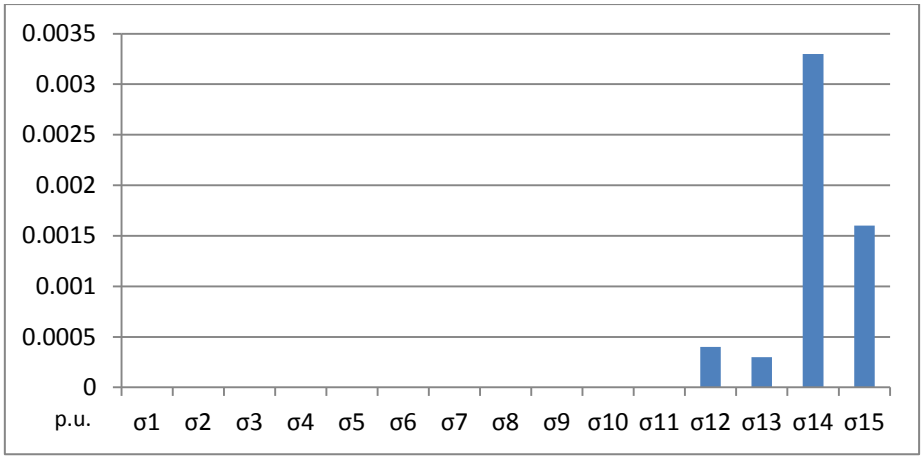

Figure 6.14 Sensitivity of modal damping to M16

6.8.1 Estimation with Redundant Measurements

With redundant measurements, when FME is at ±0.5%, ±2% and ±10% respectively, no results can be produced by the proposed method due to the divergence. At ±5% FME, convergence is also unavailable when DME is over ±5%. However, the estimation errors are slightly reduced in this simulation in comparison with those provided by frequency method.

Table 6. 38 Estimation based on s_1

FME(%) / DME(%)		±0.2	±0.5	±0.8	±1	±2	±5	±10
±5	M1	0.39	N/A	0.92	1.49	N/A	1.28	N/A
	M10	0.29	N/A	1.01	1.28	N/A	21.54	N/A
	M14	3.86	N/A	12.76	10.20	N/A	16.65	N/A
	M15	1.01	N/A	4.95	2.04	N/A	13.53	N/A
	M16	2.93	N/A	8.43	8.09	N/A	16.69	N/A
		4 steps	N/A	4 steps	4 steps	N/A	12 steps	N/A
±10	M1	0.41	N/A	1.11	1.81	N/A	N/A	N/A
	M10	0.29	N/A	1.06	1.37	N/A	N/A	N/A
	M14	4.04	N/A	13.37	11.51	N/A	N/A	N/A
	M15	1.05	N/A	4.84	1.96	N/A	N/A	N/A
	M16	3.04	N/A	8.63	8.63	N/A	N/A	N/A
		4 steps	N/A	7 steps	7 steps	N/A	N/A	N/A
±20	M1	0.42	N/A	1.32	2.14	N/A	N/A	N/A
	M10	0.30	N/A	1.16	1.53	N/A	N/A	N/A
	M14	0.04	N/A	13.58	11.87	N/A	N/A	N/A
	M15	1.04	N/A	4.86	1.99	N/A	N/A	N/A
	M16	3.02	N/A	8.82	8.96	N/A	N/A	N/A
		4 steps	N/A	6 steps	6 steps	N/A	N/A	N/A

Table 6. 39 Estimation based on s_2

FME(%) / DME(%)		±0.2	±0.5	±0.8	±1	±2	±5	±10
±5	M1	0.38	N/A	1.02	1.48	N/A	0.02	N/A
	M10	0.28	N/A	1.08	1.20	N/A	20.66	N/A
	M14	3.78	N/A	12.73	10.01	N/A	16.11	N/A
	M15	0.98	N/A	4.94	1.99	N/A	13.36	N/A
	M16	2.88	N/A	8.41	7.96	N/A	16.43	N/A
		4 steps	N/A	4 steps	4 steps	N/A	17 steps	N/A
±10	M1	0.40	N/A	1.20	1.78	N/A	N/A	N/A
	M10	0.28	N/A	1.13	1.29	N/A	N/A	N/A
	M14	3.97	N/A	13.39	11.42	N/A	N/A	N/A
	M15	1.03	N/A	4.84	1.94	N/A	N/A	N/A
	M16	2.99	N/A	8.64	8.57	N/A	N/A	N/A
		5 steps	N/A	7 steps	7 steps	N/A	N/A	N/A
±20	M1	0.41	N/A	1.40	2.10	N/A	N/A	N/A
	M10	0.29	N/A	1.24	1.47	N/A	N/A	N/A
	M14	3.93	N/A	13.60	11.78	N/A	N/A	N/A
	M15	1.01	N/A	4.86	1.97	N/A	N/A	N/A
	M16	2.97	N/A	8.83	8.89	N/A	N/A	N/A
		4 steps	N/A	6 steps	6 steps	N/A	N/A	N/A

6.8.2 Estimation with Inadequate Measurements

The frequency-damping method cannot deal with the situation when the number of parameters to be estimated is more than that of the measurements. As shown in Table 6.40, no estimation results can be provided due to algorithm divergence, since the damping measurements do not contribute much to the iterative estimation in (6.7). In other words, it is caused by the fact that the sensitivity of modal damping is much lower than that of modal frequency.

Table 6. 40 Estimation based on s_3

FME(%) / DME(%)		±0.2	±0.5	±0.8	±1	±2	±5	±10
±5	M1	N/A	N/A	N/A	N/A	N/A	N/A	N/A
	M10	N/A	N/A	N/A	N/A	N/A	N/A	N/A
	M14	N/A	N/A	N/A	N/A	N/A	N/A	N/A
	M15	N/A	N/A	N/A	N/A	N/A	N/A	N/A
	M16	N/A	N/A	N/A	N/A	N/A	N/A	N/A
		N/A	N/A	N/A	N/A	N/A	N/A	N/A
±10	M1	N/A	N/A	N/A	N/A	N/A	N/A	N/A
	M10	N/A	N/A	N/A	N/A	N/A	N/A	N/A
	M14	N/A	N/A	N/A	N/A	N/A	N/A	N/A
	M15	N/A	N/A	N/A	N/A	N/A	N/A	N/A
	M16	N/A	N/A	N/A	N/A	N/A	N/A	N/A
		N/A	N/A	N/A	N/A	N/A	N/A	N/A
±20	M1	N/A	N/A	N/A	N/A	N/A	N/A	N/A
	M10	N/A	N/A	N/A	N/A	N/A	N/A	N/A
	M14	N/A	N/A	N/A	N/A	N/A	N/A	N/A
	M15	N/A	N/A	N/A	N/A	N/A	N/A	N/A
	M16	N/A	N/A	N/A	N/A	N/A	N/A	N/A
		N/A	N/A	N/A	N/A	N/A	N/A	N/A

6.9 Summary of Frequency-Damping Method

It was found that the frequency method was not capable to deal with the case when there are fewer measurements than parameters. To circumvent this problem, frequency-damping method which includes both frequency and damping into the objective function has been developed. Thus, the estimated results are produced to move both frequency and damping as close as possible to the measured values. The simulation results showed that the estimation errors could be reduced for some cases when the damping was weighted higher.

Generally, the performance of this method also has poor robustness at different levels of FME and DME due to the fact that the high nonlinearity of the model. Thus, the frequency-damping method still cannot deal with the scenarios when there is a lack of measurement data, which significantly restricts the practical implementation of this method.

It should be note that the estimation errors increase with the growth of measurement error levels, and they are more sensitive to FME than DME. In other words, the FME level determines the estimation error levels mainly. This again can be interpreted by the sensitivity difference between the two types of measurements. Algorithm divergence can also be caused by particular measurement errors. This is due to the nonlinearity of the algorithm, thus the results are highly dependent on input measurement errrors.

6.10 Conclusions

In this chapter, two approaches have been proposed for the use of estimating the inertia constants of synchronous generators using system modal measurements with different levels of errors.

The frequency method seeks the optimal solutions through the minimisation of the difference between the estimated system modal frequencies and the measured modal frequencies. The algorithm only requires the information of modal frequencies. The initial tests of this method on two-area system showed that it could produce accurate results when the measured frequencies were at low FME, but incorrect estimation results occurred when FME was high. Moreover, it could not guarantee the convergence of the algorithm. Convergence is highly dependent on a particular FME. Furthermore, the method was also tested in the NY-NE system with two conditions, redundant measurements and inadequate measurements. It was discovered that the proposed method could not converge and deal with the condition of inadequate measurements. Practically, it cannot be avoided that the number of measurements is smaller than the number of parameters to be updated. Thus, the implementation of the proposed method is highly restricted.

By minimising the difference between measured modes and estimated modes, frequency-damping method was developed by introducing extra measurements into the estimation. The tests for both two-area system and NY-NE systems showed that the estimation errors were reduced slightly for some tests. Similarly for frequency method, the frequency-damping method cannot deal with the

situation when the number of parameters to be estimated is more than that of the measurements due to damping measurements do not contribute much to the optimisation search.

From the estimated results in this chapter, it also can be seen that the two proposed algorithms have poor performance in some tests even when there are more measurements than parameters, and they are completely invalid to deal with the situation that lacks of measurement data.

Chapter 7 Iterative Parameter Estimation With Pseudomeasurement

7.1 Introduction

In this chapter, two measurement-parameter-based methods are proposed in order to solve the divergence problems which occurred frequently in the measurement-based methods. The main reason that caused the algorithm to diverge is because the number of unknown parameters exceeded the number of measured modes, equation (6.2) and (6.7) become under-determined. Thus, there are an infinite number of sets of parameter differences that satisfy these two equations. It was suggested in [102] that the set that produces the smallest parameter changes is preferable. Based on the existing two measurement-based methods, two measurement-parameter-based methods will be explained in this chapter.

In order to minimise parameter changes, initial guess of unknown parameters were selected as reference. Moreover, the initial guess of unknown parameters mainly plays as pseudo-measurements in the estimation, for the purpose of introducing more measurements.

7.2 Frequency-Pseudomeasurements Method

The frequency-pseudomeasurements method was developed in terms of frequency method by adding a term which reflects the change of parameters into the objective function in (7.1). The objective function for this method is then written as,

$$J(\Delta M) = \varepsilon_f^T W_f \varepsilon_f + (M - M_0)^T W_p (M - M_0) \quad (7.1)$$

where $M_0$is the initial guess for inertia constant and W_p is the parameter weighting matrix.

W_p is diagonal matrix and positive definite. The diagonal elements in W_p are the reciprocals of the estimated variance of the corresponding parameters. W_p is important because the parameter estimation are not equally accurate. Thus, it is desirable to assign accordingly to the weight of each

parameter. To determine the variance, some engineering insight was required. Normally, the method to estimate the elements in the parameter weighting matrix is based on the predicted Standard Deviation (SD) which provides a quantitative estimation of the uncertainty.

The optimal solution can be achieved and presented in (7.2),

$$\Delta M = \left[S_f^{k^T} W_f S_f^k + W_p\right]^{-1} \left[S_f^{k^T} W_f(\omega_m - \omega_k) - W_p(M_k - M_0)\right] \quad (7.2)$$

where S_f is modal frequency sensitivity matrix which is defined in (6.3).

Equation (7.2) can be further expanded into an iterative form as is shown in (7.3),

$$M_{k+1} = M_k + \left[S_f^{k^T} W_f S_f^k + W_p\right]^{-1} \left[S_f^{k^T} W_f(\omega_m - \omega_k) - W_p(M_k - M_0)\right] \quad (7.3)$$

The frequency-pseudomeasurements method can be outlined in a flow chart as shown in Figure 7.1. The oval shapes represent the input data and the rectangular shapes represent the necessary steps in the algorithm. In this method, only modal frequency measurements and parameter initial guess are needed.

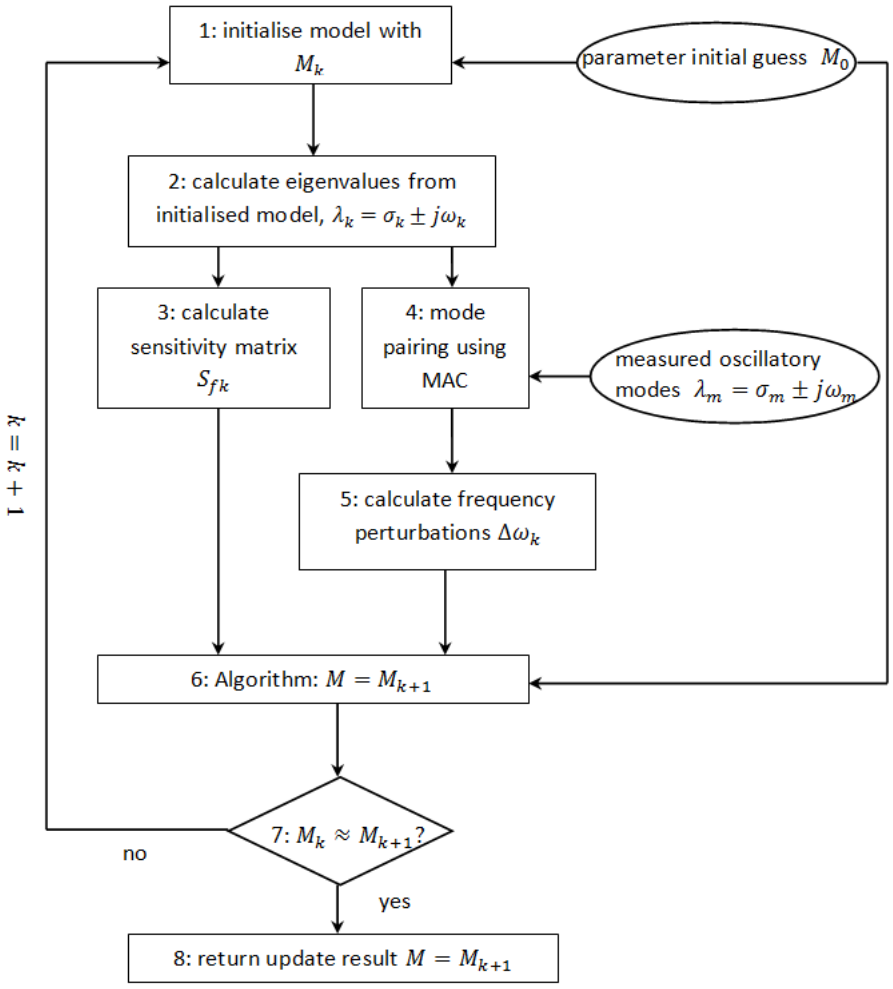

Figure 7. 1 Frequency-Pseudomeasurements method

The estimation errors are calculated based on (6.4). The FME is set as $\pm$0.2%, $\pm$0.5% $\pm$0.8%, $\pm$1.0%, $\pm$2.0%, $\pm$5.0% and $\pm$10% respectively to investigate the robustness of the method. DME was not considered in this method, since only the modal frequencies are involved in the algorithm. The flow chart is summarised as,

1. Initialise system model with M_k (M_0, for the first time);
2. Calculate the eigenvalues of the initialised system model;
3. Calculate sensitivity matrix of modal frequency;
4. Pair eigenvalues calculated at step 2, with the measured eigenvalues;
5. Calculate perturbations between corresponding calculated frequencies and measured frequencies;

6. Update inertia constants using equation (7.3);
7. If the updated results are approximately equal to last update, then return results. Otherwise, go back to step 1.

7.3 Test on Two-Area System

The initial guess and actual values of inertia constants in this system were shown in Table 5.1. To calculate the weighting matrix of parameter changes, W_p, standard deviation of estimating M1, M2, M3 and M4 are all set as 10% as a target of the simulation. Three types of tests were conducted based on the number of inertia constants to be estimated with full observability. The change of inertia constant confirms with that was stated in Chapter 6. The modal frequency sensitivity matrix is provided in Table 6.2.

7.3.1 Single-Machine Estimation

It can be seen from Table 7.1 and 7.2, accurate estimation were achieved when FME is less than $\pm$2% for the estimation of M1 and M2. It should be noted that the estimation error for both M1 and M2 dropped at $\pm$5% FME to an acceptable estimation error range. However, the general trend of errors increases with the increase of FME.

FME (%)	$\pm$0.2	$\pm$0.5	$\pm$0.8	$\pm$1	$\pm$2	$\pm$5	$\pm$10
M1 Estimation Error (%)	1.07	0.69	2.78	5.95	9.94	5.40	11.00
steps	3 steps	3 steps	3 steps	2 steps	2 steps	3 steps	3 steps

Table 7. 1 Estimation of M1

FME (%)	$\pm$0.2	$\pm$0.5	$\pm$0.8	$\pm$1	$\pm$2	$\pm$5	$\pm$10
M2 Estimation Error (%)	0.66	1.03	2.61	3.66	7.16	2.36	10.87
steps	3 steps	3 steps	3 steps	3 steps	2 steps	5 steps	3 steps

Table 7. 2 Estimation of M2

The proposed method performs slightly better when estimating M3 and M4 individually. As it is shown in Table 7.3 and 7.4, precise estimates are obtained when FME is up to $\pm$5%. In all four cases,

single-machine estimation can be completed within very short time and the main trend of errors is growing with the increase of FME.

Table 7. 3 Estimation of M3

FME (%)	0.2%	0.5%	0.8%	1%	2%	5%	10%
M3 Estimation Error (%)	0.01	0.01	0.68	0.55	2.63	6.17	8.17
steps	3 steps	4 steps	3 steps	3 steps	3 steps	2 steps	2 steps

Table 7. 4 Estimation of M4

FME (%)	0.2%	0.5%	0.8%	1%	2%	5%	10%
M4 Estimation Error (%)	0.19	0.44	0.10	1.43	3.81	7.39	9.16
steps	3 steps	3 steps	3 steps	4 steps	3 steps	3 steps	3 steps

7.3.2 Two-Machine Estimation

When estimating the inertias of two machines, the proposed method produced a precise estimation when FME is below $\pm$1%, as shown in Table 7.5 to Table 7.10. The estimation can be completed within short steps. However, in the estimation of M3 and M4, small estimation errors were achieved when FME is up to $\pm$5%.

Table 7. 5 Estimation of M1 and M2

FME (%)	$\pm$0.2	$\pm$0.5	$\pm$0.8	$\pm$1	$\pm$2	$\pm$5	$\pm$10
M1 Estimation Error (%)	2.50	5.47	1.72	6.73	7.38	5.38	10.29
M2 Estimation Error (%)	0.99	4.38	3.90	0.36	3.57	1.42	10.20
steps	3 steps	4 steps	4 steps	5 steps	4 steps	5 steps	3 steps

Table 7. 6 Estimation of M1 and M3

FME (%)	$\pm$0.2	$\pm$0.5	$\pm$0.8	$\pm$1	$\pm$2	$\pm$5	$\pm$10
M1 Estimation Error (%)	1.14	0.73	3.13	6.50	10.91	5.96	11.21
M3 Estimation Error (%)	0.20	0.14	1.17	1.60	3.94	6.49	8.38
steps	3 steps	3 steps	4 steps	3 steps	3 steps	4 steps	3 steps

Table 7. 7 Estimation of M1 and M4

FME (%)	$\pm$0.2	$\pm$0.5	$\pm$0.8	$\pm$1	$\pm$2	$\pm$5	$\pm$10
M1 Estimation Error (%)	1.16	0.59	2.81	6.52	10.83	5.91	11.17
M4 Estimation Error (%)	0.33	0.38	0.20	2.14	4.70	7.62	9.32
steps	3 steps	3 steps	3 steps	4 steps	3 steps	3 steps	4 steps

Table 7. 8 Estimation of M2 and M3

FME (%)	±0.2	±0.5	±0.8	±1	±2	±5	±10
M2 Estimation Error (%)	0.66	1.02	2.64	3.72	7.32	2.50	10.93
M3 Estimation Error (%)	0.03	0.06	0.79	0.73	2.88	6.23	8.22
steps	3 steps	3 steps	3 steps	3 steps	3 steps	4 steps	3 steps

Table 7. 9 Estimation of M2 and M4

FME (%)	±0.2	±0.5	±0.8	±1	±2	±5	±10
M2 Estimation Error (%)	0.67	1.01	2.60	3.73	7.29	2.47	10.91
M4 Estimation Error (%)	0.21	0.42	0.04	1.53	3.96	7.43	9.20
steps	3 steps	3 steps	3 steps	3 steps	3 steps	4 steps	3 steps

Table 7. 10 Estimation of M3 and M4

FME (%)	±0.2	±0.5	±0.8	±1	±2	±5	±10
M3 Estimation Error (%)	2.30	3.68	3.04	3.38	0.07	4.53	7.39
M4 Estimation Error (%)	2.21	3.60	2.84	4.29	4.13	6.30	8.51
steps	3 steps	4 steps	12 steps	5 steps	4 steps	3 steps	3 steps

7.3.3 Three-Machine Estimation

The estimation errors for M1 are larger than those of M2, M3 and M4 when FME is more than 1%, as shown in Table 7.11, 7.12 and 7.13. Convergence of the algorithm takes longer to estimate M1, M3 and M4 at ±0.8% FME, and M2, M3 and M4 at ±0.8%, which are 22 steps and 19 steps respectively. Accurate estimates were obtained for all three inertias in the estimation of M2, M3 and M4 when FME is within ±1%.

Table 7. 11 Estimation of M1, M2 and M3

FME (%)	±0.2	±0.5	±0.8	±1	±2	±5	±10
M1 Estimation Error (%)	5.44	8.58	0.89	9.07	8.13	5.97	10.50
M2 Estimation Error (%)	2.77	5.93	3.35	1.54	3.06	1.44	10.24
M3 Estimation Error (%)	0.86	1.26	0.70	2.02	3.89	6.56	8.42
steps	4 steps	5 steps	4 steps	5 steps	4 steps	5 steps	3 steps

Table 7. 12 Estimation of M1, M2 and M4

FME (%)	±0.2	±0.5	±0.8	±1	±2	±5	±10
M1 Estimation Error (%)	4.31	7.93	1.92	8.94	8.72	5.91	10.47
M2 Estimation Error (%)	2.10	5.66	4.04	1.49	3.06	1.41	10.23
M4 Estimation Error (%)	0.66	1.26	0.20	2.41	4.65	7.66	9.35
steps	4 steps	5 steps	4 steps	6 steps	5 steps	5 steps	3 steps

Table 7. 13 Estimation of M1, M3 and M4

FME (%)	±0.2	±0.5	±0.8	±1	±2	±5	±10
M1 Estimation Error (%)	0.95	1.09	3.13	6.31	10.93	6.21	11.34
M3 Estimation Error (%)	1.68	4.24	3.65	1.56	1.25	4.80	7.59
M4 Estimation Error (%)	1.79	3.93	3.04	3.47	4.08	6.44	8.65
steps	3 steps	5 steps	22 steps	5 steps	5 steps	3 steps	3 steps

Table 7. 14 Estimation of M2, M3 and M4

FME (%)	±0.2	±0.5	±0.8	±1	±2	±5	±10
M2 Estimation Error (%)	0.62	1.09	2.66	3.68	7.34	2.58	10.96
M3 Estimation Error (%)	2.18	3.86	3.22	3.01	0.22	4.59	7.44
M4 Estimation Error (%)	2.11	3.71	2.92	4.10	4.08	6.32	8.54
steps	3 steps	5 steps	19 steps	4 steps	4 steps	4 steps	3 steps

7.4 Test on NY-NE System

Initial guess and actual values of M1, M10, M14, M15 and M16 in NY-NE system were given in Table 6.17. The sensitivity matrix presented in Table 6.18 was utilised in this test. The tests in this section are also executed in terms of the two conditions that introduced in Chapter 6. The chosen sets of measurements, s_1, s_2 and s_3 were presented in Chapter 6.

7.4.1 Estimation with Redundant Measurements

The proposed method aim to solve the divergence problems which frequently occurs in the estimation using measurement-based methods. The estimation results based on the full observability are described in Table 7.15 where the estimates are highly accurate when FME is not more than ±1%. Acceptable estimation results were achieved when FME is not more than ±2%. However, large errors can occur when the FME is high, which is shown in the last two columns in the table.

Through the comparison of Table 7.16 and Table 7.15, the reduction in the number of measurements in this case merely changes the accuracy of the estimation. The difference between the estimation calculated based on s_1 and s_2 was negligible. The convergence was reached within a small number of steps for both cases.

Table 7. 15 Estimation based on s_1

FME (%)	$\pm$0.2	$\pm$0.5	$\pm$0.8	$\pm$1	$\pm$2	$\pm$5	$\pm$10
M1 Estimation Error (%)	0.39	1.06	0.78	1.26	5.12	2.60	6.49
M10 Estimation Error (%)	0.27	1.00	0.64	0.73	5.63	4.36	13.04
M14 Estimation Error (%)	1.99	1.15	0.04	0.63	2.93	9.36	10.06
M15 Estimation Error (%)	0.43	1.40	1.72	0.49	6.69	7.83	8.80
M16 Estimation Error (%)	1.75	0.48	1.21	2.18	0.88	9.31	9.47
steps	4 steps	5 steps	4 steps	3 steps	4 steps	4 steps	7 steps

Table 7. 16 Estimation based on s_2

FME (%)	$\pm$0.2	$\pm$0.5	$\pm$0.8	$\pm$1	$\pm$2	$\pm$5	$\pm$10
M1 Estimation Error (%)	0.37	1.03	0.84	1.19	4.98	2.51	6.59
M10 Estimation Error (%)	0.26	1.06	0.73	0.68	5.81	3.95	13.72
M14 Estimation Error (%)	1.91	1.23	0.06	0.66	2.94	9.36	10.06
M15 Estimation Error (%)	0.40	1.38	1.73	0.49	6.69	7.82	8.80
M16 Estimation Error (%)	1.70	0.55	1.23	2.15	0.13	9.37	9.45
steps	4 steps	4 steps	4 steps	3 steps	4 steps	4 steps	5 steps

7.4.2 Estimation with Inadequate Measurements

Convergence was reached for all levels of FME in this simulation. Small estimation errors were achieved when FME is not greater than $\pm$1%. Acceptable accuracy was also obtained when FME as at $\pm$2%, but the error of the estimates of M14 and M16 increased to 5.37% and 4.57% respectively. Steps to convergence were almost twice of those of estimation based on s_1 and s_2.

Table 7. 17 Estimation based on s_3

FME (%)	$\pm$0.2	$\pm$0.5	$\pm$0.8	$\pm$1	$\pm$2	$\pm$5	$\pm$10
M1 Estimation Error (%)	0.37	1.03	0.83	1.18	4.98	2.53	6.60
M10 Estimation Error (%)	0.26	1.06	0.74	0.70	5.81	3.87	13.68
M14 Estimation Error (%)	0.29	0.94	1.49	0.23	5.37	9.43	9.50
M15 Estimation Error (%)	0.11	1.30	1.83	0.61	5.61	9.51	9.59
M16 Estimation Error (%)	0.58	0.55	1.05	0.10	4.57	8.15	8.19
steps	8 steps	8 steps	7 steps	8 steps	5 steps	4 steps	5 steps

7.5 Summary of Frequency-Pseudomeasurements Method

Frequency-pseudomeasurements method was designed to introduce the parameter perturbation objective component into the objective function of the frequency method. The frequency-

pseudomeasurements method significantly improved the accuracy of estimation. Moreover, the divergence caused by measurement noise or lack of measurements could be effectively circumvented. Highly accurate results were achieved when FME was not more than $\pm$1% in the tests on both two-area model and NY-NE model. Acceptable estimation precision could be obtained when FME was not greater than $\pm$2%.

7.6 Frequency-Damping-Pseudomeasurements Method

Through the introduction of parameter changes into the objective function (6.5), a new objective function is formed in (7.4).

$$J(\Delta M) = \varepsilon_f^T W_f \varepsilon_f + \varepsilon_d^T W_d \varepsilon_d + (M - M_0)^T W_p (M - M_0) \quad (7.4)$$

Through the minimisation of the objective function, the optimal solution is presented in (7.5),

$$\Delta M = \left(S_f^T W_f S_f + S_d^T W_d S_d + W_p\right)^{-1} [S_d^T W_d \Delta\sigma + S_f^T W_f \Delta\omega - (M - M_0)^T W_p] \quad (7.5)$$

Equation (7.5) can be rewritten in an iterative form,

$$M_{k+1} = M_k + \left(S_f^T W_f S_f + S_d^T W_d S_d + W_p\right)^{-1} [S_d^T W_d (\sigma_m - \sigma_k) + S_f^T W_f (\omega_m - \omega_k) - (M_k - M0)TWp] \quad (7.6)$$

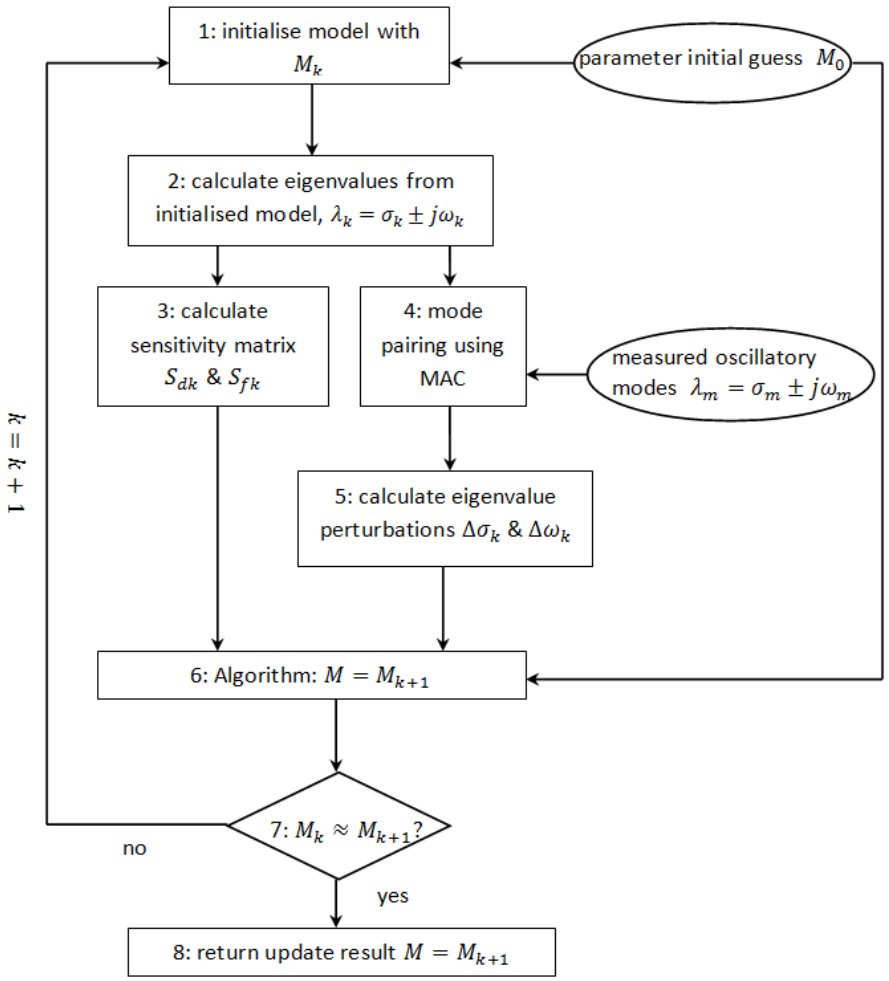

Figure 7. 2 Frequency-damping-pseudomeasurements method

In Figure 7.2, the oval shapes represent the inputs which are the measurements that need to be provided to execute the algorithm. The rectangular shapes contain the procedures of the algorithm. Besides modal frequency measurements and parameter initial guess, the method presented in this section also requires modal damping measurements. The flow chart can be summarised as,

1. Initialise system model with M_k (M_0, for the first time);
2. Calculate the eigenvalues of the initialised system model;
3. Calculate sensitivity matrices of modal frequency and modal damping;
4. Pair eigenvalues calculated at step 2, with the measured eigenvalues;
5. Calculate perturbations between corresponding calculated eigenvalues and measured eigenvalues;

6. Update inertia constants using equation (7.6);
7. If the updated results are approximately equal to last update, then return results. Otherwise, go back to step 1.

7.7 Test on Two-Area System

This section shows the estimation results of Frequency-damping-pseudomeasurements method applied to the two-area system. The standard deviations of uncertainty for the estimation of all four inertias are all set to 10%. Since modal damping measurements are used in this method, it is necessary to consider the Damping Measurement Error (DME) which varies from ±5% to ±20%. The tests are conducted in three divisions, the estimation of a single inertia, two inertias and three inertias.

7.7.1 Single-Machine Estimation

The resultant estimation of a single machine is presented from Table 7.18 to 7.21. Generally, accuracy can be guaranteed when FME is not greater than ±1%. However, accurate results can also be achieved through the estimation of M3 and M4 at ±2% FME. The variation of DME is not affected when the FME is not greater than ±2%. Nevertheless, during the estimation, the same inertia, it was found that estimation errors at ±10% DME were relatively small compared to those at ±5% and ±20% DME.

Table 7. 18 Estimation of M1

FME(%) / DME(%)	±0.2	±0.5	±0.8	±1	±2	±5	±10
±5	1.08	0.58	2.72	5.43	7.64	3.86	6.92
	4 steps	4 steps	4 steps	4 steps	5 steps	6 steps	13 steps
±10	1.03	0.95	2.08	4.75	6.57	0.44	4.35
	4 steps	4 steps	3 steps	3 steps	3 steps	6 steps	6 steps
±20	1.09	0.62	2.92	6.12	10.20	6.28	11.40
	4 steps	4 steps	4 steps	3 steps	3 steps	4 steps	6 steps

Table 7. 19 Estimation of M2

FME(%) / DME(%)	±0.2	±0.5	±0.8	±1	±2	±5	±10
±5	0.67	0.97	2.69	3.76	7.16	3.33	10.11
	4 steps	4 steps	4 steps	5 steps	5 steps	6 steps	8 steps
±10	0.64	1.11	2.37	3.29	5.88	0.79	7.04
	4 steps	4 steps	4 steps	4 steps	3 steps	5 steps	5 steps
±20	0.66	1.01	2.64	3.71	7.24	2.80	10.90
	4 steps	4 steps	4 steps	4 steps	3 steps	4 steps	7 steps

Table 7. 20 Estimation of M3

FME(%) / DME(%)	±0.2	±0.5	±0.8	±1	±2	±5	±10
±5	0.02	0.14	1.03	1.10	3.97	8.32	10.26
	4 steps	4 steps	4 steps	4 steps	3 steps	4 steps	5 steps
±10	0.03	0.11	0.44	0.18	1.48	3.31	4.40
	4 steps	4 steps	4 steps	4 steps	4 steps	4 steps	5 steps
±20	0.01	0.00	0.71	6.02	2.78	6.51	8.60
	4 steps	4 steps	4 steps	4 steps	4 steps	3 steps	4 steps

Table 7. 21 Estimation of M4

FME(%) / DME(%)	±0.2	±0.5	±0.8	±1	±2	±5	±10
±5	0.21	0.56	0.18	1.83	4.80	9.13	10.98
	4 steps	4 steps	4 steps	4 steps	4 steps	4 steps	4 steps
±10	0.17	0.37	0.28	1.15	2.90	4.95	5.88
	4 steps	4 steps	4 steps	4 steps	4 steps	3 steps	4 steps
±20	0.19	0.45	0.08	1.47	3.93	7.72	9.60
	4 steps	4 steps	4 steps	4 steps	4 steps	4 steps	4 steps

7.7.2 Two-Machine Estimation

The frequency-damping-pseudomeasurements method also had an excellent performance when estimating the inertias of two machines at the same time, which is shown from Table 7.22 to 7.27. Precise outcomes are obtained when FME was not greater than ±1%. The estimation of M3 and M4, shown in Table 7.27 had slightly higher accuracy than the other scenarios.

Table 7. 22 Estimation of M1 and M2

FME(%) / DME(%)		±0.2	±0.5	±0.8	±1	±2	±5	±10
±5	M1	2.53	5.93	2.22	5.69	4.36	3.64	3.61
	M2	1.01	4.63	4.53	0.11	4.53	1.58	8.47
		4 steps	6 steps	8 steps	9 steps	9 steps	12 steps	13 steps
±10	M1	2.19	4.13	3.44	3.96	3.47	0.04	3.20
	M2	0.81	3.71	4.94	0.86	4.12	0.60	6.41
		4 steps	4 steps	4 steps	8 steps	5 steps	6 steps	6 steps
±20	M1	2.56	5.58	1.02	6.94	7.71	5.98	10.52
	M2	1.03	4.42	3.41	0.44	3.46	1.52	9.99
		4 steps	5 steps	5 steps	4 steps	3 steps	5 steps	6 steps

Table 7. 23 Estimation of M1 and M3

FME(%) / DME(%)		±0.2	±0.5	±0.8	±1	±2	±5	±10
±5	M1	1.16	0.55	3.10	5.94	8.12	3.38	6.00
	M3	0.22	0.06	1.47	1.93	4.54	8.19	9.78
		4 steps	4 steps	4 steps	4 steps	6 steps	8 steps	7 steps
±10	M1	1.09	1.03	2.30	5.06	7.03	0.28	4.32
	M3	0.17	0.29	0.79	0.98	2.27	3.31	4.39
		4 steps	4 steps	4 steps	4 steps	4 steps	5 steps	6 steps
±20	M1	1.15	0.64	3.29	6.68	11.15	6.78	11.55
	M3	0.20	0.11	1.22	1.67	4.10	6.84	8.77
		4 steps	4 steps	4 steps	4 steps	4 steps	4 steps	5 steps

Table 7. 24 Estimation of M1 and M4

FME(%) / DME(%)		±0.2	±0.5	±0.8	±1	±2	±5	±10
±5	M1	1.17	0.44	2.81	5.92	8.05	3.45	6.16
	M4	0.35	0.51	0.45	2.39	5.21	9.08	10.66
		4 steps	4 steps	5 steps	4 steps	5 steps	6 steps	9 steps
±10	M1	1.11	0.87	2.04	5.16	7.07	0.30	4.28
	M4	0.31	0.26	0.07	1.70	3.45	4.91	5.85
		4 steps	4 steps	4 steps	4 steps	4 steps	6 steps	7 steps
±20	M1	1.17	0.51	2.96	6.69	11.05	6.72	11.53
	M4	0.33	0.39	0.24	2.19	4.83	7.96	9.75
		4 steps	4 steps	4 steps	4 steps	4 steps	4 steps	5 steps

Table 7. 25 Estimation of M2 and M3

FME(%) / DME(%)		±0.2	±0.5	±0.8	±1	±2	±5	±10
±5	M2	0.67	0.96	2.74	3.83	7.18	2.69	9.17
	M3	0.05	0.11	1.13	1.23	3.99	8.24	9.70
		4 steps	4 steps	4 steps	4 steps	6 steps	7 steps	9 steps
±10	M2	0.64	1.11	2.39	3.33	5.97	0.76	6.99
	M3	0.01	0.16	0.54	0.33	1.66	0.33	4.34
		4 steps	4 steps	4 steps	4 steps	4 steps	6 steps	5 steps
±20	M2	0.67	1.01	2.68	3.77	7.39	2.91	10.92
	M3	0.03	0.04	0.83	0.78	3.02	6.56	8.62
		4 steps	4 steps	4 steps	4 steps	4 steps	4 steps	5 steps

Table 7. 26 Estimation of M2 and M4

FME(%) / DME(%)		±0.2	±0.5	±0.8	±1	±2	±5	±10
±5	M2	0.68	0.95	2.70	3.82	7.14	2.78	9.33
	M4	0.23	0.54	0.23	1.90	4.80	9.08	10.59
		4 steps	4 steps	4 steps	4 steps	5 steps	7 steps	12 steps
±10	M2	0.65	1.10	2.35	3.33	5.94	0.82	6.94
	M4	0.19	0.34	0.23	1.23	2.99	4.93	5.83
		4 steps	4 steps	4 steps	5 steps	4 steps	6 steps	5 steps
±20	M2	0.67	0.99	2.63	3.77	7.36	2.88	10.91
	M4	0.21	0.43	0.02	1.57	4.07	7.74	9.62
		4 steps	4 steps	4 steps	4 steps	4 steps	5 steps	5 steps

Table 7. 27 Estimation of M3 and M4

FME(%) / DME(%)		±0.2	±0.5	±0.8	±1	±2	±5	±10
±5	M3	2.23	3.38	3.54	2.66	1.05	5.62	7.77
	M4	2.17	3.48	3.00	4.14	4.34	6.90	8.60
		4 steps	5 steps	13 steps	5 steps	6 steps	5 steps	5 steps
±10	M3	2.34	3.86	2.68	3.82	1.05	2.05	3.59
	M4	2.23	3.67	2.71	4.34	3.83	4.45	5.32
		4 steps	5 steps	13 steps	5 steps	5 steps	4 steps	5 steps
±20	M3	2.30	3.68	3.10	3.37	0.01	4.74	7.68
	M4	2.21	3.61	2.87	4.32	4.21	6.51	8.82
		4 steps	5 steps	13 steps	5 steps	5 steps	4 steps	4 steps

7.7.3 Three-Machine Estimation

The estimation errors increased when the proposed method was used to estimate three inertias at the same time. The results are shown from Table 7.28 to 7.31. The growth of estimation errors can

be easily seen from Table 7.28 and 7.29 when FME is ±0.5%. However, this algorithm effectively avoids divergence problems that occurred within the previous methods.

Generally, more steps are required for this algorithm to converge, in comparison to the frequency-pseudomeasurements method. For example, when estimating the combination M1, M2 and M3, it can take up to 12 steps to reach convergence, whilst a maximum 5 steps is required through the utilisation of the frequency-pseudomeasurements method. Similar findings also can be seen through the estimation of the other combinations.

Table 7. 28 Estimation of M1, M2 and M3

FME(%) / DME(%)		±0.2	±0.5	±0.8	±1	±2	±5	±10
±5	M1	5.63	8.62	1.02	7.86	5.36	3.39	2.99
	M2	2.87	5.99	3.65	1.15	3.86	1.09	7.85
	M3	0.91	1.28	1.03	2.23	4.41	8.17	9.50
		6 steps	6 steps	9 steps	9 steps	9 steps	12 steps	12 steps
±10	M1	4.64	5.88	3.32	5.04	4.11	0.13	3.18
	M2	2.31	4.68	4.87	0.26	3.87	0.63	6.35
	M3	0.72	0.73	0.14	1.06	2.11	3.35	4.34
		5 steps	6 steps	5 steps	6 steps	5 steps	6 steps	7 steps
±20	M1	5.52	8.62	0.09	9.20	9.07	6.51	10.68
	M2	2.81	5.99	2.80	1.57	2.98	1.52	10.00
	M3	0.88	1.28	0.84	2.08	4.04	6.88	8.79
		5 steps	6 steps	5 steps	4 steps	4 steps	5 steps	6 steps

Table 7. 29 Estimation of M1, M2 and M4

FME(%) / DME(%)		±0.2	±0.5	±0.8	±1	±2	±5	±10
±5	M1	4.42	8.48	2.09	7.71	5.28	3.41	3.06
	M2	2.17	5.97	4.44	1.08	3.86	1.11	7.91
	M4	0.69	1.41	0.08	2.59	5.10	9.06	10.46
		6 steps	7 steps	8 steps	7 steps	8 steps	12 steps	33 steps
±10	M1	3.80	5.94	3.95	5.40	4.24	0.12	3.13
	M2	1.81	4.71	5.31	0.05	3.77	0.69	6.30
	M4	0.60	0.96	0.57	1.76	3.31	4.90	5.79
		5 steps	6 steps	5 steps	8 steps	5 steps	6 steps	6 steps
±20	M1	4.36	7.95	1.15	9.02	8.95	6.44	10.66
	M2	2.13	5.66	3.49	1.50	3.00	1.50	10.00
	M4	0.67	1.27	0.11	2.46	4.77	7.97	9.76
		5 steps	5 steps	5 steps	5 steps	4 steps	5 steps	6 steps

Table 7. 30 Estimation of M1, M3 and M4

FME(%) / DME(%)		±0.2	±0.5	±0.8	±1	±2	±5	±10
±5	M1	0.98	0.86	3.12	5.76	8.07	3.21	5.61
	M3	1.60	3.83	4.06	1.19	1.59	5.47	7.36
	M4	1.74	3.75	3.15	3.46	4.32	6.90	8.43
		4 steps	5 steps	17 steps	7 steps	6 steps	7 steps	7 steps
±10	M1	0.89	1.40	2.29	4.82	7.02	0.25	4.24
	M3	1.77	4.54	3.13	2.45	0.26	2.06	3.58
	M4	1.84	4.06	2.87	3.73	3.80	4.41	5.29
		4 steps	5 steps	16 steps	5 steps	6 steps	5 steps	6 steps
±20	M1	0.96	1.01	3.28	6.44	11.15	6.97	11.65
	M3	1.67	4.18	3.74	1.49	1.34	5.02	7.83
	M4	1.78	3.91	3.08	3.47	4.16	6.66	8.95
		4 steps	5 steps	17 steps	5 steps	5 steps	5 steps	6 steps

Table 7. 31 Estimation of M2, M3 and M4

FME(%) / DME(%)		±0.2	±0.5	±0.8	±1	±2	±5	±10
±5	M2	0.63	1.01	2.76	3.81	7.18	2.52	8.77
	M3	2.11	3.53	3.69	2.37	1.07	5.54	7.30
	M4	2.07	3.58	3.07	3.98	4.32	6.88	8.38
		4 steps	5 steps	14 steps	8 steps	6 steps	8 steps	10 steps
±10	M2	0.61	1.19	2.39	3.27	5.96	0.79	6.90
	M3	2.22	4.04	2.84	3.51	0.84	2.09	3.54
	M4	2.14	3.77	2.80	4.17	3.79	4.41	5.28
		4 steps	5 steps	14 steps	7 steps	6 steps	5 steps	5 steps
±20	M2	0.62	1.07	2.68	3.72	7.39	2.94	10.92
	M3	2.17	3.85	3.28	2.99	2.92	4.79	7.70
	M4	2.11	3.71	2.95	4.12	4.16	6.53	8.84
		4 steps	5 steps	14 steps	5 steps	5 steps	5 steps	5 steps

7.8 Test on NY-NE System

The same sensitivity matrix shown in Table 6.37 will be used in this section due to damping discrepancies in frequency-damping-pseudomeasurements method. Simulation tests are conducted for two scenarios.

7.8.1 Estimation with Redundant Measurements

Full observability was employed to produce the results given in Table 7.32. It shows the capability of the algorithm to avoid divergence. Since modal damping components are less sensitive to the

variation of inertias, the changes of DME at the same FME can hardly cause an effect on the estimation results. High precision can be guaranteed when FME was not greater than $\pm$1%. The estimation accuracy was acceptable when FME is $\pm$2%. In comparison to the estimates presented in Table 7.15, the estimation errors can be slightly reduced.

Table 7. 32 Estimation based on s_1

FME(%) / DME(%)		$\pm$0.2	$\pm$0.5	$\pm$0.8	$\pm$1	$\pm$2	$\pm$5	$\pm$10
$\pm$5	M1	0.37	1.16	0.45	0.74	5.42	4.71	6.48
	M10	0.26	1.01	0.55	0.59	4.90	21.06	21.80
	M14	1.85	1.25	0.15	0.87	2.79	7.33	7.46
	M15	0.39	1.44	1.84	0.28	7.30	8.84	9.62
	M16	1.66	0.54	1.10	2.03	0.09	7.57	7.14
		4 steps	5 steps	5 steps	5 steps	9 steps	5 steps	6 steps
$\pm$10	M1	0.38	1.11	0.62	1.01	5.59	4.75	8.02
	M10	0.26	1.01	0.60	0.65	5.14	20.50	23.07
	M14	2.03	0.95	0.28	0.43	2.28	7.41	7.51
	M15	0.43	1.45	1.75	0.49	6.63	7.36	8.22
	M16	1.77	0.38	1.27	2.17	0.15	8.03	8.89
		3 steps	6 steps	3 steps	4 steps	5 steps	4 steps	5 steps
$\pm$20	M1	0.39	1.04	0.81	1.30	4.80	1.92	5.06
	M10	0.27	0.99	0.68	0.79	5.53	3.81	12.80
	M14	1.97	1.12	0.08	0.63	2.68	8.60	9.05
	M15	0.42	1.39	1.67	0.58	6.56	7.44	8.22
	M16	1.74	0.46	1.21	2.16	0.06	8.96	8.89
		4 steps	7 steps	4 steps	4 steps	4 steps	7 steps	8 steps

Estimation results based on s_2 are quite similar to those that were obtained for full observability. The reduction of the number of measurements does not have significant impacts on estimation accuracy when the sensitive modes were involved in the estimation.

Table 7. 33 Estimation based on s_2

FME(%) / DME(%)		±0.2	±0.5	±0.8	±1	±2	±5	±10
±5	M1	0.36	1.12	0.54	0.73	5.19	4.21	6.09
	M10	0.25	1.09	0.61	0.50	5.37	20.20	21.21
	M14	1.76	1.33	0.14	0.90	2.81	7.33	7.45
	M15	0.36	1.42	1.84	0.29	7.31	8.85	9.64
	M16	1.60	0.61	1.10	1.98	0.17	7.53	7.03
		6 steps	7 steps	4 steps	4 steps	8 steps	4 steps	4 steps
±10	M1	0.36	1.08	0.70	0.97	5.39	3.93	7.82
	M10	0.25	1.08	0.66	0.57	5.51	3.65	22.68
	M14	1.95	1.03	0.29	0.46	2.28	7.39	7.51
	M15	0.42	1.43	1.76	0.49	6.64	7.34	7.89
	M16	1.72	0.45	1.29	2.14	0.19	8.06	7.57
		4 steps	7 steps	3 steps	3 steps	6 steps	15 steps	5 steps
±20	M1	0.38	1.01	0.89	1.27	4.60	1.62	4.76
	M10	0.26	1.06	0.75	0.72	5.89	4.03	14.61
	M14	1.89	1.19	0.09	0.65	2.69	8.60	9.04
	M15	0.39	1.37	1.68	0.59	6.56	7.44	8.22
	M16	1.68	0.53	1.23	2.12	0.11	8.99	8.85
		4 steps	6 steps	4 steps	4 steps	4 steps	6 steps	33 steps

7.8.2 Estimation with Inadequate Measurements

The frequency-damping method does not perform well when the number of parameters to be estimated is more than that of the measurements. As it is shown in Table 6.40, no estimation results can be provided. Convergence was reached again by using pseudomeasurements in the estimation when the number of measurements was less than the number of parameters to be estimated.

Through the comparison of the results in Table 7.34 against those estimated based on redundant measurements, the accuracy level remains the same. Only at ±2% FME, the errors of M16 increase from less than ±0.2% to about 4.92%. However, this does not degrade the entire estimation accuracy.

By comparing against frequency-pseudomeasurements method, the estimation accuracy of frequency-damping-pseudomeasurements, was not improved through the inclusion of the modal damping component in the optimisation objective function. This is because the sensitivity of modal damping to inertia was much smaller than that of the frequency to inertia.

Table 7. 34 Estimation based on s_3

FME(%) / DME(%)		±0.2	±0.5	±0.8	±1	±2	±5	±10
±5	M1	0.35	1.12	0.53	0.72	5.19	4.23	6.10
	M10	0.25	1.09	0.62	0.51	5.39	20.18	21.21
	M14	0.24	1.46	2.05	0.89	6.05	10.10	10.27
	M15	0.05	1.19	1.78	0.61	5.83	9.95	10.18
	M16	1.02	0.14	0.71	0.40	4.49	8.34	8.45
		8 steps	7 steps	7 steps	7 steps	7 steps	4 steps	4 steps
±10	M1	0.36	1.08	0.69	0.97	5.39	3.95	7.83
	M10	0.26	1.08	0.67	0.58	5.52	3.61	22.67
	M14	0.05	1.23	1.74	0.50	5.34	8.80	8.63
	M15	0.11	1.08	1.60	0.34	5.26	8.78	8.64
	M16	0.06	1.05	1.54	0.36	4.92	8.16	7.92
		8 steps	8 steps	8 steps	10 steps	6 steps	15 steps	4 steps
±20	M1	0.38	1.01	0.88	1.26	4.60	1.63	4.76
	M10	0.26	1.06	0.76	0.73	5.90	3.96	14.60
	M14	0.03	1.21	1.72	0.47	5.35	8.95	8.84
	M15	0.10	1.10	1.61	0.35	5.29	8.95	8.85
	M16	0.09	1.01	1.48	0.32	4.82	8.08	7.96
		9 steps	7 steps	7 steps	8 steps	5 steps	7 steps	31 steps

7.9 Summary of Frequency-Damping-Pseudomeasurements Method

The effect to include the parameter perturbation within the objective function was demonstrated in this method. By comparing against the methods presented in Chapter 6, with the frequency-pseudomeasurements method the advantages of this method are similar. However, the inclusion of the modal damping term within the optimisation algorithm does not improve the estimation accuracy significantly in comparison to the results obtained from the frequency-pseudomeasurements method.

7.10 Conclusions

In this chapter, two methods based on modal measurements and pseudomeasurements were designed. In comparison to the methods proposed in Chapter 6, the two methods in this chapter have effectively solved the divergence problems due to nonlinearity and inadequate available measurements. This facilitates practical implementation when there is a lack of modal measurements.

Generally, frequency-damping-pseudomeasurements method can be applied to identify parameters associated with oscillatory modes. However, it is well known that generator inertia is more related to modal frequencies. This can be also proved through the investigation of the sensitivity matrix. Thus, theoretically, the estimation accuracy should not be different to those using frequency-pseudomeasurements method and frequency-damping-pseudomeasurements method in order to obtain the inertia constants. The theory was supported by the simulation results obtained within this chapter.

Chapter 8 Conclusions

Input: Power system oscillations are commonly detected in modern power systems, through measurements, such as power flow, system frequency, and voltage angles. These measurements normally contain oscillations of several modes. These modes are associated with the system dynamic properties. Techniques to extract these dynamic characteristics from measurements were comprehensively studied in the literature. Benefits from these techniques, continuous modal frequencies and damping which are treated as input to the estimation methods can be achieved in near-real-time base, depending on the size of the system.

Estimation: Power system dynamics of a power system is mainly reflected by the generator dynamic properties within and outside of the power system, thus it highly depends on the operating condition which is time variant. The timely operating condition determines the parameters of generators that contribute towards the dynamic characteristics of a power system. It indicates that the power system model can hardly be represented by a set or sets of fixed data. An adaptive estimation of the generator parameters relating to the changes of operating condition plays a significant role in the reveal of the potential risks. The estimation methods developed in this work can be implemented to estimate generator parameters of an external network equivalents and also internal networks. Besides inertia constants, the methodology can also be used to estimate other parameters with minor modification.

The estimation techniques proposed simply compare the modal measurements with the modal data which are calculated based on initial guesses of the parameters. The discrepancies of modal data were then calculated accordingly. These differences imply that the parameters of generators within or outside the system under examination may undergo certain changes which have an impact on the system's dynamic properties. By using WLS method, the estimation methods are extended to an iterative estimation to update the parameters, and prompt the original modal data to move towards to the measured modal data. It was found that the methods which utilise modal data only have poor

performance. Moreover, they could not reach convergence when the number of measurements is less than the number of parameters to be estimated. Hence, pseudomeasurements which are the initial guesses of these parameters are included in the estimation. This successfully circumvented the divergence problems. Prior knowledge on the system is very important to achieve reasonable initial guesses.

It should be noted that not all modes contribute to the estimation of certain sets of parameters. Therefore, modal sensitivity analysis can indicate the required parameters. It should be addressed that it is not necessary to use both modal frequencies and damping in the estimation, whilst pseudo-measurements are highly recommended. The reason is that the variation of parameters may not be adequately reflected in both modal frequencies and damping.

Output: The estimates are a set of parameters which can best reflect the system dynamics under the certain operation condition. Simulation results showed that the proposed methods can effectively produce estimation to high accuracy.

Chapter 9 Future Works

In this thesis, a methodology was developed to estimate the generator parameters adaptively. Four approaches were developed. Comparative studies were conducted in order to find their benefits and drawbacks. Simulation tests were used to estimate the generator inertia constants. The proposed methodology suitable for general use for parameters estimation which is associated with power system oscillations. Thus, it is not limited to estimate only generator inertia constants, but can also be applied to estimate other parameters such as damping coefficients. Damping coefficient is a parameter which has a significant impact on power system dynamics, since it is associated with modal damping which determines the stability of the system. Therefore, it is suggested estimated damping coefficients to be executed in future studies. This can make contributions to power system management and tuning of Power System Stabilisers (PSS).

Modal frequencies and damping data used in the estimation are corrupted with different levels of noise. However, only one test is conducted in terms of each level. It is highly suggested to apply Monte-Carlo simulation to the test at each measurement error level.

It is also suggested that the proposed methodology to be used to reconstruct external network with high renewable energy penetration. Since the amount of generation from renewable energy is increasing significantly, it is useful if we can demonstrate the use of the proposed methodology in this field.

Reference

1. J. Machowski., J. W. Bialek, and J. R. Bumby, *Power system dynamics - stability and control* 2nd ed.. UK: John Wiley & Sons, 2008.
2. C4.601, *Review of on-line dynamic security assessment tools and techniques*, in *CIGRE Technical Brochure* 2007.
3. G. Rogers, *Power system oscillations. New York:* Kluwer Academic Publishers, 1983.
4. Y. N. Yu, *Electric power system dynamics*. Vancouver: Academic Press, 1983.
5. M. Klein, G. Rogers, and P. Kundur, "A fundamental study of inter-area oscillations in power systems," *IEEE Trans. Power Syst.*, vol. 6, no. 3, pp. 914-921, 1991.
6. J. M. Undrill and A. E. Turner, "Construction of power system electromechanical equivalents by modal analysis," *IEEE Trans. Power App. Syst.*, vol. PAS-90, no. 5, pp. 2049-2059, 1971.
7. D. J. Trudnowski and J. W. Pierre. "Overview of algorithms for estimating swing modes from measured responses," in *Proc. Power Eng. Soc. General Meeting,* Calgary, Canada, 2009.
8. N. Zhou, et al., "Electromechanical mode online estimation using regularized robust RLS methods," *IEEE Trans. Power Syst.*, vol. 23, no. 4, pp. 1670-1680, 2008.
9. Ning, Z., J.W. Pierre, and J.F. Hauer, "Initial results in power system identification from injected probing signals using a subspace method, " *IEEE Trans. Power Syst.*, vol. 21, no. 3, pp. 1296-1302, 2006
10. Zhou, N., J.W. Pierre, and D. Trudnowski. "A Bootstrap Method for Statistical Power System Mode Estimation and Probing Signal Selection," in *Proc. Power Systems Conference and Exposition,* 2006.
11. F. B. Hildebrand, *Introduction to numerical analysis*. 2nd ed. New York: Dover Publications, 1987.
12. S. M. Kay and S. L. Marple Jr, "Spectrum analysis- a modern perspective," in *Proc. of the IEEE*, vol. 69, no. 11, pp. 1380-1419, 1981.
13. A. Poggio, et al., "Evaluation of a processing technique for transient data," *IEEE Trans. Antennas Propagat.*, vol. 26, no. 1, pp. 165-173, 1978.
14. M. VanBlaricum and R. Mittra, "Problems and solutions associated with Prony's method for processing transient data," *IEEE Trans. Antennas Propagat.*, vol. 26, no. 1, pp. 174-182, 1978.
15. J. F. Hauer, "Application of Prony analysis to the determination of modal content and equivalent models for measured power system response," *IEEE Trans. Power Syst.*, vol. 6, no.3, pp. 1062-1068, 1991.
16. J. J. Sanchez-Gasca and J. H. Chow, "Performance comparison of three identification methods for the analysis of electromechanical oscillations," *IEEE Trans. Power Syst.*, vol. 14, no. 3, pp. 995-1002, 1999.
17. J .F. Hauer, C. Demeure, and L. Scharf, "Initial results in Prony analysis of power system response signals," *IEEE Trans. Power Syst.,* vol. 5, no. 1, pp. 80-89, 1990.
18. C. Grund, et al., "Comparison of Prony and eigenanalysis for power system control design," *IEEE Trans. Power Syst.,* vol. 8, no. 3, pp. 964-971, 1993.
19. D. Trudnowski, J. Johnson, and J. Hauer, "Making Prony analysis more accurate using multiple signals," *IEEE Trans. Power Syst.,* vol. 14, no. 1, pp. 226-231, 1999.
20. D. Pierre, D. Trudnowski, and J. Hauer, "Identifying linear reduced-order models for systems with arbitrary initial conditions using Prony signal analysis," *IEEE Trans. Autom. Control*, vol. 37, no. 6, pp. 831-835, 1992.
21. J. Hauer, "Application of Prony analysis to the determination of modal content and equivalent models for measured power system response," *IEEE Trans. Power Syst.,* vol. 6, no. 3, pp. 1062-1068, 1991.
22. D. Trudnowski, M. Donnelly, and J. Hauer, "Advances in the identification of transfer function models using Prony analysis," in *Proc. of IEEE American Control Conference, 1993*.

23. D. Pierre, et al., "General formulation of a Prony based method for simultaneous identification of transfer functions and initial conditions," in *Proc. of 31st IEEE Conf. Decision and Control, 1992.*
24. I. Kamwa, et al., "A minimal realization approach to reduced-order modelling and modal analysis for power system response signals," *IEEE Trans. Power Syst.,* vol. 8, no. 3, pp. 1020-1029, 1993.
25. I. Kamwa, G. Trudel, and L. GerinLajoie, "Low-order black-box models for control system design in large power systems," *IEEE Trans. Power Syst.*, vol. 11, no. 1, pp. 303-311, 1996.
26. J. J. Sanchez-Gasca and J. H. Chow, "Computation of power system low-order models from time domain simulations using a Hankel matrix," *IEEE Trans. Power Syst.*, vol. 12, no. 4, pp. 1461-1467.
27. M. L. Crow and A. Singh, "The matrix pencil for power system modal extraction," *IEEE Trans. Power Syst.*, vol. 20, no. 1, pp. 501-502, 2005.
28. T. K. Sarkar and O. Pereira, "Using the matrix pencil method to estimate the parameters of a sum of complex exponentials," *IEEE Trans. Antennas Propagat.*, vol. 37, no. 1, pp. 48-55, 1995.
29. Y. Hua and T. K. Sarkar, "Generalized pencil-of-function method for extracting poles of an EM system from its transient response," *IEEE Trans. Antennas Propagat.*, vol. 37, no. 2, pp. 229-234, 1989.
30. L. Guoping, J. Quintero, and V. Venkatasubramanian, "Oscillation monitoring system based on wide area synchrophasors in power systems," in *Bulk Power System Dynamics and Control - VII. Revitalizing Operational Reliability, iREP Symposium*, 2007.
31. J. W. Pierre, D. J. Trudnowski, and M. K. Donnelly, "Initial results in electromechanical mode identification from ambient data, ". *IEEE Trans. Power Syst.*, vol. 12, no. 3, pp. 1245-1250, 1997.
32. R. W. Wies, J. W. Pierre, and D. J. Trudnowski, "Use of ARMA block processing for estimating stationary low-frequency electromechanical modes of power systems," *IEEE Trans. Power Syst.*, vol. 18, no. 1, pp. 167-173, 2003.
33. M. Andersron, et al., "Bootstrap-based confidence interval estimates for electromechanical modes from multiple output analysis of measured ambient data," in *Proc. Power Eng. Soc. General Meeting,* 2005.
34. H. Ghasemi, C. Canizares, and A. Moshref, "Oscillatory stability limit prediction using stochastic subspace identification," *IEEE Trans. Power Syst.*, vol. 21, no. 2, pp. 736-745.
35. C. Y. Chung, and D. Bo, "A Combined TSA-SPA Algorithm for Computing Most Sensitive Eigenvalues in Large-Scale Power Systems," *IEEE Trans. Power Syst.* vol. 28, no. 1, pp. 149-157, 2013.
36. J. Ni, C. Shen, and F. Liu. "Estimating the electromechanical oscillation characteristics of power system based on measured ambient data utilizing stochastic subspace method," in *Proc. Power Eng. Soc. General Meeting,* 2011.
37. R. W. Wies, J. W. Pierre, and D. J. Trudnowski, "Use of least mean squares (LMS) adaptive filtering technique for estimating low-frequency electromechanical modes in power systems," in *Proc. Power Eng. Soc. General Meeting,* 2004.
38. N. Zhou, et al., "Robust RLS methods for online estimation of power system electromechanical modes," *IEEE Trans. Power Syst.*, vol. 22, no. 3: pp. 1240-1249, 2007.
39. L. Dosiek and J. W. Pierre, "Estimating electromechanical modes and mode shapes using the multichannel ARMAX model," *IEEE Trans. Power Syst.* vol. 28, no. 2, pp. 1950-1959, 2013.
40. L. Dosiek, J. W. Pierre, and J. Follum, "A recursive maximum likelihood estimator for the online estimation of electromechanical modes with error bounds," *IEEE Trans. Power Syst.*, vol. 28, no. 1, pp. 441-451, 2013.

41. S. A. Nezam Sarmadi and V. Venkatasubramanian, "Electromechanical mode estimation using recursive adaptive stochastic subspace identification," *IEEE Trans. Power Syst.*, vol. 29, no. 1, pp. 349-358, 2013.
42. F. J. De Marco, et al., "Efficient online estimation of electromechanical modes in large power systems," *IEEE Fourth LASCAS,* 2013.
43. A. R. Messina, and V. Vittal, "Nonlinear, non-stationary analysis of interarea oscillations via Hilbert spectral analysis," *IEEE Trans. Power Syst.*, vol. 21, no. 3, pp. 1234-1241, 2006.
44. A. Messina, et al., "Interpretation and visualization of wide-area PMU measurements using Hilbert analysis," *IEEE Trans. Power Syst.*, vol. 21, no. 4, pp. 1763-1771, 2006.
45. M. A. Andrade, et al., "Identification of instantaneous attributes of torsional shaft signals using the Hilbert transform," *IEEE Trans. Power Syst.*, vol. 19, no. 3, pp. 1422-1429, 2004.
46. S. L. Hahn, *Hilbert transforms in signal processing*. Vol. 2. 1996: Artech House Boston.
47. N. E. Huang, et al., "The empirical mode decomposition and the Hilbert spectrum for nonlinear and non-stationary time series analysis," *Proc. of the Royal Society of London*. Series A: Mathematical, Physical and Engineering Sciences, 1998. 454(1971): p. 903-995.
48. A. Messina and V. Vittal, "Extraction of dynamic patterns from wide-area measurements using empirical orthogonal functions," *IEEE Trans. Power Syst.*, vol. 22, no. 2, pp. 682-692, 2007.
49. T. J. Browne, et al., "A comparative assessment of two techniques for modal identification from power system measurements," *IEEE Trans. Power Syst.*, vol. 23, no. 3, pp. 1408-1415, 2008.
50. B. L. Kokanos and G. G. Karady, "Associate Hermite Expansion Small Signal Mode Estimation," *IEEE Trans. Power Syst.*, vol. 25, no. 2, pp. 999-1006, 2010.
51. B. L. Kokanos and G. G. Karady, "Comparison of various power system electromechanical mode estimators," in *Proc. IEEE PowerTech,* Trondheim, 2011.
52. L. Oatts, "External network modeling-recent practical experience," *IEEE Trans. Power Syst.*, vol. 9, no. 1, pp. 216-228, 1994..
53. J. H. Chow, "Time-scale modeling of dynamic networks with applications to power systems," 1982: Springer-Verlag.
54. U. D. Annakkage, et al., "Dynamic System Equivalents: A Survey of Available Techniques," *IEEE Trans. Power Del.*, vol. 27, no. 1, pp. 411-420, 2012.
55. J. M. Undrill, et al., "Electromechanical Equivalents for Use in Power System Stability Studies," *IEEE Trans. Power App. Syst.*, vol. PAS-90, no. 5, pp. 2060-2071, 1971.
56. W. Price, et al., "Testing of the modal dynamic equivalents technique," *IEEE Trans. Power App. Syst.*, vol. PAS-97, no. 4, pp. 1366-1372, 1978.
57. I. J. Perez-Arriaga, G.C. Verghese, and F.C. Schweppe, "Selective Modal Analysis with Applications to Electric Power Systems, PART I: Heuristic Introduction," *IEEE Trans. Power App. Syst.*, vol. PAS-101, no. 9, pp. 3117-3125, 1982.
58. G. C. Verghese, I. J. Perez-Arriaga, and F. C. Schweppe, "Selective Modal Analysis With Applications to Electric Power Systems, Part II: The Dynamic Stability Problem," *IEEE Trans. Power App. Syst.*, vol. PAS-101, no. 9, pp. 3126-3134, 1982.
59. I. J. Perez-Arriaga, et al., "Developments in selective modal analysis of small-signal stability in electric power systems," *Automatica*, vol. 26, no. 2, pp. 215-231, 1990..
60. Wang, L., et al., "Dynamic reduction of large power systems for stability studies," *IEEE Trans. Power Syst.*, vol. 22, no. 2, pp. 889-895, 1997.
61. X. Lei, D. Povh, and O. Ruhle, "Industrial approaches for dynamic equivalents of large power systems," in *Proc. Power Eng. Soc. Winter Meeting,* 2002.
62. R. Podmore, "Identification of coherent generators for dynamic equivalents," *IEEE Trans. Power App. Syst.*, vol. PAS-97, no. 4, pp. 1344-1354, 1978.
63. A. J. Germond and R. Podmore, "Dynamic Aggregation of Generating Unit Models," *IEEE Trans. Power App. Syst.*, vol. PAS-97, no. 4, pp. 1060-1069, 1978.

64. A. M. Gallai, "Coherency-based dynamic equivalents for transient-stability studies of power systems," 1980: Cornell University.
65. S. B. Yusof, , G. J. Rogers, and R. T. H. Alden, "Slow coherency based network partitioning including load buses," *IEEE Trans. Power Syst.*, vol. 8, no. 3, pp. 1375-1382, 1993.
66. M. L. Ourari, L.A. Dessaint, and D. Van-Que, "Dynamic equivalent modeling of large power systems using structure preservation technique," *IEEE Trans. Power Syst.*, vol. 21, no. 3, pp. 1284-1295, 2006.
67. E. Muljadi and B. Parsons, "Comparing single and multiple turbine representations in a wind farm simulation," *National Renewable Energy Laboratory*, 2006.
68. L. M. Fernandez, , J. R. Saenz, and F. Jurado, "Dynamic models of wind farms with fixed speed wind turbines," *Renewable Energy*, vol. 31, no. 8, pp. 1203-1230, 2006.
69. Q. Wei, R. G. Harley, and G. K. Venayagamoorthy, "Dynamic modeling of wind farms with fixed-speed wind turbine generators," in *Power Eng. Soc. General Meeting,* 2007.
70. V. Akhmatov and H. Knudsen, "An aggregate model of a grid-connected, large-scale, offshore wind farm for power stability investigations-importance of windmill mechanical system," *International Journal of Electrical Power & Energy Systems*, vol. 24, no. 9, pp. 709-717, 2002.
71. D. J. Trudnowski, et al., "Fixed-speed wind-generator and wind-park modeling for transient stability studies," *IEEE Trans. Power Syst.*, vol. 19, no. 4, pp. 1911-1917, 2004.
72. M. A. Poller, "Doubly-fed induction machine models for stability assessment of wind farms," in *Proc. Power Tech Conf., Bologna*, 2003.
73. S. Geeves, "A modal-coherency technique for deriving dynamic equivalents," *IEEE Trans. Power Syst.*, vol. 3, no. 1, pp. 44-51, 1988.
74. A. Chakrabortty, J. H. Chow, and A. Salazar, "A measurement-based framework for dynamic equivalencing of large power systems using wide-area phasor measurements," *IEEE Trans. Smart Grid*, vol. 2, no. 1 pp. 68-81, 2011.
75. X. Feng, Z. Lubosny, and J. W. Bialek, "Identification based dynamic equivalencing," in *Proc. Power Tech, Lausanne*, 2007.
76. X. Feng, Z. Lubosny, and J. W. Bialek, "Dynamic equivalencing of distribution network with high penetration of distributed generation," in *Proc. UPEC,* 2006.
77. Z. Huang, et al., "Generator dynamic model validation and parameter calibration using phasor measurements at the point of connection. *IEEE Trans. Power Syst.,* vol. 28, no. 2, pp. 1939-1949.
78. J. V. Milanovic and S. Mat Zali, Validation of equivalent dynamic model of active distribution network cell*. IEEE Trans. Power Syst.,* vol. 28, no. 3, pp. 2101-2110.
79. R. Hecht-Nielsen, *Neurocomputer applications*, in *Neural computers*. 1988, Springer. p. 445-453.
80. P. D. Wasserman, *Neural computing: theory and practice*. 1989: Van Nostrand Reinhold Co.
81. T. Khanna, *Foundations of neural networks.* 1990.
82. J. Freeman and D. Skapura, *Neural networks, algorithms, applications, and programming techniques.* 1991.
83. Y. Pao, *Adaptive pattern recognition and neural networks.* 1989.
84. V. S. S. Vankayala and N.D. Rao, "Artificial neural networks and their applications to power systems-a bibliographical survey," *Electric Power Systems Research*, vol. 28, no. 1, pp. 67-79, 1993.
85. A. M. Stankovic, A.T. Saric, and M. Milosevic, "Identification of nonparametric dynamic power system equivalents with artificial neural networks," *IEEE Trans. Power Syst.*, vol. 18, no. 4, pp. 1478-1486, 2003.
86. A. M. Azmy and I. N. Erlich. "Identification of dynamic equivalents for distribution power networks using recurrent ANNs," in *Proc. Power Systems Conference and Exposition, 2004.*

87. A. Rahim and A. Al-Ramadhan, "Dynamic equivalent of external power system and its parameter estimation through artificial neural networks," *International journal of electrical power & energy systems*, vol. 24, no. 2, pp. 113-120, 2002.
88. H. Shakouri G and H. R. Radmanesh, "Identification of a continuous time nonlinear state space model for the external power system dynamic equivalent by neural networks," *International journal of electrical power & energy systems*, vol. 31, no. 3, pp. 334-344, 2009.
89. M. Feng and V. Vittal, "A Hybrid Dynamic Equivalent Using ANN-Based Boundary Matching Technique," *IEEE Trans. Power Syst.* vol. 27, no. 3, pp. 1494-1502, 2012.
90. J. MacQueen, "Some methods for classification and analysis of multivariate observations," in *Proc. the 5th Berkeley symposium on mathematical statistics and probability*, California, 1967.
91. S. M. Zali, N. Woolley, and J. Milanovic, Development of equivalent dynamic model of distribution network using clustering procedure. in *Proc. 17th PSCC.*
92. M. Melanie, *An introduction to genetic algorithms.* Cambridge, Massachusetts London, England, 5th printing, 1999.
93. S. Orero and M. Irving, "A genetic algorithm for generator scheduling in power systems," *International journal of electrical power & energy systems*, vol. 18, no. 1, pp. 19-26, 1996.
94. A. G. Bakirtzis, et al., "Optimal power flow by enhanced genetic algorithm," *IEEE Trans. Power Syst.* vol. 17, no. 2, pp. 229-236, 2002.
95. A. Shahat and H. Shewy, "Permanent magnet synchronous motor dynamic modeling with genetic algorithm performance improvement," *International Journal of Engineering, Science and Technology*. vol. 2, no. 2, pp. 93-106, 2010.
96. J. Ramfirez, and R. G. A. Valle, "A technique to reduce power systems electromechanical models," *IEEE Trans. Energy Convers*, vol. 19, no. 2, pp. 456-458, 2004.
97. M. Gavrilas, O. Ivanov, and G. Gavrilas, "REI equivalent design for electric power systems with genetic algorithms," *WSEAS Transactions on Circuits and Systems*, vol. 7, no. 10, pp. 911-921, 2008.
98. D. H. Wilson, K. Hay, and G. J. Rogers, "Dynamic model verification using a continuous modal parameter estimator," in *Proc. Power Tech Conference,* 2003.
99. Y. Qixun, B. Tianshu, and W. Jingtao, "WAMS implementation in China and the challenges for bulk power system protection,". in *Proc. Power Eng. Soc. General Meeting, 2007.*
100. *2011 National Electricity Transmission System Seven Year Statement*. 2011, National Grid.
101. P. Kundur, *Power System Stability and Control*. 1993: McGraw-Hill.
102. M. I. Friswell and J. E. Mottershead, *Finite Element Model Updating in Structural Dynamics*. 1995: Kluwer Academic Publishers.
103. S. Guo and J. Bialek, "Synchronous machine inertia constants updating using wide area measurements," in *Proc. ISGT*, Berlin, 2012.